C18C6

NASA TECHNICAL MEMORANDUM

NASA TM-82524

STS-2, -3, -4 INDUCED ENVIRONMENT CONTAMINATION MONITOR (IECM) SUMMARY REPORT

Edited by E. R. Miller
Space Science Laboratory

February 1983

NASA

George C. Marshall Space Flight Center
Marshall Space Flight Center, Alabama

TECHNICAL REPORT STANDARD TITLE PAGE

1. REPORT NO.	2. GOVERNMENT ACCESSION NO.	3. RECIPIENT'S CATALOG NO.
NASA TM-82524		

4. TITLE AND SUBTITLE	5. REPORT DATE
STS-2, -3, -4 Induced Environment Contamination Monitor (IECM) Summary Report	February 1983
	6. PERFORMING ORGANIZATION CODE
7. AUTHOR(S)	8. PERFORMING ORGANIZATION REPORT #
Edited by E. R. Miller	
9. PERFORMING ORGANIZATION NAME AND ADDRESS	10. WORK UNIT NO.
George C. Marshall Space Flight Center Marshall Space Flight Center, Alabama 35812	11. CONTRACT OR GRANT NO.
	13. TYPE OF REPORT & PERIOD COVERED
12. SPONSORING AGENCY NAME AND ADDRESS	Technical Memorandum
National Aeronautics and Space Administration Washington, D. C. 20546	14. SPONSORING AGENCY CODE

15. SUPPLEMENTARY NOTES

Prepared by Space Science Laboratory, Science and Engineering Directorate.

16. ABSTRACT

A brief description of the STS-2, -3, and -4 missions is given with the location of the IECM in the payload bay and the Shuttle coordinate systems used in this report. Measurement results from the three flights are given in the following sections for each instrument with comparisons to original goals for preflight environment and induced environment contamination. These results include very low levels of molecular mass accumulation rates, absence of molecular films on optical samples, outgassing species above 50 amu undetectable, general low levels of on-orbit particulates, and decay rates for early mission and water dump particulates. Results of exposure of several optical materials and coatings to atomic oxygen are also presented. From these results, it is concluded that the Space Shuttle has met the established induced environment contamination goals.

17. KEY WORDS	18. DISTRIBUTION STATEMENT
Space Shuttle, Spacecraft Contamination	Unclassified - Unlimited

19. SECURITY CLASSIF. (of this report)	20. SECURITY CLASSIF. (of this page)	21. NO. OF PAGES	22. PRICE
Unclassified	Unclassified	107	NTIS

MSFC - Form 3292 (May 1969)

For sale by National Technical Information Service, Springfield, Virginia 22151

ACKNOWLEDGMENTS

The editor and authors would like to recognize the many people that contributed to the successful flights of the IECM on STS-2, -3, and -4. Some of the major contributors not otherwise recognized in this report are listed here:

Development, Engineering, and Testing:

Larry W. Russell, Marion L. Teal, Charles W. Davis, James W. Berry, Warren S. Streeter, Eli G. Osburn, Jonathan R. Scheidt, Herman E. Kesler, J. B. Stanley, John L. Frazier, William A. Davis, Adrian V. Clark, Bobby H. Futral, William G. Horn, and Gary M. Arnett, all of MSFC.

Integration, Flight Planning, and Operations:

Lubert J. Leger, Stephen Jacobs, Horst K. Ehlers, Angienetta R. Johnson, Joe H. Engle, Richard H. Truly, Jack R. Lousma, G. Gordon Fullerton, Thomas K. Mattingly, and Henry W. Hartsfield, JSC; Edwin C. Johnson, Jr., Lee Harrison, KSC; John B. Gembitsky, Pete Reninger, Charles L. Gross, Rockwell/KSC; Gerald Wittenstein, Robert P. Little, Marvis A. Sanders, Byron J. Schrick, Keith B. Chandler, and Charles A. Lundquist, MSFC.

TABLE OF CONTENTS

TECHNICAL MEMORANDUM

STS-2, -3, -4 INDUCED ENVIRONMENT CONTAMINATION MONITOR (IECM) SUMMARY REPORT

I. INTRODUCTION

E. R. Miller

The Induced Environment Contamination Monitor (IECM) (Fig. I-1) is a desk size (121.3 cm long by 82.2 cm wide by 79.1 cm high) package consisting of 10 instruments designed to obtain environment and induced contamination measurements during preflight ground operations, ascent, on-orbit, descent, and postlanding.[1] The 10 instruments and their functions are (1) Humidity Monitor; (2) Dew Point Hygrometer, which measures water vapor content and air temperature on the ground and during ascent and descent; (3) Air Sampler, which provides sampling for hydrocarbons, HCl, and NO products in the cargo bay; (4) Cascade Impactor, which measures size and quantity of airborne particulates in the cargo bay; (5) Optical Effects Module; (6) Passive Sample Array, which provides measure of molecular contamination effects on optical properties as well as size distribution and effects of particulate accumulation; (7) Temperature-Controlled and (8) Cryogenic Quartz Crystal Microbalance, which measures nonvolatile residue at various temperatures; (9) Camera/Photometer, which measures size, range, and velocity of on-orbit particulates as well as background brightness; and (10) Mass Spectrometer, which measures quantity and mass of molecular flux.

This report provides a summary of results to date of the Shuttle/IECM flights. Section II briefly describes the STS-1 through -4 mission parameters, payloads, and major attitudes. Technical discussions and results from the 10 instruments are given in Sections III through IX. Finally, conclusions that can be made at this time from the three flights of IECM are given in Section X. Further results from continuing analyses will be published as these studies are completed.

1. An Induced Environment Contamination Monitor for the Space Shuttle, edited by Edgar R. Miller and Rudolf Decher, NASA TM-78193, August 1978.

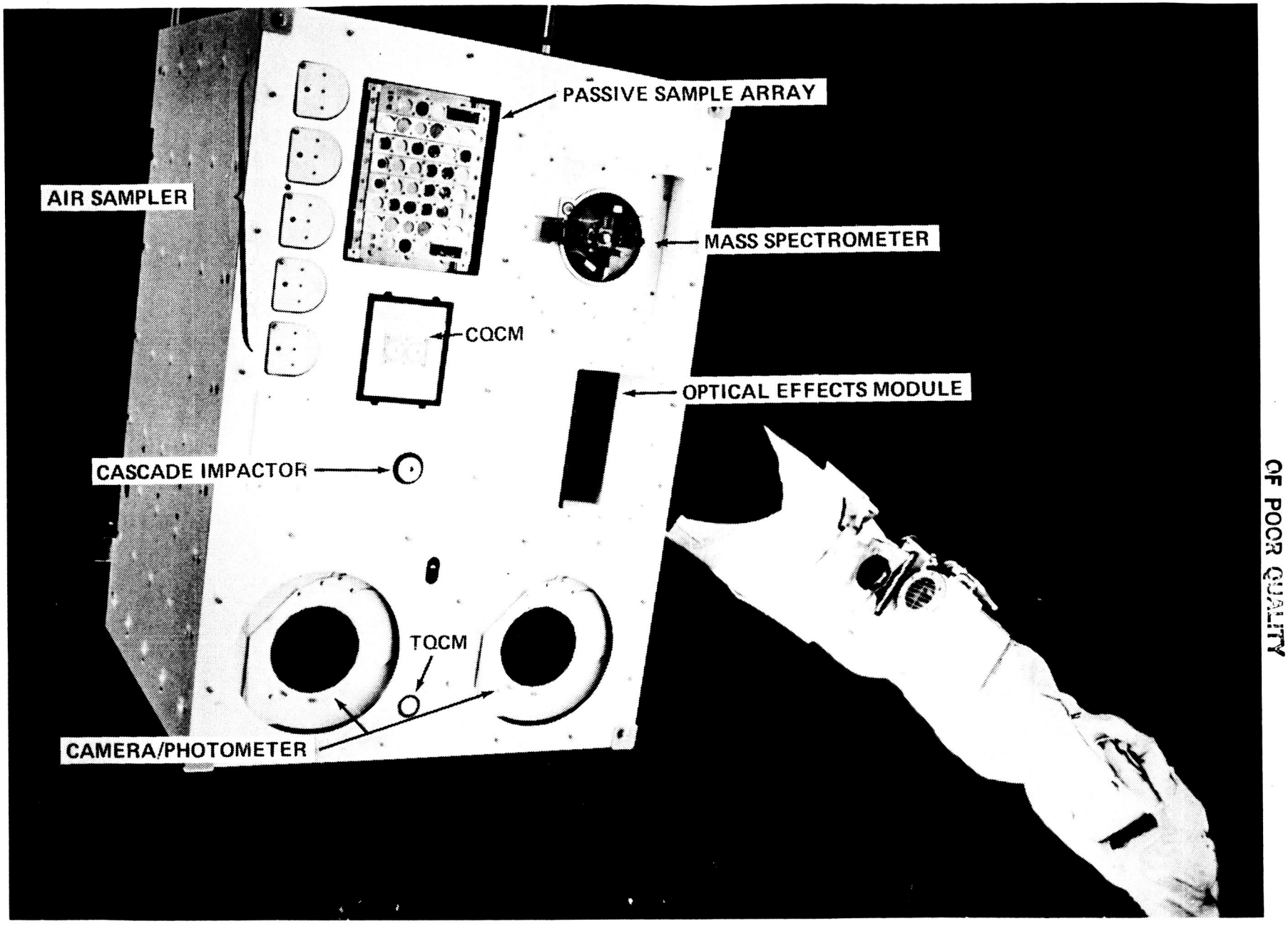

Figure I-1. Induced Environment Contamination Monitor.

II. OFT/IECM MISSIONS DESCRIPTION

E. R. Miller

The IECM flew on the Orbiter Flight Tests (OFT), STS-2, -3, and -4 [II-1,II-2]. In addition, one tray (containing six optical samples) of the IECM Passive Sample Array flew on STS-1 [II-3]. The IECM payload bay location (top center of IECM) for all three missions was approximately 15.16 m (49.75 ft) from the forward bulkhead, 3.25 m (10.67 ft) from the rear bulkhead, 1.19 m (3.92 ft) above the payload bay door sill line, and centered on the Y axis (Fig. II-1). Mounting was accomplished through the Release/Engage Mechanism (REM) which was mounted on special rails attached to the Development Flight Instrumentation (DFI) pallet.

The OFT flights were primarily designed to test the Space Transportation System (STS). During these flights, the Orbiter was subjected to extreme thermal conditions with payload bay door cyclings, primary thrust firings, water dumps, and flash evaporator operations with few requirements or attempts to minimize induced contamination. Consequently, the IECM obtained measurements during these extremes as well as during conditions more representative of operational missions, such as long periods at given attitudes with minimal test operations contributing to the induced contamination environment. An overall summary of the missions is given in Table II-1.

The payload bay (-Z axis) co-elevation angle with the velocity vector (Fig. II-1) as a function of mission elapsed time (MET) is given for STS-4 in Figure II-2. Similar information for STS-2 and -3 is available in References II-2 and II-3, respectively.

TABLE II-1. STS MISSIONS DESCRIPTION

MISSION PARAMETER	STS–1	STS–2	STS–3	STS–4
LAUNCH DATE	4–12–81	11–12–81	3–22–82	6–27 -82
DURATION, HR.	54	54	192	168
INCLINATION/BETA ANGLE, °	40/–26 TO –19	38/–50 TO –45	38/–36 TO –23	28.5/–1 TO +20
ALTITUDE, km (N. MI.)	240–278 (130–150)	222–259 (120–140)	241 (130)	306 (165)
MAJOR ATTITUDE(S)	–ZLV, Y–POP PAYLOAD BAY TO EARTH	–ZLV, Y–POP PAYLOAD BAY TO EARTH	TAIL TO SUN 24 HRS. NOSE TO SUN 80 HRS. BAY TO SUN 27 HRS. PASSIVE THERMAL CONTROL (PTC) 23 HRS.	TAIL TO SUN 61 HRS. BOTTOM TO SUN 32 HRS. TOP TO SUN 7.5 HRS. PTC 72 HRS. GRAVITY GRADIENT 7 HRS.
PAYLOAD(S)	DEVELOPMENT FLIGHT INSTRUMENTATION (DFI)	OSTA–1 IECM + DFI	OSS–1, IECM, AND DFI	DOD 82–1, IECM, AND DFI
COMMENT		GAS RELEASE	DOOR TESTS	DOOR TEST, CONTAMINATION SURVEY GAS RELEASE

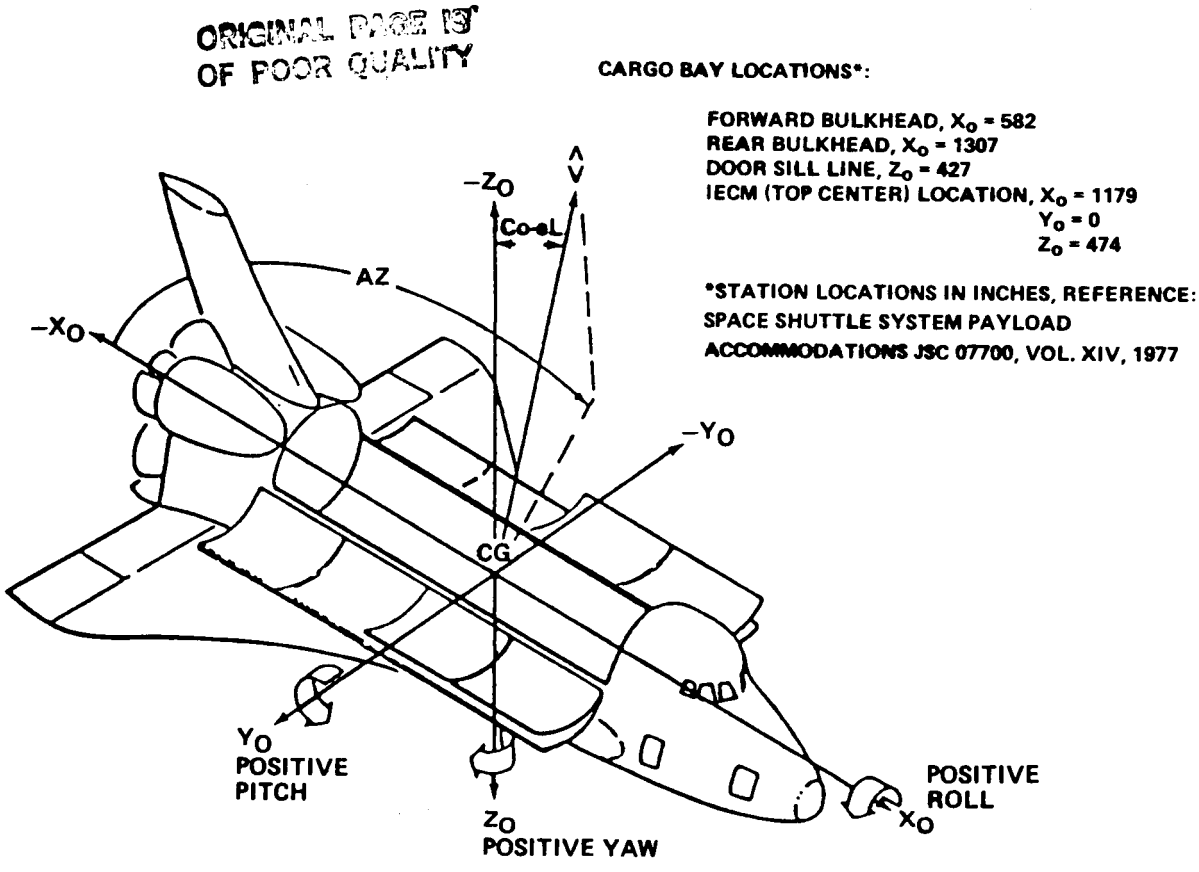

Figure II-1. Orbiter body coordinate system and azimuth, co-elevation coordinates.

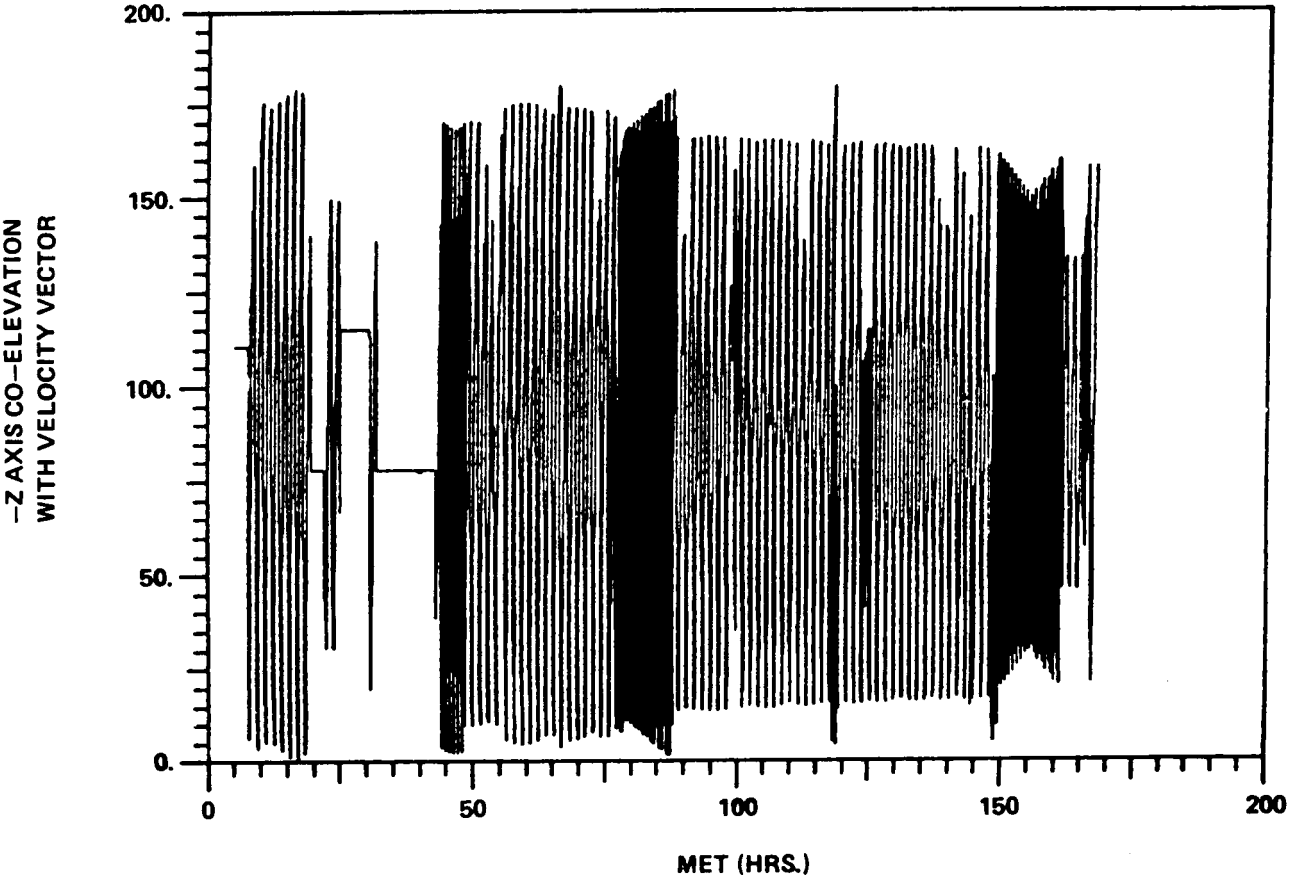

Figure II-2. STS-4 mission elapsed time.

REFERENCES

II-1. Linton, Roger C., Miller, Edgar R., and Susko, Michael: Passive Optical Sample Assembly (POSA). NASA TM-92446, August 1981.

II-2. Miller, E. R. (Editor): STS-2 Induced Environment Contamination Monitor (IECM) – Quick-Look Report. NASA TM-82457, January 1982.

II-3. Miller, E. R. and Fountain, J. A. (Editors): STS-3 Induced Environment Contamination Monitor (IECM) – Quick-Look Report. NASA TM-82489, June 1982.

III. HUMIDITY MONITOR AND DEW POINT HYGROMETER

H. W. Parker

The Humidity Monitor operates over a range of 0 to 100 percent relative humidity with an accuracy of ±4 percent. The Dew Point Hygrometer operates over a range of -6.7°C (20°F) to 26.7°C (80°F) with an accuracy of 0.5°C. The temperature is measured over a range of 0 to 100°C with an accuracy of 0.5°C.

The sensors for the Humidity Monitor and Dew Point Hygrometer are located in the air manifold within the air sampler system. The air is piped into the manifold at a flow rate of 1 liter/min.

The Humidity Monitor measured zero relative humidity during ascent, reflecting the environment provided by the cargo bay dry nitrogen purge gas prior to launch. The Dew Point Hygrometer correspondingly indicated a dew point below its measuring range of -6.7°C (20°F).

The results of relative humidity and temperature measurements during descent are shown in Figures III-1 and III-2. The air pumps were turned on at an altitude of approximately 22.875 km (75,000 ft) and remained on until approximately 30 min after landing on STS-2 and 44 min after landing on STS-3 and -4. The relative humidity rose to near constant levels of approximately 15 percent on STS-2 and -3 and to about 25 percent on STS-4. The air temperature remained between approximately 10° and 20°C. The dew point remained well below -6.7°C operating range of the hygrometer on STS-2 and -3 and near this value on STS-4.

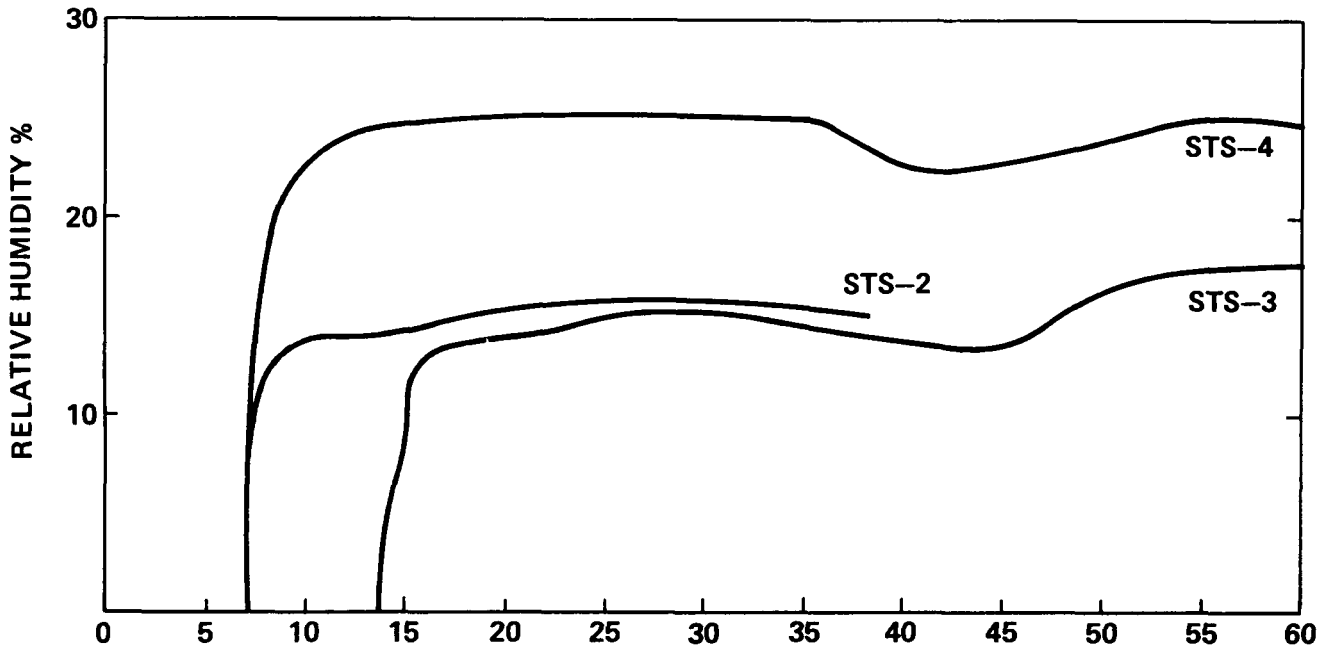

Figure III-1. IECM reentry Humidity Monitor for STS-2, STS-3, and STS-4.

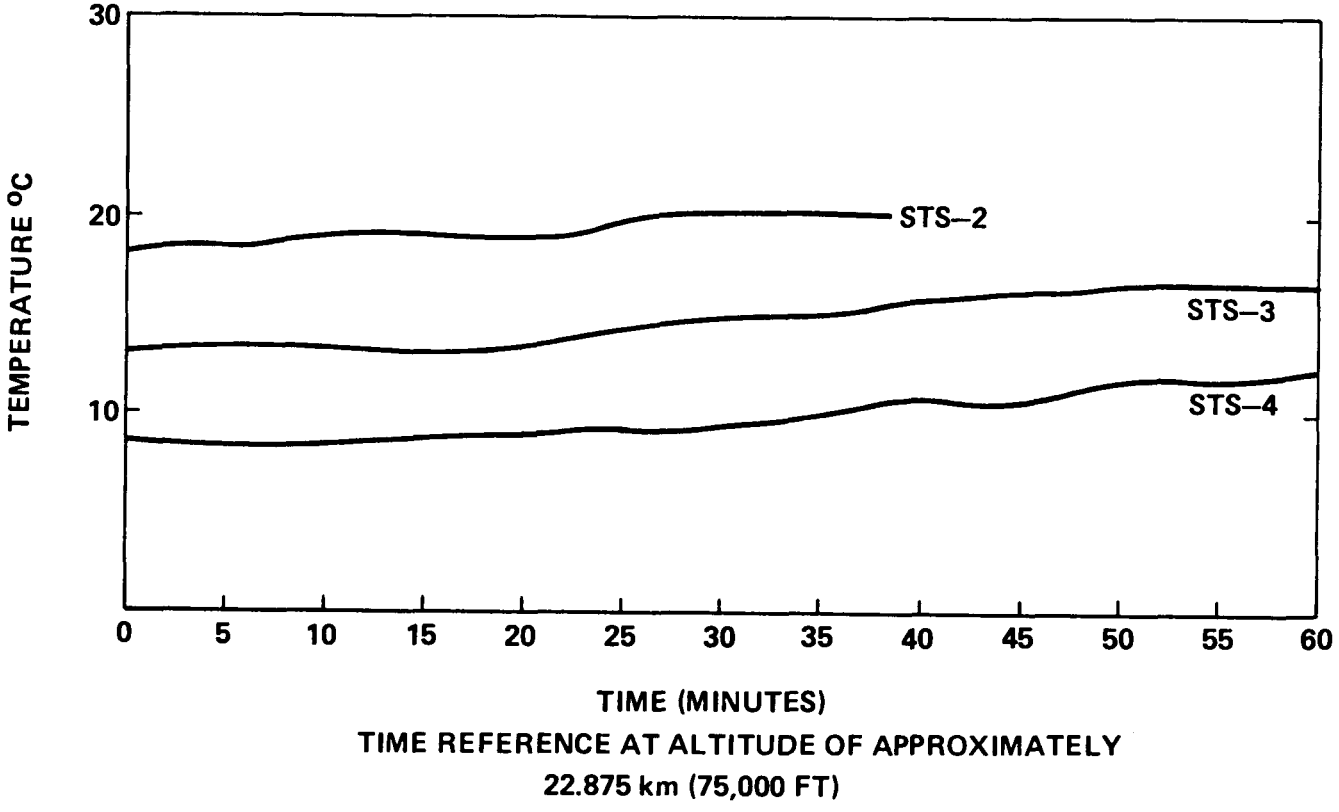

Figure III-2. IECM reentry temperature (air sampler) for STS-2, STS-3, and STS-4.

IV. AIR SAMPLER

P. N. Peters, H. B. Hester, W. Bertsch,[1] H. Mayfield,[1] and D. Zatko[2]

Preflight ground, ascent, and descent air samples of the ambient environment taken during the STS missions 2 through 4 were collected. Quick-look results from the STS-2 and -3 flights have been reported [IV-1, IV-2]. This report summarizes the results to date from STS-2, -3, and -4. Analyses made for volatile species by concentration on adsorbents and postflight measurements with gas chromatography/mass spectroscopy indicated that the ground level requirement goal of less than 15 ppm total hydrocarbons was met during the ground sampling periods (typical total hydrocarbons was 1 to 2 ppm by weight relative to air). Although higher percentage levels of volatiles were expected during ascent, no a priori requirements were provided for this highly transient phase of flight where partial vacuums evaporated such species. Unexpectedly large background levels as evidenced in control samples prevented accurate analyses for species with gas chromatograph retention times of less than 2 to 3 min (the maximum retention times utilized in the analyses typically exceeded 45 min). After control sample background subtractions, a typical level of total volatiles detected during ascent was 55 ppm by weight relative to air or <15 ppm by volume (average molecule was heavier than air). Examples of volatiles detected are shown in Table IV-1.

Similar methods of analyses were used for volatile compounds sampled during descent except elastomer-sealed solenoid valves were used in opening and closing the adsorbent containers as compared to metal-to-metal sealed pyrovalves for the ascent sampling containers. A typical total hydrocarbon analysis for descent gave approximately 18 ppm by weight in air or <5 ppm by volume. Again, no guidelines were specified for the levels of hydrocarbons to be expected in descent samples; however, the relatively higher contamination levels obtained for descent compared to ground sampling levels were not anticipated, since materials within the cargo bay should have been outgassing in orbit before reentry. Conceivably repressurization of the cargo bay during descent could have provided a purging effect to help release trapped vapors outgassed in the multilayers of insulating blankets or other areas particularly restricted in the free-molecular-flow regime. For comparison, it was observed that dry nitrogen purging of the vacuum jackets of multilayer insulated dewars used for liquid helium storage reduces the time required to remove helium trapped in such blankets; also, chambers vented after evacuation usually exhibit a strong smell. However, no firm model is proposed to explain the indicated intermediate levels of volatile species present during descent. It should be noted that in terms of total micrograms of mass collected, the ascent samples were highest, the ground samples least, and the descent samples intermediate. However, in terms of air volume sampled, the ground level volume was highest, the ascent volume least, and the descent volume intermediate.

Analyses for HCl and reactive nitrogen compounds were negative. Only on STS-3 was a positive indication of chemical reaction noted, and this resulted from SO_2 or other reactive-sulfur species which the Air Sampler was not required to identify or quantify. A distinctive peak at 64 amu was first noted on analysis of the residual gas in the free volume of the adsorbent containers which sampled descent air. This peak was assumed to be from SO_2 and was determined to be present at a level on the order of 1 ppm. When these containers were opened, it was noted that silver oxide/hydroxide sample surfaces were discolored. Subsequent analysis verified that a sulfide was present on the discolored surfaces. An attempt was made to associate the observed SO_2 with the eruption of El Chichon, a volcano which

1. The University of Alabama.
2. Sperry Univac.

initially erupted on March 28, 1982. Although, STS-3 landed 2 days later on March 30, the major eruption of El Chichon did not occur until April 4, 1982, and weather satellite photographs taken during the March 28-30 time frame and orbital tracking data did not appear to support a theory that gases from El Chichon were sampled by STS-3. A more likely candidate for the source of SO_2 would be nearby smelters or other industries that may have released such gases in the vicinity of the White Sands landing site, which was uniquely associated with STS-3.

CONCLUSIONS

During the ground sampling periods the applicable specifications for total hydrocarbon levels were met. During ascent the percentage levels of volatiles were considerably higher than ground levels (55 versus 1 to 2 ppm by weight relative to air), as should be expected from reduction in pressure; however, quartz crystal microbalance and other measurements suggested that transient rather than permanent effects occurred from exposure of numerous surfaces to these higher levels. Descent levels (18 ppm by weight relative to air) for percent total hydrocarbons, although intermediate and without detectable permanent effects, were higher than might be anticipated from surfaces outgassed in orbit. While none of the originally anticipated reactive species were detected, the identification of apparently non-Shuttle related SO_2 on one flight provided evidence that the detection system for the reactives was functioning properly.

TABLE IV-1. SOME VOLATILE COMPOUNDS IDENTIFIED FROM ADSORBENTS USED DURING STS MISSIONS – QUANTITIES ARE LISTED AS PARTS PER MILLION RELATIVE TO AIR (29 amu)

Compound	Ascent	Descent
Hexamethyldisiloxane	–	0.5 to 0.7
Methylbenzene	0.2 to 4.5	0.6 to 0.7
Tetrachloroethane	1.7 to 3.5	<0.1
C_8 Hydrocarbon	–	<0.3
2,4 Dimethylhexane	0.4 to 0.6	–
Hexamethylcyclotrisiloxane	2.0 to 10.0	3.0 to 10.0
C_2 Benzene	1.0 to 3.0	0.1 to 0.3
C_9 Hydrocarbon	0.6 to 1.0	0.2 to 0.6
Acetic acid	0.6 to 6.0	0.4 to 3.0
C_{10} Hydrocarbon	<1.0	–
Decane	0.8 to 1.4	0.1 to 0.3
Octamethylcyclotetrasiloxane	1.3 to 7.0	~2.0
C_{11} Hydrocarbon	0.4 to 1.4	–

REFERENCES

VI-1. STS-2 Induced Environment Contamination Monitor (IECM) – Quick Look Report. NASA TM-82457, edited by E. R. Miller, January 1982.

VI-2. STS-2 Induced Environment Contamination Monitor (IECM) – Quick-Look Report. NASA TM-82489, edited by E. R. Miller and J. A. Fountain, June 1982.

V. CASCADE IMPACTOR

B. J. Duncan

INTRODUCTION

The Cascade Impactor instrument consists of three stages of quartz crystal microbalances, each operating directly behind an impact nozzle. Sampled air flows sequentially through the stages whose individual nozzles are sized to provide size discrimination in three ranges from 0.3 μm to greater than 5.0 μm in diameter. The sensors for these three particulate size ranges function during spacecraft ascent and descent.

In addition to the three particulate measuring stages, an exposed crystal (Fig. I-1) measures the nonvolatile residue (i.e., the excess of condensation over evaporation at any given time) at ambient temperature.

Table V-1 is a capsule summary of results from measurements on the three OFT missions.

TABLE V-1. STS-2, -3, -4 SUMMARY RESULTS – CASCADE IMPACTOR

Measurement	Requirements	Results		
Non-volatile Residue	$<10^{-5}$ g/cm^2-2π sr 30 day mission	STS-2 $\sim 2 \times 10^{-6}$ g/cm^2-2π sr STS-3 peaks to 3×10^{-6} g/cm^2-2π sr STS-4 $\sim 2 \times 10^{-5}$ g/cm^2-2π sr		
>5μm size particulates	<375 μg/m^3 (assuming $\bar{d}$=25μm, ρ=2g/cm^3	STS-2	Ascent Descent	$\sim$ 30 μg/m^3 $\sim$ 10 "
		STS-3	Ascent Descent	$\sim$ 10 " $\sim$ 10 "
		STS-4	Ascent Descent	Non functional $\sim$ 20 μg/m^3
1μm to 5μm size particles	<100 μg/m^3 (assuming $\bar{d}$=5μm, ρ=2 g/cm^3	STS-2	Ascent Descent	$\sim$ 500 μg/m^3 $\sim$ 250 "
		STS-3	Ascent Descent	<10 μg/m^3 <10 "
		STS-4	Ascent Descent	$\sim$ 400 μg/m^3 <10 "
0.3μm to 1μm size	<10 μg/m^3 (assuming $\bar{d}$=1μm, ρ=2 g/cm^3	STS-2	Ascent Descent	$\sim$ 250 μg/m^3 $\sim$ 125 μg/m^3
		STS-3	Ascent Descent	<10 μg/m^3 <10 "
		STS-4	Ascent Descent	$\sim$ 150 μg/m^3 Non functional

DESCRIPTION

Each stage of the Cascade Impactor consists of a pair of 10 MHz "AT"-cut quartz crystals operating in an electronic oscillator circuit. One of the crystals is used as a sensing element and the other as a reference element, with signals combined in a mixer whose output is a beat frequency. In addition to the reduced bandwidth of the beat frequency and the resultant simplification in data signal handling, temperature compensation advantages are obtained by having the reference and sensing crystals in proximity. Coupled with the nearly zero temperature coefficient of the "AT"-cut crystals, this added compensation minimizes thermal effects. A hybrid mixer-oscillator chip in a T05 plug-in package completes the small electronic module, so that only low audio frequency signals need be transmitted from the sensor head.

In the cascade stages, the reference crystal is mechanically shielded from the incoming contaminant particles; thus, the beat frequency output is proportional to the mass deposited on the sensing element, due to the piezoelectric property of quartz. A small, vane-type pump maintains a constant volumetric flow rate (250 ml/min) through the cascade of nozzles. Therefore, the rate of change of mass collected on the impact plate becomes a measure of the volumetric concentration of mass of particulates of a given size range in the sampled environment.

The accelerated particles are acted upon principally by two forces: inertial, which tends to cause impact on the crystal, and aerodynamic viscous drag, which tends to turn the particle along flow steamlines, thus missing the impact plate and proceeding to the next stage. Size discrimination results from the balance attained between these two opposing factors. The nozzles are sized for particle discrimination such that each stage has a 50 percent probability of impact for particles of 5.0, 1.0, and 0.3 μm diameter, respectively. The volumetric concentrations are proportional to the rate of change of frequency as a constant flow rate of sampled air is maintained. Crystal sensitivity falls off exponentially with the square of the distance from the center. However, since the nozzle openings are so relatively small, the peak sensitivity may be assumed for the total collected mass. With this assumption, the mass concentration measured at any point in time is $C(\mu g/m^3) = 2.15\ [(\mu g/m^3)/(Hz/min)]\ \Delta f/\Delta t$ (Hz/min).

Figure V-1 represents the size discrimination characteristics of the impactor stage (assuming particle density of 2 $\mu g/cm^3$).

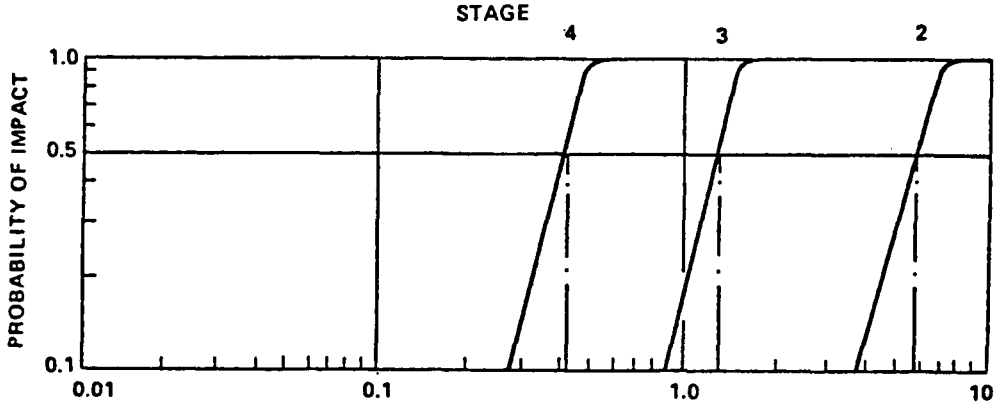

Figure V-1. Cascade stage cutoff characteristics.

The nonvolatile residue (NVR) stage measures the cumulative airborne molecular residue at ambient temperature. In the NVR stage, the reference crystal is enclosed in a hermetically-sealed can such that it is isolated from potential ambient molecular deposition. Thus, mass deposited on the sensing crystal is proportional to the low-frequency beat signal from the sensing and reference oscillators. The remaining electronics are identical to that of the cascade stages.

Calibration for the NVR stage is determined by the basic sensitivity of the "AT"-cut quartz crystals operating at 10 MHz; i.e., mass deposition per unit area, M/A ($\mu g/cm^2$) = 4.43 x 10^{-3} [($\mu g/cm^3$)/ Hz] x Δf (Hz).

RESULTS

Figures V-2, -3, and -4 are differential plots resulting from frequency measurements of the particulate stages for STS-2, -3, and -4, respectively. The ordinate of the plots is in units of suspended mass concentration in $\mu g/m^3$. This sampled mass concentration is plotted versus Mission Elapsed Time (MET) for both the ascent and descent portions of the mission.

During ascent, the 0.3 μm to 1.0 μm stage measured mass concentrations up to 250 $\mu g/m^3$ on STS-2. The 1 μm to 5 μm stage gave even higher mass readings of up to 500 $\mu g/m^3$ during the ascent phase, while the larger size stage (>5 μm) showed negligible particulates in this range. The excessive concentrations of smaller size particulates during ascent are felt to be resultant from the vibratory environment of lift-off and consequent dislodging of particles from other payload items and thermal blankets not previously flown. However, it must be pointed out that these stages, particularly the smaller one, were operating at or near saturation. This occurred due to the 11-hr countdown hold for STS-2 which resulted in 11 hr of on-pad instrumentation operation prior to flight.[1]

During descent, the two smaller particle stages again show apparent peaks of relatively high magnitude (100 and 250 $\mu g/m^3$) in mass concentration. However, this is felt to be purely a thermal effect due to "blasting" the sensing crystals with a stream of cold air when the pump was operated during descent, since the payload bay is vented to very cold air at spacecraft altitudes during deorbit and descent. These stages as well as the larger particle-size stage settled down to very low indicated mass accumulations (< 50 $\mu g/m^3$) for the remainder of the descent and after touchdown.

On the STS-3 mission, particulate concentrations were measured as less than 10 $\mu g/m^3$ for all three size ranges during ascent. The mission appears to have been much cleaner than STS-2. The thermal effect of descent is again evident (instrumental effect only), with final reading stabilizing to within a 10 $\mu g/m^3$ environment.

On STS-4, the large (>5 μm) particle stage was inoperative during ascent. The smaller particle concentrations were almost as high as they were on STS-2 (approximately 400 $\mu g/m^3$ and 200 $\mu g/m^3$, respectively, for the 1.0 μm to 5.0 μm and the 0.3 μm to 1.0 μm particles). During descent, the small (0.3 μm to 1.0 μm) particle stage was inoperative, while the other two stages measured negligible amounts of particulates.

---

1. Miller, E. R. (Editor), STS-2 Induced Environment Contamination Monitor (IECM) – Quick-Look Report, NASA TM-82457, January 1982.

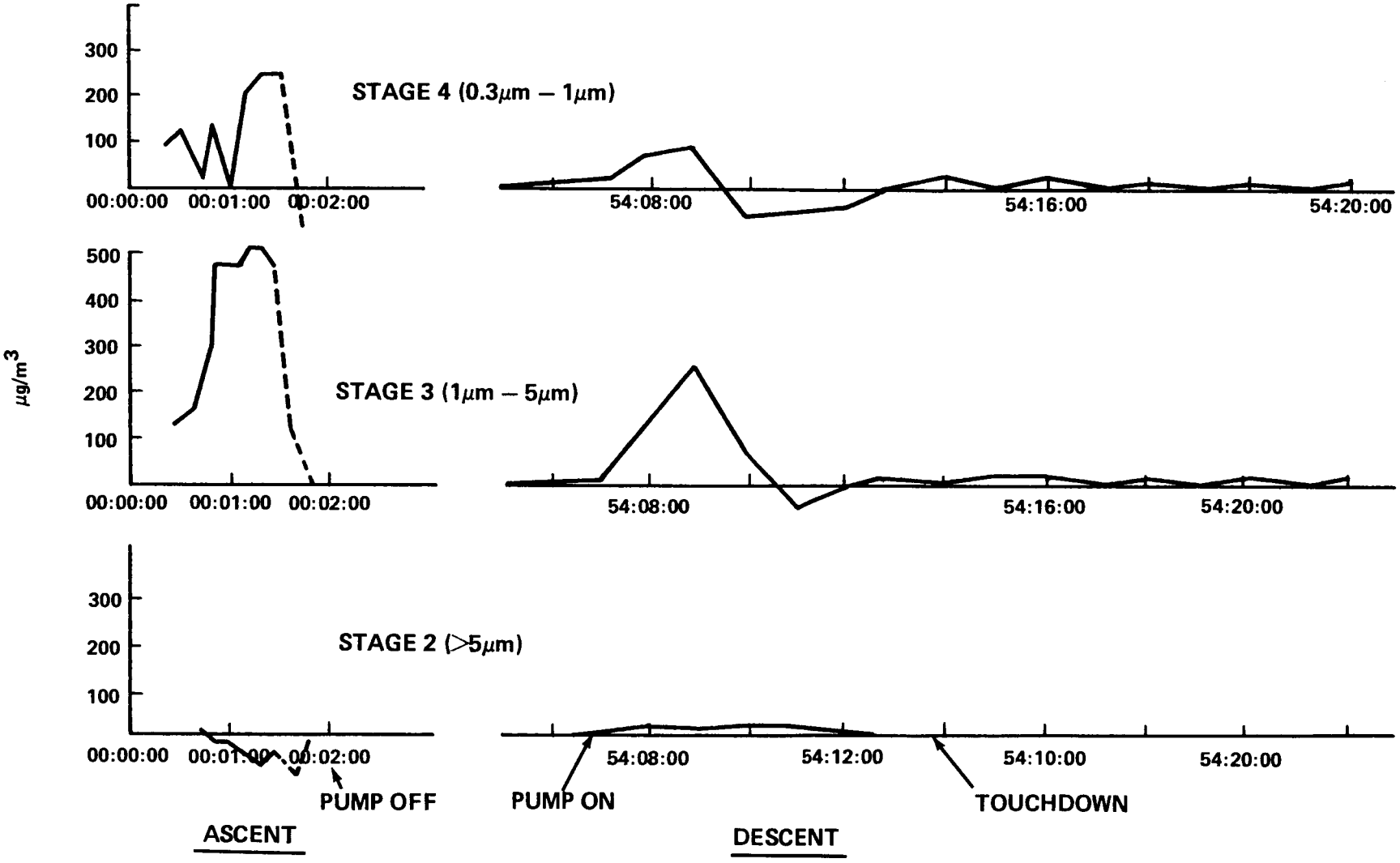

Figure V-2. STS-2 mass concentrations as a function of mission time (hr:min:sec).

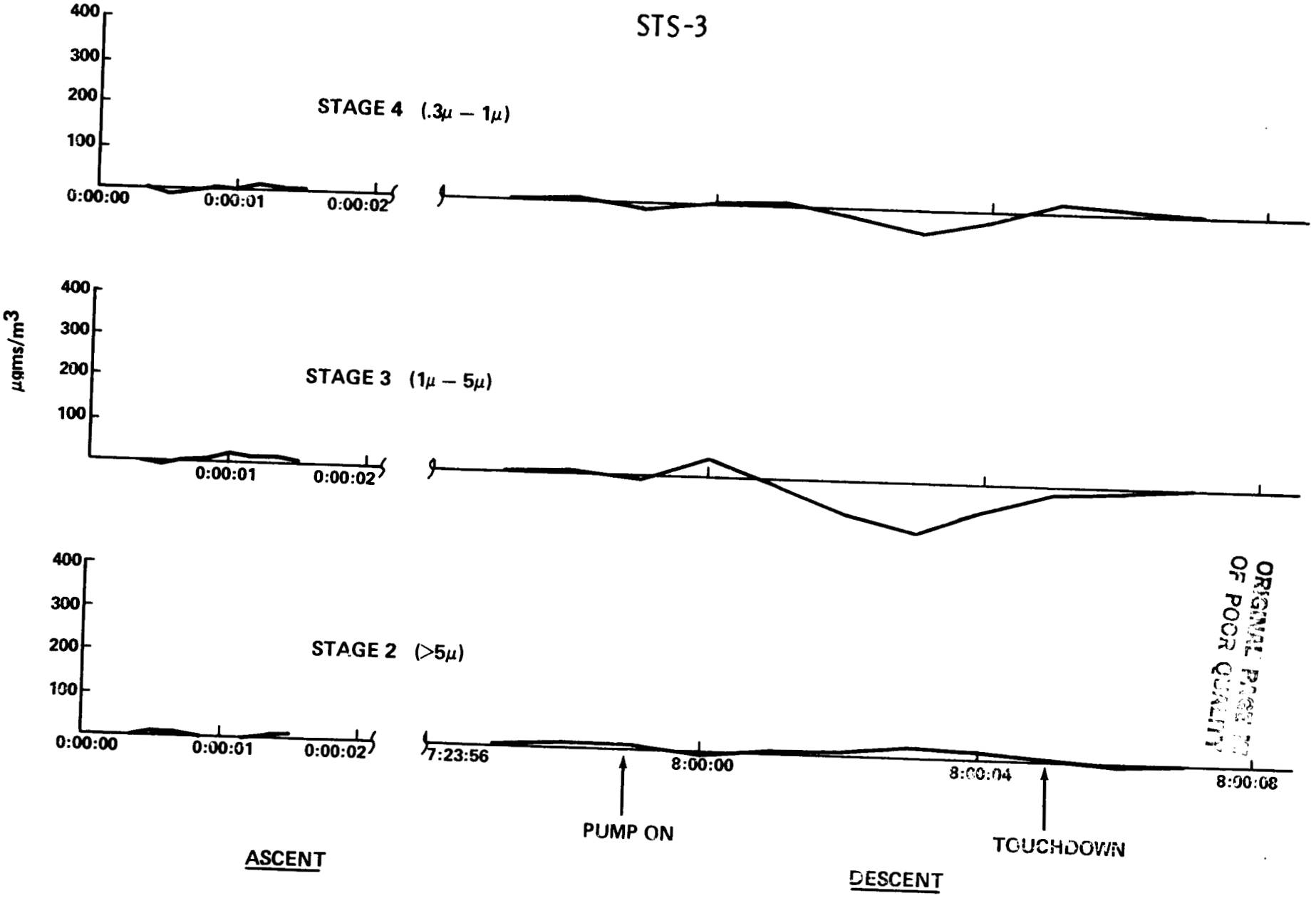

Figure V-3. STS-3 mass concentrations as a function of mission time (day:hr:min).

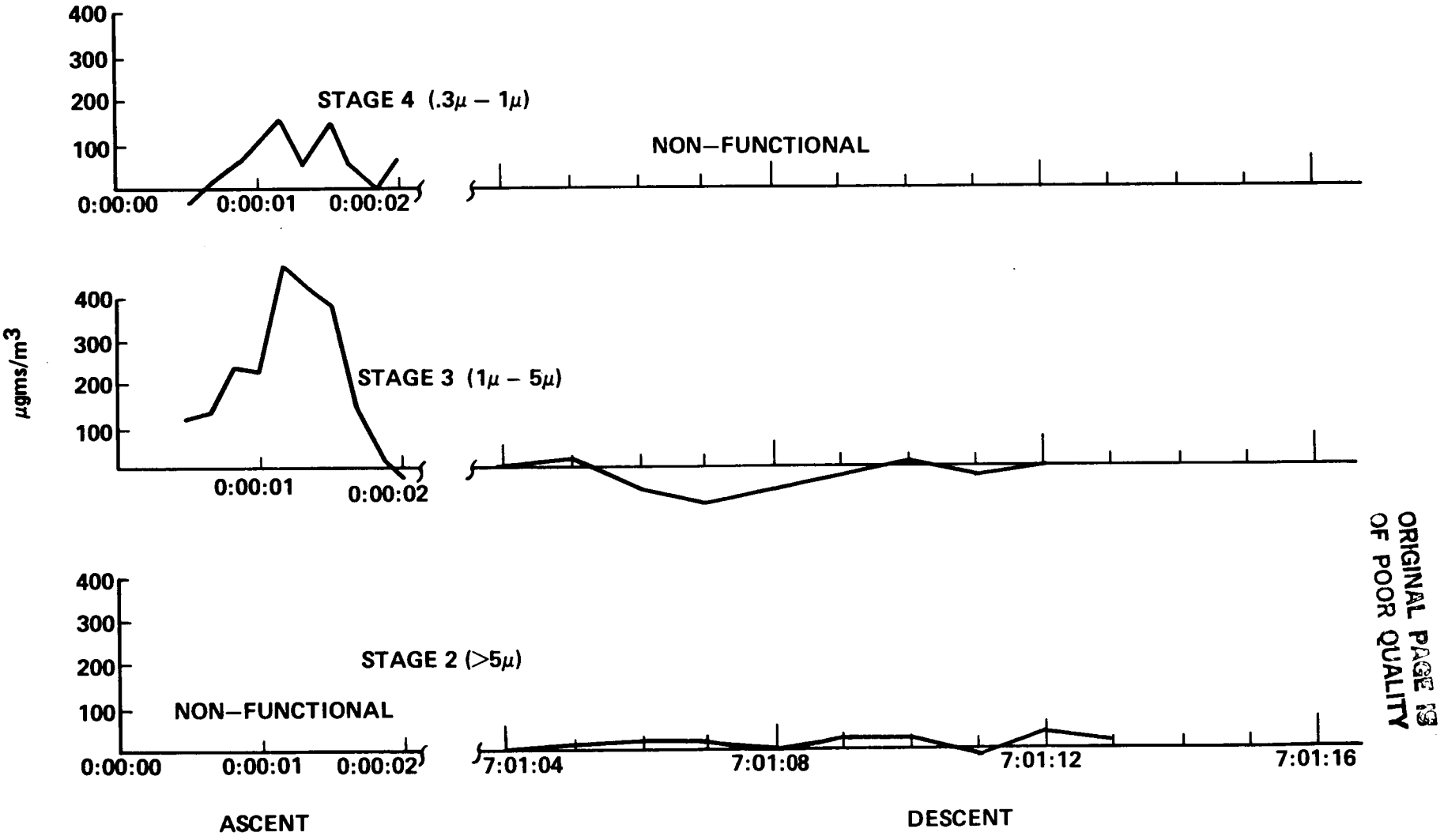

Figure V-4. STS-4 mass concentrations as a function of mission time (day:hr:min).

Nonvolatile residue measurements were obtained at last access in the Orbiter Processing Facility (OPF) during preflight ground operations on STS-2 and -3, and on the launch pad on STS-4. No change could be detected in frequency output of the NVR stage, indicating mass depositions during these ground operations were less than 10^{-7} gm/cm^2.

POSTFLIGHT EXAMINATION

Following each flight, the sensing crystals were removed from the cascade stages, and the collected particulates were examined with a scanning electron microscope. Figures V-5, V-6, and V-7 are relatively low magnification photographs showing the particle distributions for each stage. The size discrimination capability of the three stages is readily apparent. The previously mentioned saturation of the fourth stage on STS-2 due to the 11-hr operation resulting from the launch hold is evident in the high mound of particles. On all three flights, the relative sparsity of particles on the larger size stage is apparent. Numerous fiber-shaped particles are collected on the third stage (1 μm to 5 μm particles) of all three flights, and to a lesser extent on the smallest size stage. These fibers are assumed to originate from the Shuttle thermal tiles. X-ray spectral analysis shows the fibers consist mostly of silicon.

CONCLUSIONS

The particle concentrations of particles larger than 5 μm diameter were at least an order of magnitude below the 100 K clean room requirement of the CDRG specifications for all three of the OFT Shuttle flights. The intermediate size (1 μm to 5 μm) particle concentrations exceeded the CRDG levels on STS-2 and during ascent on STS-4. STS-3 levels were very low for all stages. On STS-2 and STS-4, the smallest size particles (0.3 μm to 1.0 μm) also exceeded the concentration recommendations, but to a lesser extent. The two smaller size stages show some accumulation of fibers containing silicon, presumably from the thermal tiles, on all three flights.

ACKNOWLEDGMENTS

The assistance of Alice Dorries in the analytical work done with the Scanning Electron Microscope and Energy Dispersive Spectrometer is greatly appreciated. Consultation on instrument calibration and data reduction with Don Wallace of Berkeley Instruments has been invaluable. Collaboration of the other instrument scientists and project personnel has been very productive.

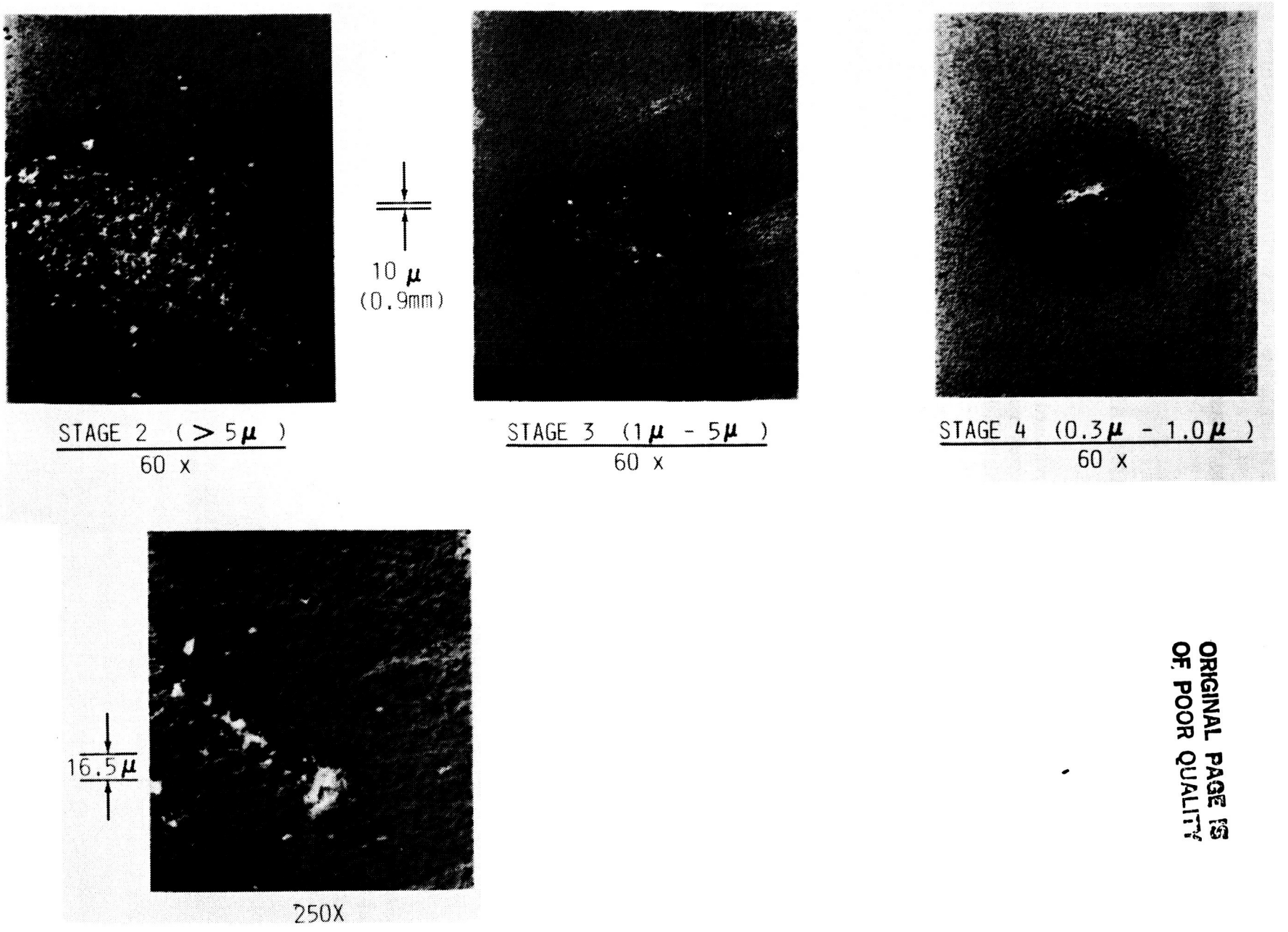

Figure V-5. STS-2 cascade sensor crystals – post flight.

Figure V-6. STS-3 sensing crystals – post flight.

Figure V-7. STS-4 cascade sensor crystals – post flight.

VI. OPTICAL EFFECTS MODULE AND PASSIVE SAMPLE ARRAY

R. C. Linton and D. R. Wilkes

INTRODUCTION

The optical effects of the deposition of contamination from the Shuttle cargo bay environment were monitored in situ by the Optical Effects Module (OEM) and the Passive Sample Array (PSA). The results have provided information concerning the effects of the natural as well as the induced environment on a variety of optical materials representative of components of present-day and projected spaceflight instrumentation. While the application of these results must be approached with careful consideration, due to the limitations of the instruments, some generalizations will be developed.

Previous reports [VI-1,VI-2] have summarized the results for the STS-2 and STS-3 missions. Some of these results will be reproduced in this report in conjunction with previously unpublished data for STS-4 to provide a basis for comparison and summation.

The OEM was developed under contract with Advanced Kinetics, Inc., of Costa Mesa, California. This instrument is an active monitor of monochromatic (253.7 nm) ultraviolet transmittance and scatter, which operated during the orbital phases of the OFT missions. Five transmitting optical samples (2.5 cm diameter) are mounted on the periphery of a carousel that sequentially rotates in the Shuttle X-Z plane. A sixth, empty, sample holder on the carousel provides an internal calibration of the OEM light source for transmittance measurements during each operational sequence.

A complete OEM sequence includes approximately 8 min of static exposure, followed by a measuring phase lasting 77 sec. In the measuring phase, the OEM samples, including the empty hole, are sequentially "stepped" through the internal light-beam-detector path by rotation of the carousel. The initial measurement sequence (triggered by the IECM power-on command) was recorded at approximately 43, 46, and 45 min MET for the STS-2, -3, and -4 missions, respectively.

As can be seen from the system schematic shown in Figure VI-1, three of the optical samples (I2, I3, and I4) are positioned for exposure to the external environment, except during measurement cycles. The other two samples (I1 and I5) as well as the empty position (I0) are positioned within the interior of the instrument except during measurement cycles. This instrument configuration results in samples I1 and I5 being masked from the bay environment for all but approximately 7 percent of the orbital mission, the remainder of the time being exposed to the instrument interior. The other three samples were, by comparison, exposed to the cargo bay environment for approximately 93 percent of the mission.

TRANSMISSION DATA

For each of the three OFT missions, summaries of the OEM results for measurements of transmittance are included in Tables VI-1, VI-2, and VI-3. Table VI-4 is a combined average for the three missions. From these results, the sample subject to the most optical change was the sapphire window (I1). The samples in positions I1 and I5 were expected to monitor the internal self-contamination of the OEM by virtue of their position on the carousel (Fig. VI-1). The in-flight data for each mission in the interval 0 to 5 hr MET indicated considerable variation in the transmittance of the sapphire sample and,

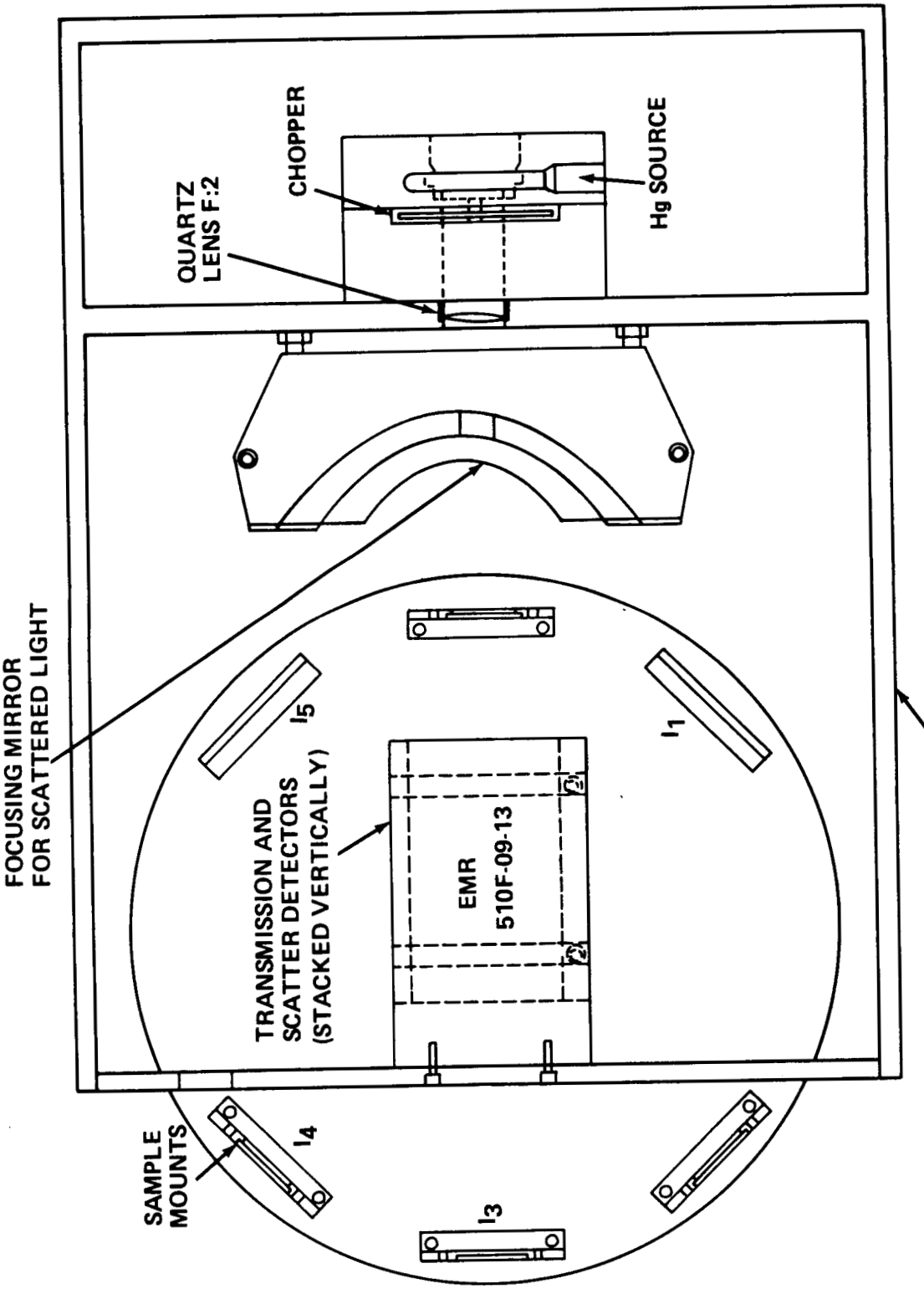

Figure VI-1. Optical Effects Module.

TABLE VI-1. OPTICAL EFFECTS MODULE, SUMMARY OF STS-2 TRANSMITTANCE RESULTS

Mission Phase	Percent Change in Transmittance (253.7 nm)				
	Samples				
	I_1	I_2	I_3	I_4	I_5
Preflight Ground Ops	-1.4	-1.2	0	-1.1	0
Ground to Orbit	-1.4	-2.3	0	-2.3	0
Inflight	-2.8	-1.2	0	-1.2	-1.2
Postlanding (Including Ferry-Flight)	-1.4	-3.6	-2.2	0	-1.2
Total Change	-5.5	-7.0	-2.2	-3.4	-2.3

TABLE VI-2. OPTICAL EFFECTS MODULE, SUMMARY OF STS-3 TRANSMITTANCE RESULTS

Mission Phase	Percent Change in Transmittance (253.7 nm)				
	Samples				
	I_1	I_2	I_3	I_4	I_5
Preflight Ground Ops	-1.3	+1.1	0	0	+1.1
Ground to Orbit	0	+1.1	-2.4	-2.2	0
Inflight	-4.1	0	+1.2	+1.1	+1.1
Postlanding (Including Ferry-Flight)	-1.0	0	0	0	0
Total Change	-1.3	+2.3	-1.2	-1.1	+2.3

TABLE VI-3. OPTICAL EFFECTS MODULE, SUMMARY OF STS-4 TRANSMITTANCE RESULTS

Mission Phase	Percent Change in Transmittance (253.7 nm)				
	Samples				
	I_1	I_2	I_3	I_4	I_5
Preflight Ground Ops	0	0	0	-1.0	*
Ground to Orbit	-1.3	-1.1	-2.1	-2.2	*
Inflight	-1.4	+2.2	+2.2	+2.0	*
Postlanding (Including) Ferry-Flight)	-1.3	0	0	0	*
Total Change	-4.0	+2.2	0	0	*

*No transmissive sample mounted in position for STS-4.

TABLE VI-4. IECM OPTICAL MEASUREMENTS, OPTICAL EFFECTS MODULE, SUMMARY OF RESULTS FOR STS-2, STS-3, AND STS-4

Mission Phase	Average Change in Transmittance (253.7 nm) (%)				
	Exposed Samples			Unexposed Samples	
	LiF_2	CaF_2	MgF_2	Sapphire	Quartz
KSC/OPF: Ground Operations	0	0	-0.7	-0.9	+0.6
Ground to Orbit	-0.8	-1.5	-2.2	-2.2	0
On-Orbit	+0.3	+1.1	+0.7	-2.8	0
Descent/Landing Ferry-Flight	-1.2	-0.7	0	-1.0	-0.6
Total	-0.8	-1.1	-1.5	-2.7	0

Notes:

1. OEM samples labeled "exposed" remain external to OEM housing 93 percent of mission duration.
2. Post-flight particle counts on OEM samples indicate accumulations no greater than level 300 to level 500.
3. Effects of discrete Shuttle events ambiguous due to limited magnitude of measured optics variations.

to a lesser extent, the quartz sample. These were generally in excess of the variations for the externally positioned samples (I2, I3, and I4). The venting of the OEM on ascent was through narrow gaps in the housing designed for passage of the sample holders during rotation of the carousel. Of course, being positioned internally, samples I1 and I5 are most subject to contamination from this source, despite the vacuum bake-outs of the IECM before each mission and other contamination control measures. This outgassing would be expected to decrease within the first few hours of the mission; this was indicated by the recorded data.

Another factor significant in explaining the optical changes of the sapphire sample during the early hours of the missions may be an unexpected increased contribution of the 184.9 nm spectral line in the output of the OEM mercury lamp. Developmental testing of the OEM did not reveal any significant intensity associated with any spectral lines other than the 253.7 nm resonance line. Low pressure mercury lamps of the type used in the OEM generally include the 184.9 nm line in the spectral output, although it is completely masked by attentuation at atmospheric pressure. The results for each of the STS missions for the sapphire sample indicate an anomalous decrease in transmittance of the sapphire sample on reaching orbit that is correspondingly reversed in magnitude following reentry and landing. No equivalent effect was noted for any of the other OEM samples. Of all the OEM samples, only the sapphire window has significant absorption at a wavelength of 184.9 nm compared to the absorption at the nominal OEM wavelength of 253.7 nm. Thus, the effect of an increased contribution of the 184.9 nm line would be expected to most strongly affect the transmittance of the sapphire sample as is indicated in the OEM data.

The OEM data for the three missions include both short- and long-term variations in the optical properties of the samples. Many, if not most, of these variations for all but the sapphire sample (I1) are restricted in magnitude to levels comparable to the measurement uncertainty. Efforts to correlate indicated optical change with particular mission events of contamination potential, such as waste dumps, etc., have not been successful.

THERMAL EFFECTS

While the spectral transmittance of optical samples of the types flown in the OEM is sensitive to temperature, the relatively restricted range of thermal variations monitored in the three flights minimized thermal effects. Recorded temperatures at three separate locations on and within the OEM indicated that the instrumental thermal design limits (0° to 70°C) were not exceeded on any of the missions. The thermal profiles for the OEM housing (and for the Passive Sample Array, for comparison), shown in Figure VI-2, are typical of all three missions. There were no temperature sensors directly on the optical samples. The thermal inertia of the more massive structures sensed by the OEM temperature probes (housing, lamp, stepping motor) results in a slower response time than for the samples. However, as previously stated, the measured changes in optical transmittance in orbit were usually small and within the range of uncertainty, so that correlation with temperature is not possible. In cases when the optical variations were significant, associated thermal variations failed to correlate in a consistent manner. Thus, thermal effects were not a significant factor in the OEM data.

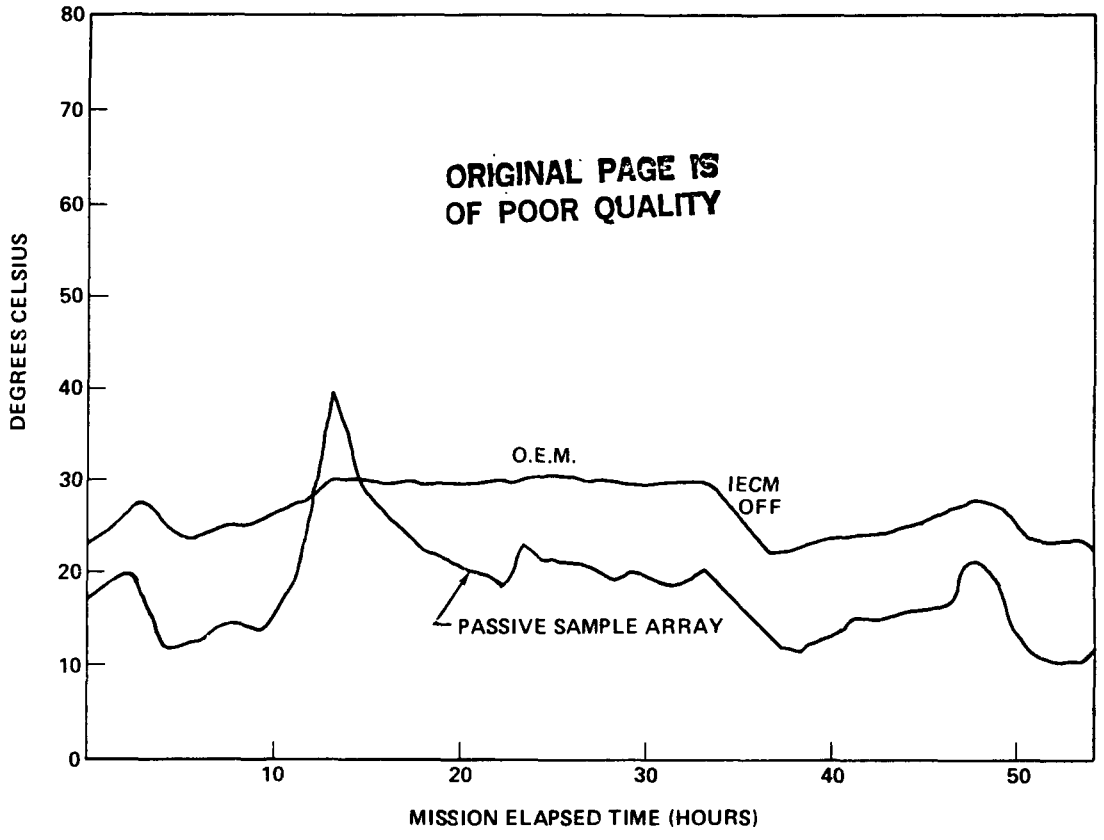

Figure VI-2. IECM flight STS-2 Optical Effects Module and Passive Sample Array housing temperature versus time

SCATTER DATA

The scatter data from the OEM result from light diffusely reflected (scattered) onto an optical element that focuses the integrated-scattered signal to a second photomultiplier sensor (Fig. VI-1). This scatter sensor is not calibrated in flight, as is the transmission sensor, and as such is subject to greater uncertainty.

The gain of the scatter sensor was set higher than that for the transmission sensor by a factor of ten to enable detection of expectedly low signals. The uncertainty associated with OEM scatter measurements is about ±2 percent absolute.

The detected scatter signal was normalized with respect to the unobstructed transmitted source light signal (Io) to reduce the effect of source variations in the scatter signal. By the nature of the measurement, increases in the scattered light intensity would result from either an increased number of particulates on a sample, source intensity increase, or detector drift.

The level of detected scattered light from samples of the OEM was about 1 to 3 percent of the incident light, nearly the same level as the scatter mode uncertainty, indicating that the particle accumulation during the flight was probably not significant. Postflight particle distribution analysis on the OEM samples agrees with this conclusion. There is inherent inaccuracy associated with the OEM method of monitoring scatter, including loss of signal by absorption, etc., in the refocusing optical element and incomplete geometry of collection.

The size of the OEM incident light-beam was approximately 1 cm^2. The decrease in transmitted light of an optical sample due to the presence of a particulate distribution corresponding to a Level 300 surface has been estimated to be 1 to 3 percent of the incident light intensity. The magnitude of scatter signal from the OEM, considering the uncertainty in the measurement, provides no significant evidence of a particulate accumulation on samples exposed to the Shuttle cargo bay environment greater than the Level 300 design criteria. Variations of the scattered light intensity (as measured) during the missions are generally on the order of the associated measurement uncertainty.

The general trend of the OEM scatter measurements on, for example STS-4, indicates a decreasing parameter (Fig. VI-3). Of course, by the nature of the measurements, the effect of an accumulation of particulate contamination would more likely result in an increase of the scattered light signal. In these data, when the factor of ten gain increase is accounted for, the low magnitude of the detected signal provides an indication that the particulate contamination remained at about the minimally detectable level, a level previously estimated to correspond to a Level 300 surface distribution. Considering the associated measurement uncertainty and the absence of an inflight calibration, there may have been (and probably were) particles deposited whose effects were not detected by the OEM scatter sensor. The post-flight evaluation of the particulate distributions on OEM samples, by independent means, provides no contradictory evidence to dispute conclusions of the flight data analysis.

OEM data indicates that, with proper shuttering of payloads with optical components, the design limit of a Level 300 surface for particulate contamination is reasonable and achievable.

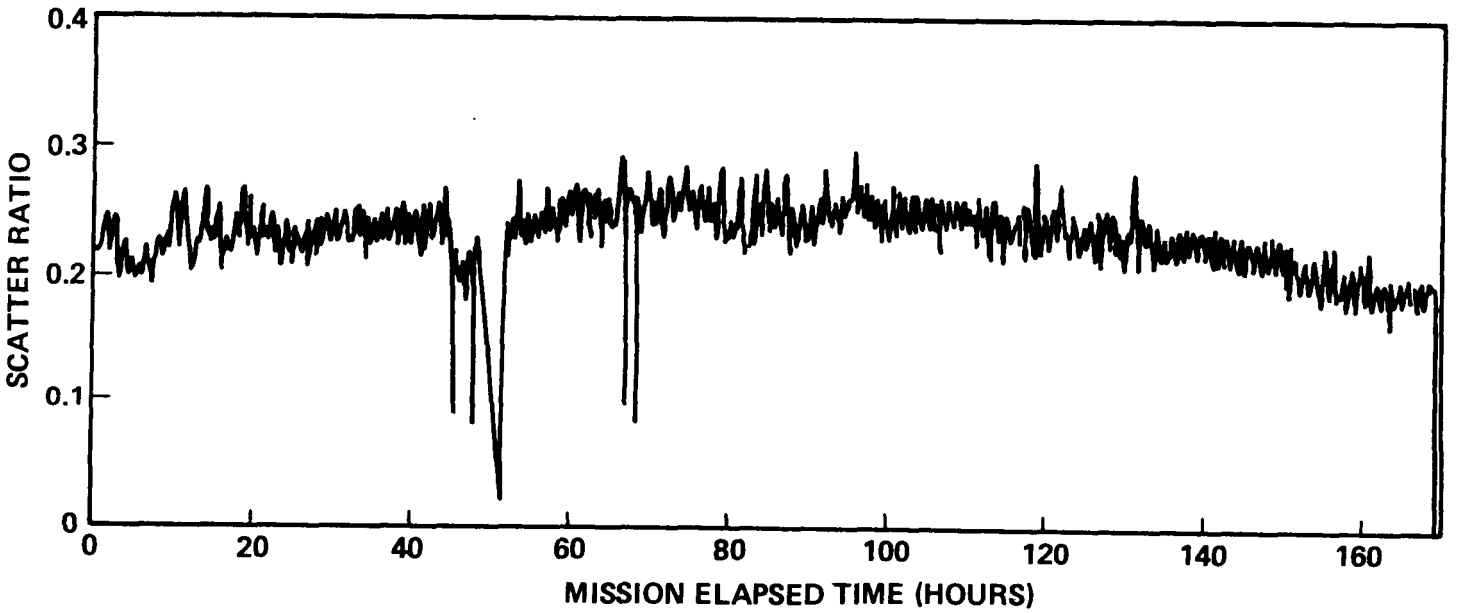

Figure VI-3. IECM flight STS-4, Optical Effects Module, channel 2 scatter ratio versus time.

PASSIVE SAMPLE ARRAY

The Passive Sample Array (PSA) was designed to accommodate a wide variety of materials (primarily optical) for exposure as witness samples. The purpose was to facilitate the extended analysis of the effects of the natural and induced environments of the Shuttle cargo bay. Each flight unit consists

of eight individually removable trays of six samples each mounted to the upper (-Z) surface of the IECM, in the Shuttle X-Y plane (Fig. II-1). Samples were exposed throughout the ascent, orbit, and descent mission phases as well as during the ferry-flight back to KSC.

After each orbital mission, prior to the ferry-flight of the Shuttle back to KSC, an additional tray of six witness samples was mounted in the cargo bay (X_O = 750) at the landing site.[1] The exposure of separate samples during the ferry-flight provided a means of estimating, and therefore differentiating, the contributions of the ferry-flight environment on the condition of samples exposed through the entire mission.

In an attempt to expose as wide a variety of materials as possible to the cargo bay environment, the contents of the PSA flight units were varied for each mission. Each array basically consisted of 42 optical samples, 2 IR absorption analysis crystals (KRS-5), and a number (4 to 8) of "electrets" (see Appendix VI-B). For each of the three Shuttle missions, two of the eight PSA trays (the ones containing the KRS-5 crystals) were supplied as guest experimenter hardware.[2] For the STS-4 mission, two modified PSA trays containing mylar, teflon, and Kapton film specimens were included as guest experimenter hardware.[3] No results for these guest samples are included in this report.

This diversity of optical materials flown as components of the PSA on the three missions can be determined from inspection of the summary listing of Table IV-5. Samples of the guest experimenter trays are excluded from this listing. The detailed specifications for the samples of each of the PSA flight units for STS-2, -3, and -4 are included with this report as Appendix VI-A. Most of these samples were selected as representative of optical coatings and windows used, or projected to be used, in the environment of space.

TABLE VI-5. PASSIVE SAMPLE ARRAY COMPOSITE LISTING FOR STS-2, STS-3, AND STS-4 (MSFC SAMPLES)

Material	Symbol (see Appendix VI-A)	Number Flown
Mirrors:		
Aluminum: Magnesium Fluoride overcoat	MgF_2/Al	24
Gold	Au	21
Platinum	Pt	10
Osmium	Os	3
Silver	Ag	1
Carbon	C	2
Vacuum Ultraviolet Filters	VUV	4
Zinc Telluride	ZnTc	1
Windows:		
Calcium Fluoride	CaF_2	3
Lithium Fluoride	LiF	1
Barium Fluoride	BaF	2
Quartz/Fused Silica	FuSi	11
Pyrex	Pyrex	1
Miscellaneous:		
Stainless Steel	SS	2
Electrets	e	20

1. For STS-2 and -4, the site was Dryden Flight Research Center; while for STS-3, the site was the White Sands Test Facility.
2. Investigator: E. N. Borson, The Aerospace Corporation, El Segundo, California.
3. Investigators: Lubert Leger and Steve Jacobs, JSC/NASA.

Contamination in the Ground-Handling Environment

Each of the eight trays in a flight configuration PSA is separately and conveniently removable. Thus, a measure of the contamination effects due to the ground-handling environment of the Shuttle was available by exposure and replacement of designated sample trays. Flight samples were not installed in the PSA until the last scheduled access to the IECM for each mission. The direct exposure of optical samples in the ground-handling or flight environment of the Shuttle is, of course, a more severe exposure than would likely occur for most payloads and components protected by detachable or movable covers, so that these results are intentionally "worst case" conditions.

For STS-2 and -3, the ground-handling environment sampling at KSC by the PSA was limited to trays exposed to the IECM activity phase in the Orbiter Processing Facility (OPF). For STS-4, exposure and replacement of trays throughout the IECM ground-handling activity phases provided a measure of the contamination to be expected in the OPF, the pad-transfer phase, and on the pad. Contaminants associated with the ground-handling environment of the Shuttle cargo bay were primarily found to be particulate in nature, as in dust, fibers, and flakes. The outgassing and subsequent deposition of molecular species is a contamination hazard more likely to be limited to lower pressure environments, as in space or vacuum testing facilities. The average measured change in reflectance or transmittance for samples exposed to the preflight KSC environment was generally found limited in magnitude to values within the range of measurement uncertainty (±2 percent) as shown in Figure VI-4. Most of the optical change for preflight exposed samples was measured as a decrease (degradation). Calculations based on the actual distribution of particles found on these samples predict a magnitude of change about equal to the 0 to 2 percent level indicated by measurements.

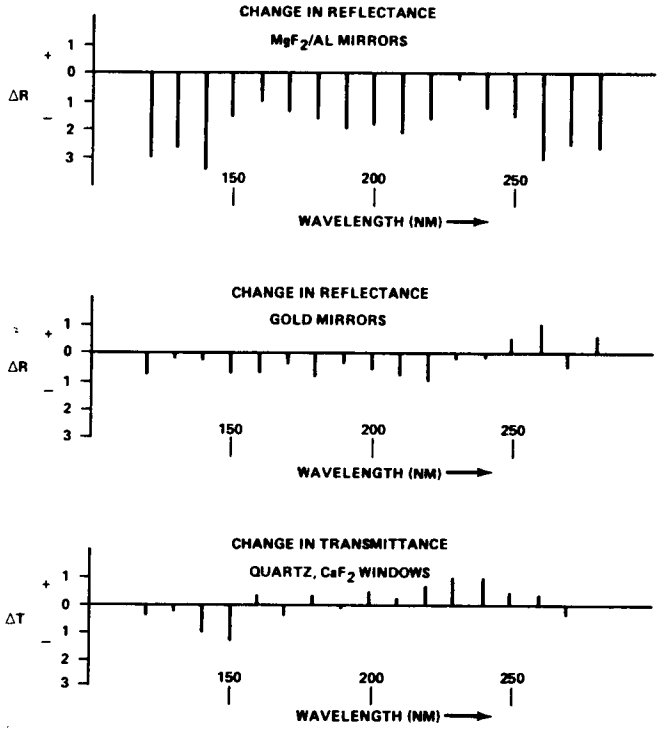

Figure VI-4. IECM/Passive Sample Array average optical effects of exposure in Orbiter Processing Facility at KSC.

Samples exposed to the OPF environment were visibly contaminated with dust and fibers (Fig. VI-5). The quantity and size distribution of particulates on these samples were measured with an imaging Bausch and Lomb Omnicon Automatic System by Mr. W. K. Witherow, MSFC. The basic contamination specification relevant to these measurements is the requirement that particulates on optical surfaces not exceed Mil Standard 1246A, Level 300. The defined particulate distribution corresponding to a Level 300 surface, and the data for a comparison of PSA samples exposed to the OPF during preflight activities for STS-2, -3, and -4, is shown in Figure VI-6. Table VI-6 is a summary of the average total particle counts of samples exposed for the three missions in the OPF and other phases of preflight activity. The decrease in particulates measured for STS-3 is attributed to a systematic clean-up and operating procedure revisions subsequent to the end of activities in the OPF for STS-2. The indicated shorter stay of Columbia in the OPF for STS-4 contributed, as expected, to less accumulation.

Additional details of the results for samples exposed during KSC preflight activities will be discussed later in this report, in conjunction with the results for samples exposed during the flight missions.

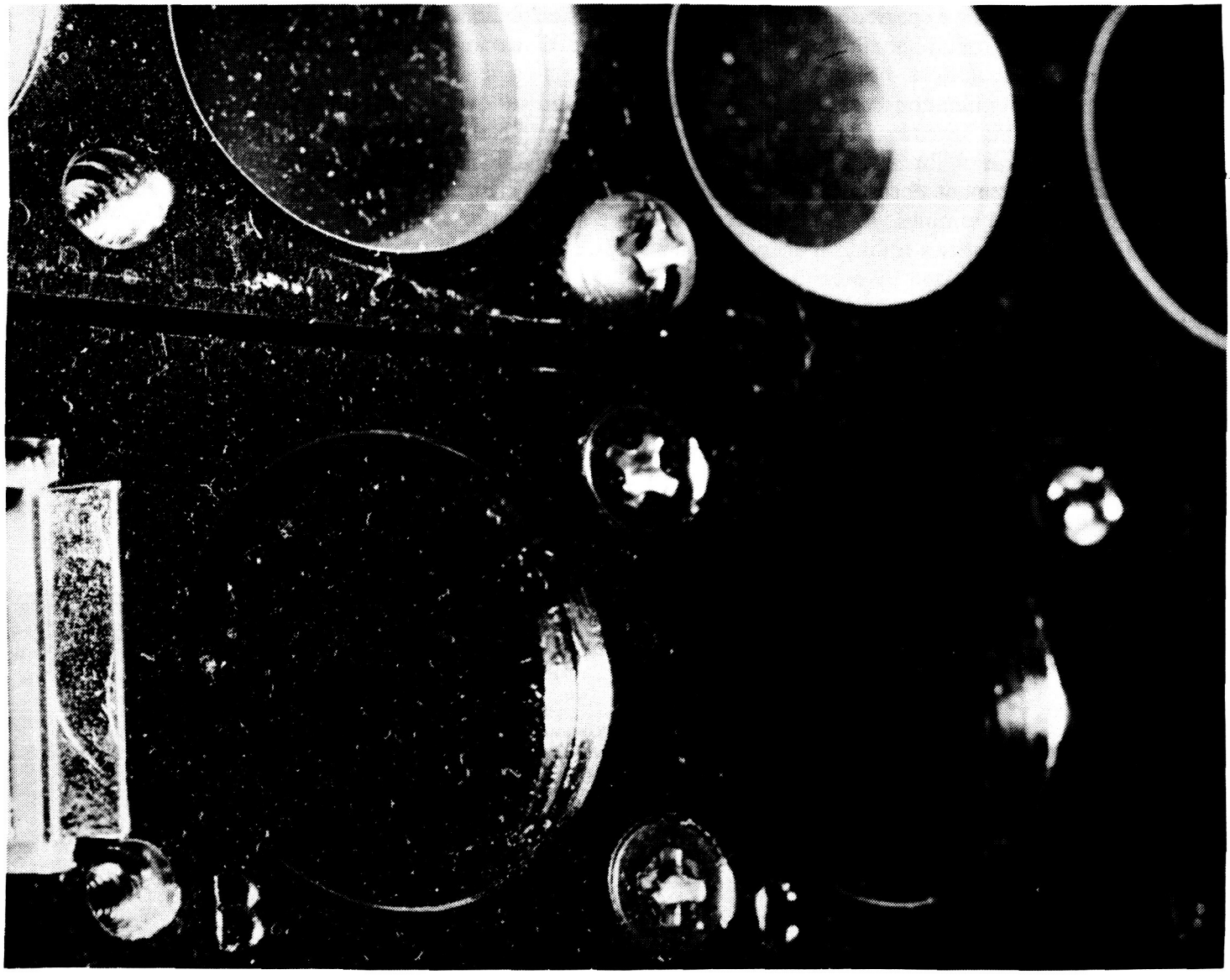

Figure VI-5. Dust and fiber contamination of sample exposed to OPF environment.

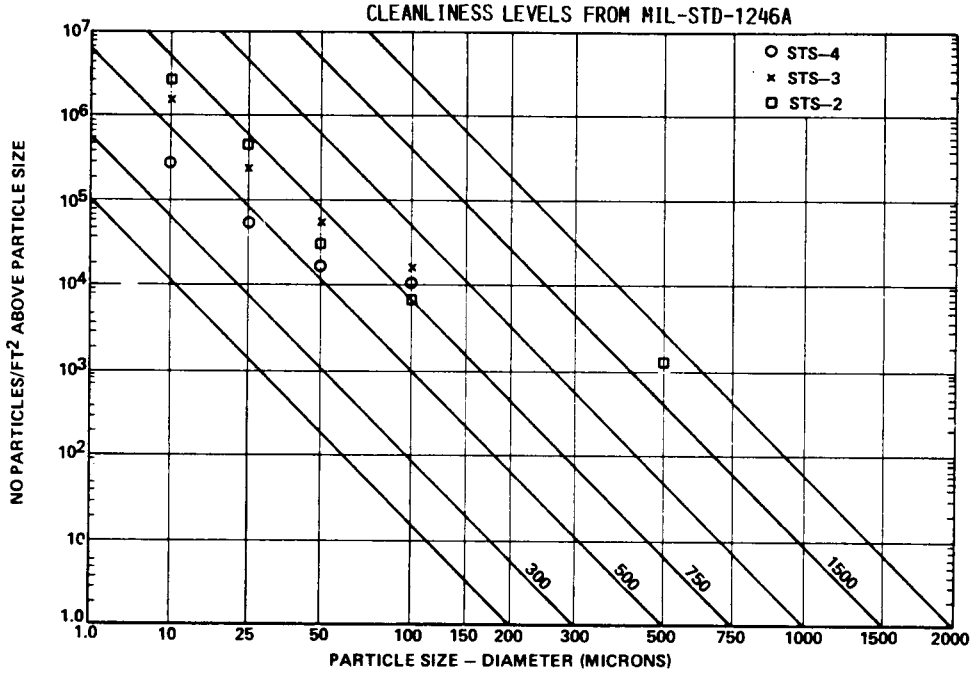

Figure VI-6. Passive Sample Array: particle size distributions for STS-2, -3, and -4, KSC operations results (Orbiter Processing Facility).

TABLE VI-6. IECM OPTICAL MEASUREMENTS, PASSIVE SAMPLE ARRAY

Contamination Specification:	Averaged Pre-Flight Exposure Results
Particle Density – Optical Surfaces $\leqslant$ Level 300 Orbiter Processing Facility (OPF) at KSC subjected to clean-up following roll-out of STS-2. During OPF operations, samples and instruments of the IECM designated for flight were protected by covers until final access prior to roll-out.	STS-2 19 days exposure: OPF $\rho = 1.4 \times 10^4$ particles/cm^2 Level 750 to 1500 STS-3 19 days exposure: OPF ρ - 6.5×10^3 particles/cm^2 Level 500 to 1500 STS-4 5 days exposure: OPF $\rho = 1.3 \times 10^3$/cm^2 Level 500 to 750 In-transit OPF-PCR (26 days) $\rho = 6.7 \times 10^2$/cm^2 Level 200 to 500 16 days exposure in PCR $\rho = 5 \times 10^2$/cm^2 Level 300 to 750 Samples exposed from first access OPF to last access PCR $\rho = 2.7 \times 10^3$/cm^2 Level 500 to 750

For each Shuttle flight, the optical properties of samples exposed to the entire flight mission, samples exposed only during the ferry-flight, and control samples were measured in a spectral region extending from the vacuum ultraviolet (120 nm) through the near infrared (2500 nm). From 120 to 290 nm, specular, spectral reflectance, and transmittance were measured at near-normal incidence. At longer wavelengths, an integrating sphere facility measuring both integrated diffuse reflectance and transmittance was utilized. For each sample, measurements were performed prior to installation in the PSA and repeated in an identical manner after the mission for comparison.

The results indicate an average change in optical properties due to exposure to the flight environment of approximately ±2 percent. For those samples with a measurable decrease in optical properties, the degradation could be attributed solely to the effects of deposited particles. The decrease in reflectance or transmittance due to absorption or scatter by deposited particles has been estimated to range from 0 to 3 percent for the particulate distributions observed. However, since the measurement uncertainty was approximately ±2 percent, these data may only indicate that the effects of exposure were minimal and perhaps not measurable in magnitude. Typical results for vacuum UV measurements of specular reflectance and transmittance, for STS-4, are shown in Figure VI-7.

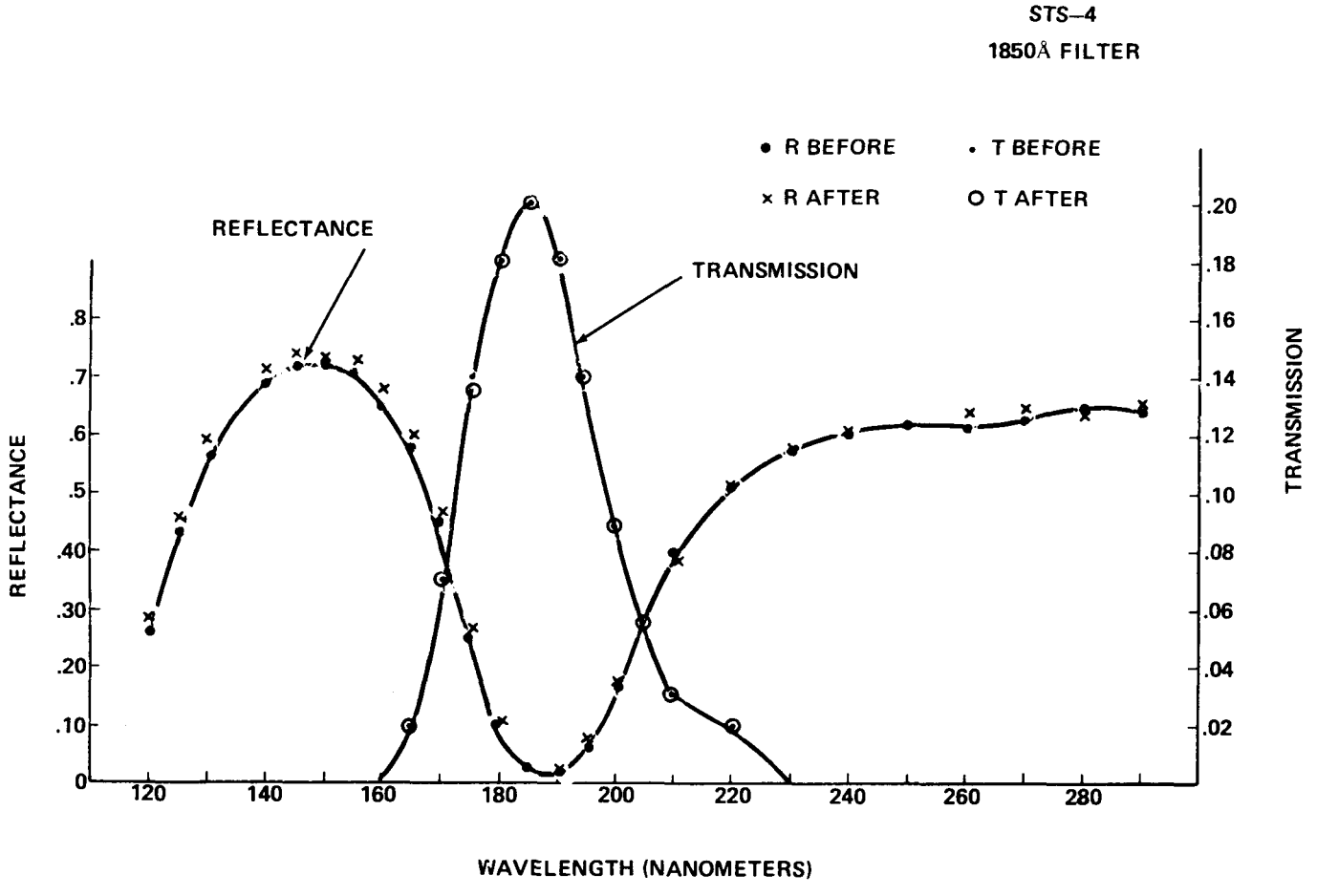

Figure VI-7. Vacuum UV measurements of specular reflectance and transmittance for STS-4.

For each flight there were, of course, a few samples whose measured optical change at a few isolated, apparently random, wavelengths exceeded the average range. No pattern was identified in the data for the samples, and the conclusion is that the data extremes probably represent random measurement error.

Previous reports [VI-1,VI-2] have included the results of optical measurements of samples exposed on STS-2 and -3. Results for four of the major types of samples included in the PSA for STS-4 are shown in Figure VI-8. The mechanism leading to the systematic increases in reflectance of the gold, platinum, and transmissive samples in the vacuum UV, as opposed to the mostly unaffected MgF_2/Al mirrors, has not been identified. The effect, though, is probably real and not a case of instrumental error, for measurements of the control samples indicate no comparable changes, and the measurements with the independent integrating sphere facility indicate similar effects, including, for example, the disparity in effects for gold mirrors compared to the aluminum mirrors. The increases may be due to volatilization in space of trace contaminants undetected in preflight measurements, or the effect may reflect interaction of the ambient environment with either trace contaminants or the mirror coatings themselves.

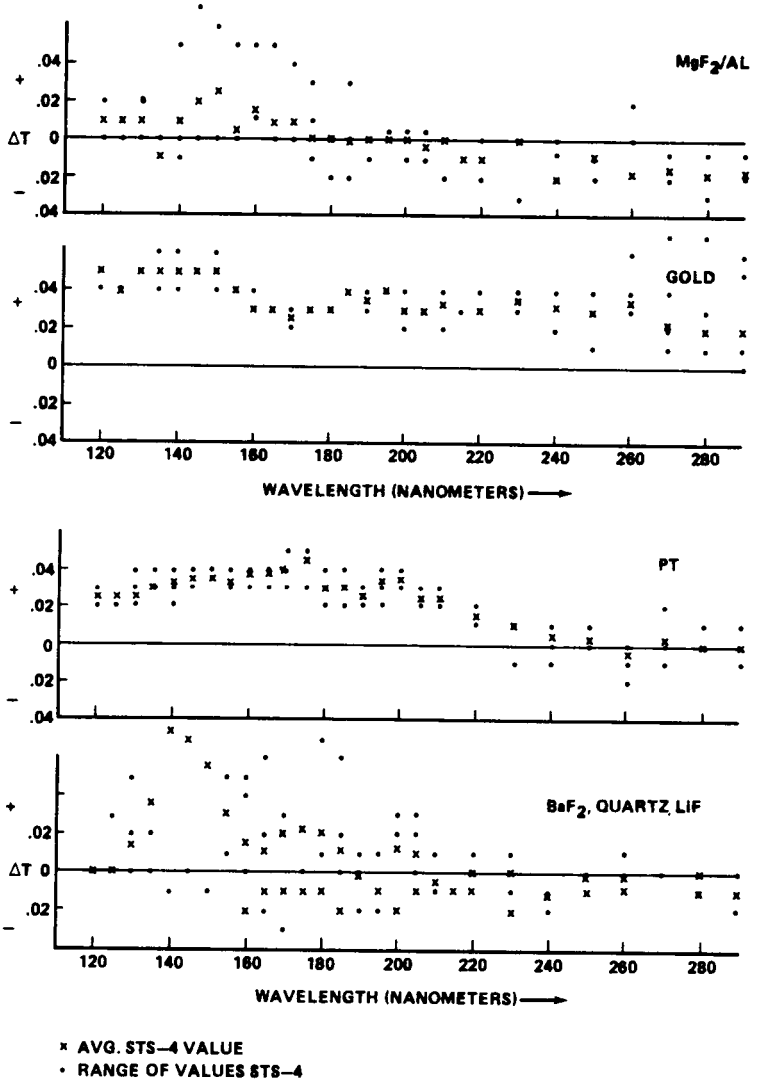

Figure VI-8. Passive Sample Array, STS-4 optical properties of exposed samples.

Combining the results of similar types of samples for all three flight missions, the average results (Table VI-4) are obtained. Since the range of uncertainty for these measurements is about ±2 percent, the effects of exposure are minimal, if not undetectable, in magnitude.

These data include the effects of exposure to the ferry-flight as well as the orbital environment, due to the enforced inaccessibility of the PSA at the landing site. The optical effects of exposure to the ferry-flight, however, are equivalent or less in magnitude to the total mission results; thus, the optical effects of exposure to the Shuttle cargo bay environment are minimal.

The flight samples and the ferry-flight samples were visibly contaminated with particles and fibers, though much less so, even visibly, than for samples exposed to preflight activities at KSC. The accumulation of particulate contamination on samples of the passive sample array was similar in quantity and size distribution on the three Shuttle missions. Averaged results for these three missions, for particles less than 30 microns diameter, are given in Figure VI-9. From these data it can be seen that a large proportion of the particles observed postflight on PSA samples were deposited during the postflight ferry-flight phase of the mission, and not during time in orbit.

The area of each sample (MSFC) in the PSA was 5.1 cm^2 (1 in. diameter); to compare the particle distribution data directly with Mil Standard 1246A, the results (particles/cm^2) were converted to particles/ft^2. Figures VI-10 and VI-11 are intended to show how the measured particles distributions relate to the various defined product cleanliness levels. Results for larger particle sizes are not included in these figures; in many cases the number of larger size (> 100 μm diameter) counted on ferry-flight samples exceeded the number counted for corresponding sizes on samples exposed to the entire mission. Of course, the POSA unit mounted in the Shuttle cargo bay for the ferry-flight was positioned forward of the IECM, in an environment that no doubt saw some differences in exposure.

Total particle counts for each of the three missions are summarized in Table VI-7.

Measurements of reflectance and transmittance were extended through the near-infrared by means of an integrating sphere attachment to a DK-2 spectrophotometer (250 to 2500 nm). These measurements were performed before and after each flight mission for a determination of the degradation caused by contamination. In general, the postflight measurements of both diffuse reflectance and transmittance in the range 0.25 to 2.5 μm were barely distinguishable from the preflight measurements. While unforeseen instrumental anomalies invalidated the STS-4 measurements at wavelengths greater than about 1 micron, typical results for two (STS-4) samples are included in Figure VI-12 to indicate the apparent increases in reflectance of gold mirrors as compared to MgF_2 overcoated aluminum mirrors. These measurements of diffuse reflectance agree within a small error margin with the specular data in the region of spectral over-lap, and most often agree with the results of the ultraviolet specular measurements indicating very little degradation of sample optical properties and, for a number of samples, small increases (improvements).

A number of the optical samples from each flight (including ones from the ferry-flight), and several control samples, were subjected to an elemental analysis using Auger spectroscopy.[4] The elements detected as contaminants were carbon, oxygen, and nitrogen, with traces of sulfur and chlorine. These elements were generally found on most of the samples submitted for Auger analysis, including the controls. It is probable from analysis of the Auger results that there were no molecular contaminant

4. Investigators: Palmer Peters, NASA/MSFC and Jack Swann, University of Alabama, Tuscaloosa.

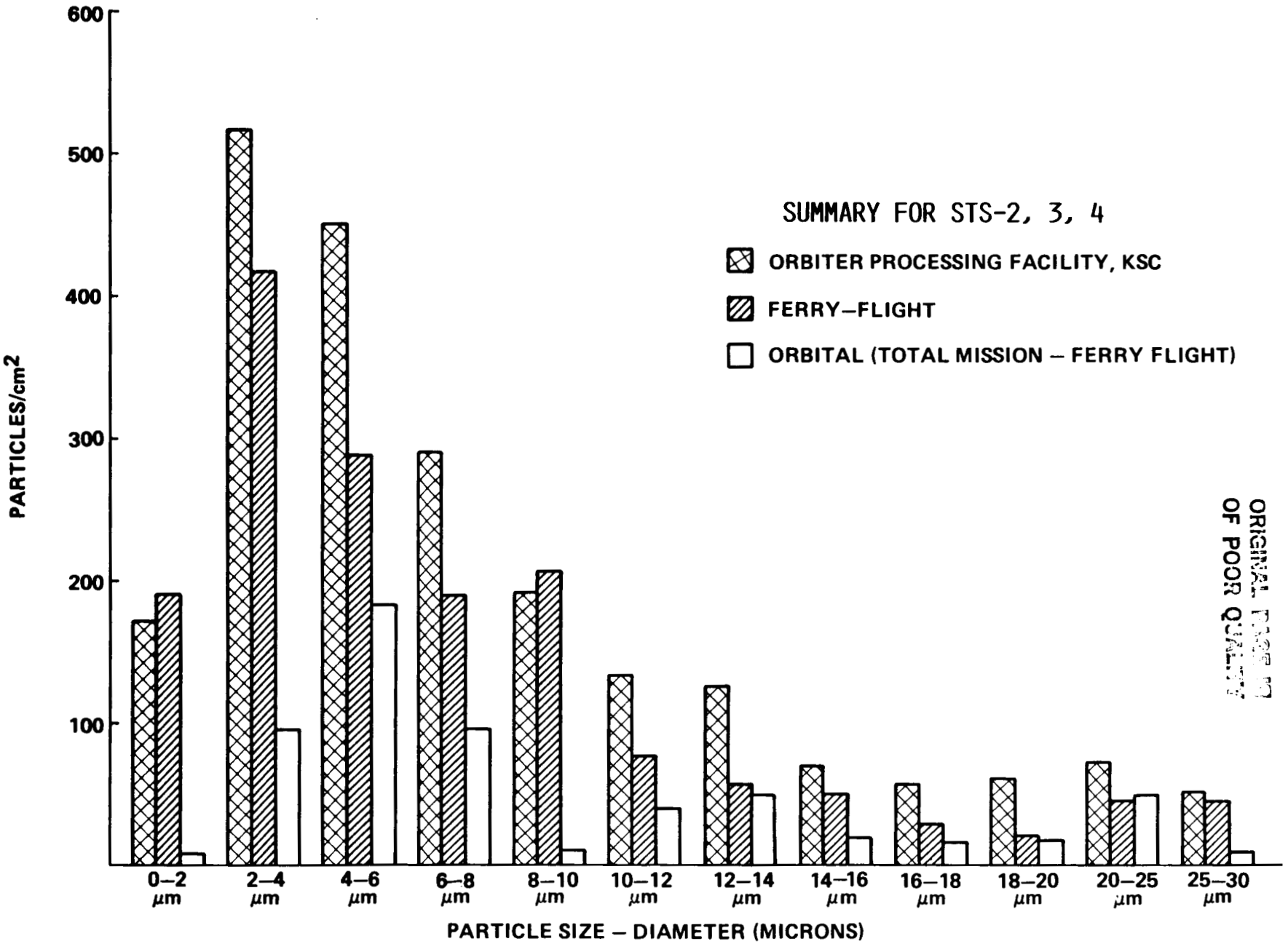

Figure VI-9. Passive Sample Array particle distributions.

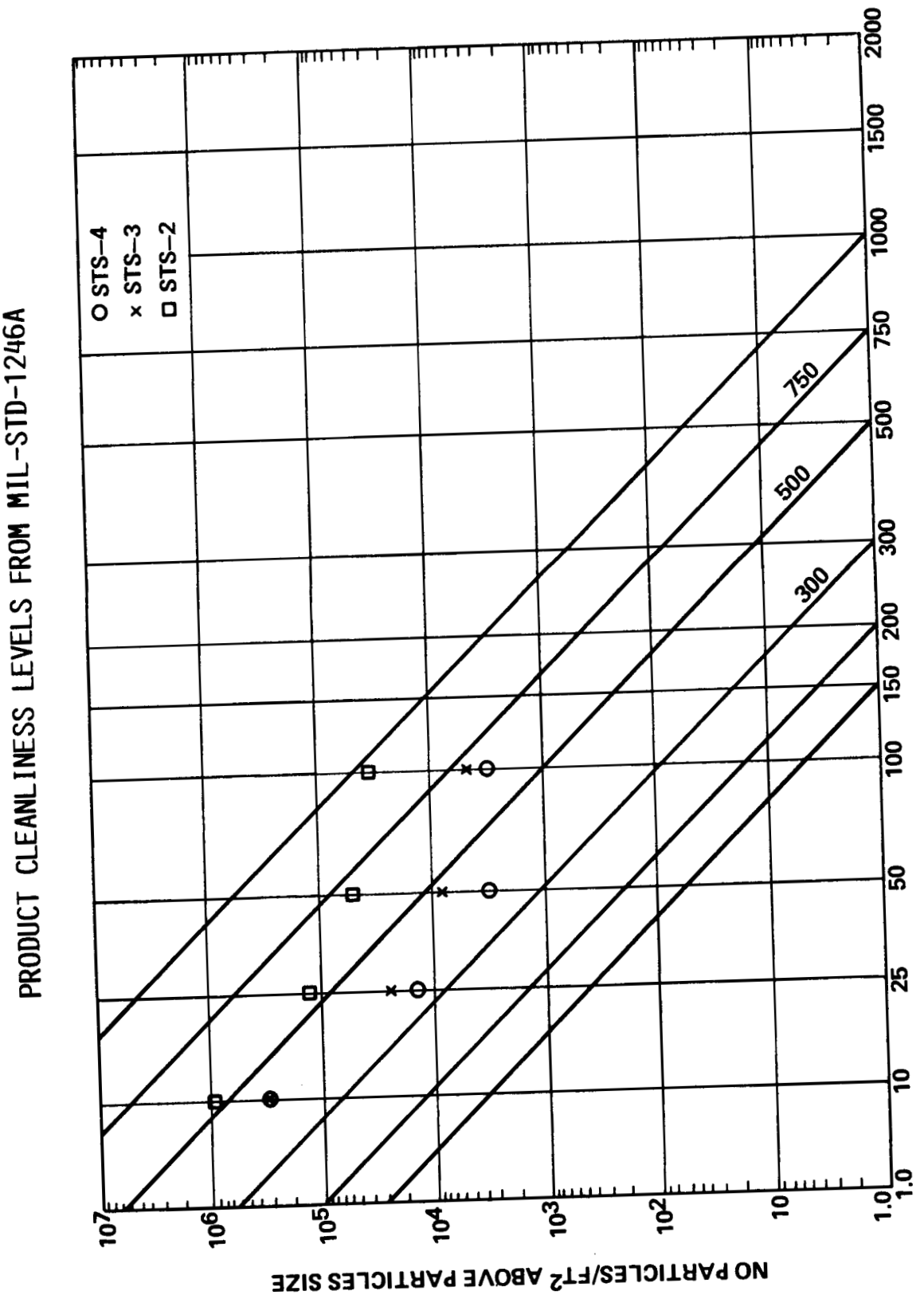

Figure VI-10. Passive Sample Array: average particle size distributions for STS-2, -3, and -4, orbital results (total mission – ferry-flight).

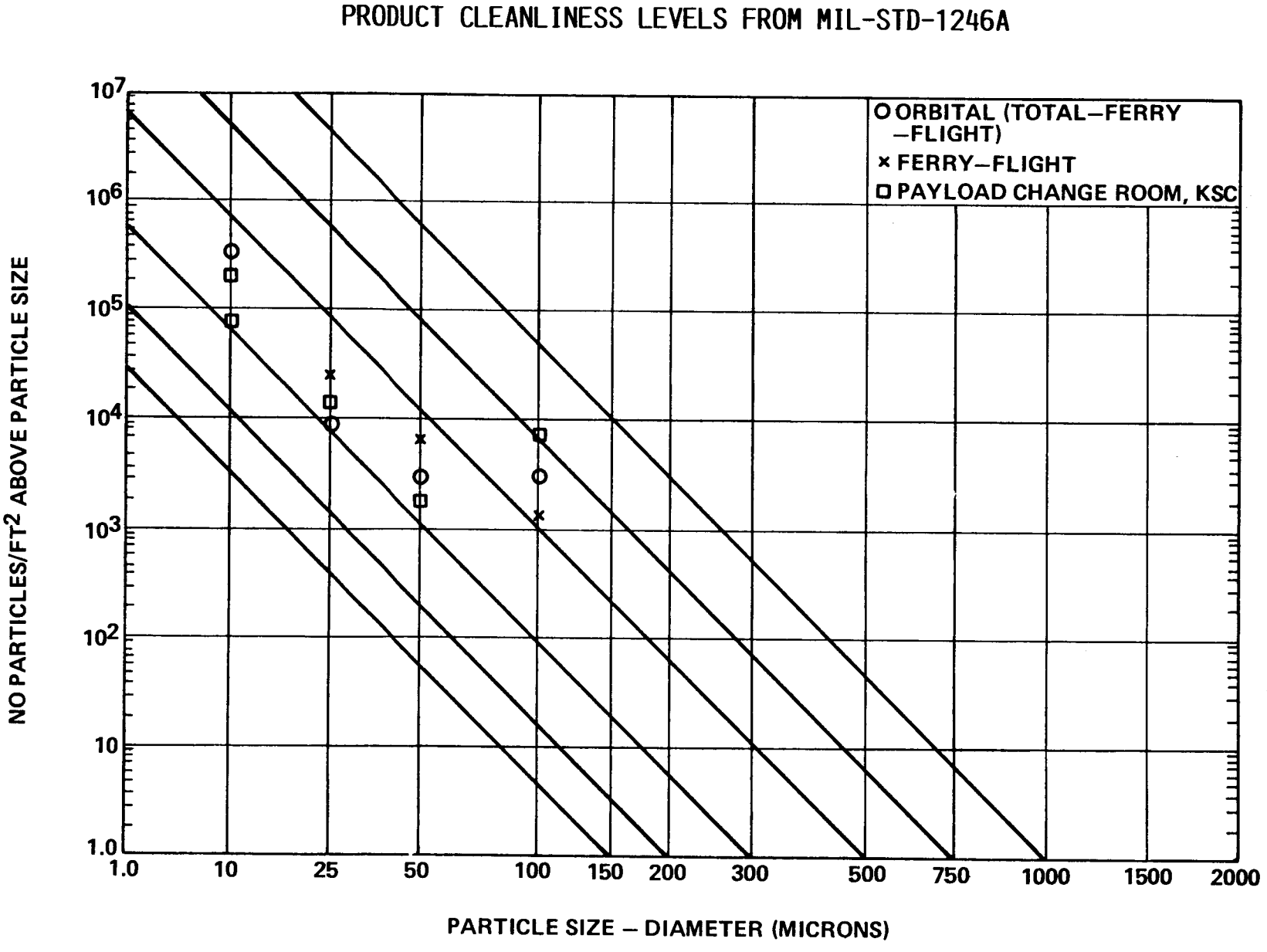

Figure VI-11. Passive Sample Array: particle size distributions for STS-4, combined mission operations.

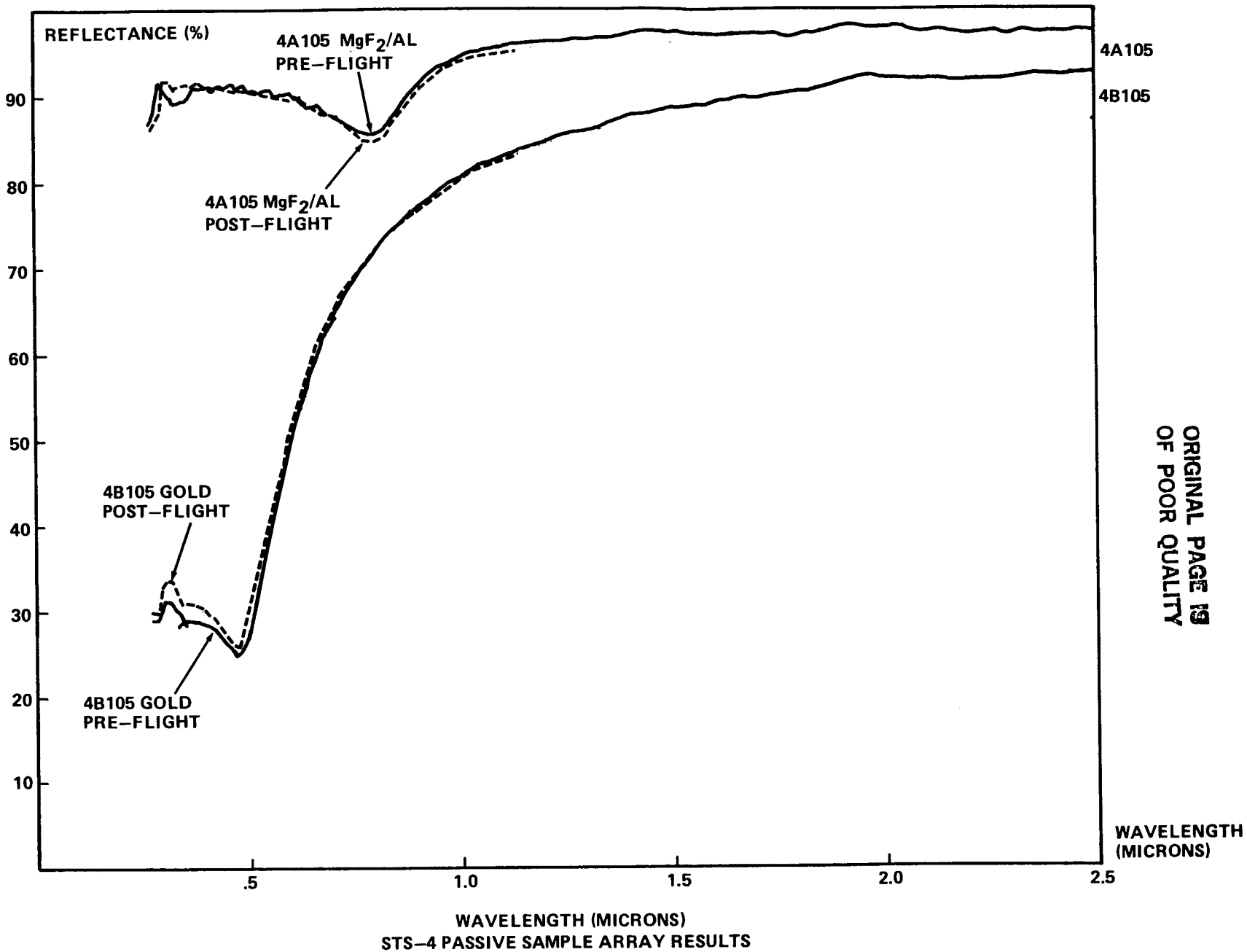

Figure VI-12. Diffuse reflectance.

TABLE VI-7. IECM OPTICAL MEASUREMENTS, PASSIVE SAMPLE ARRAY, FLIGHT MISSION RESULTS FOR STS-2, -3, AND -4

Contamination Specification:	Averaged Flight Mission Results
Particle Density – Optical Surfaces $\leqslant$ Level 300 Measurements performed with Omnicon optical imaging particle counting facility. Results shown indicate difference in levels measured on samples exposed to entire mission versus levels on samples exposed only on ferry-flight.	STS-1 $\rho = 1.7 \times 10^3$ particles/cm^2 Level 300 to 500 STS-2 $\rho = 3.8 \times 10^3$ particles/cm^2 Level 300 to 500 STS-3 $\rho = 2.7 \times 10^3$ particles/cm^2 Level 300 to 500 STS-4 $\rho = 0.5 \times 10^3$ particles/cm^2 Level 300 to 500

accumulations of monolayer thickness or more attributable to the Shuttle payload bay environment. Further examination of these samples with phase contrast microscopy and ion microprobe analysis using an electron microscope[5] revealed no significant evidence of any film contaminant layers.

The surface morphology of samples of each type included in the PSA for each of the three flight missions was studied with the aid of phase contrast microscopy and an electron microscope. Evidence of pitting, erosion, or any morphological change induced by the space environment was sought. No systematic evidence of any morphological change in any of the types of samples flown was observed. Isolated instances of minute surface abnormalities were as often found on the control as on the flight samples. The most significant features observable on any of these samples are the particles, fibers, and flakes deposited during the various mission phases, including prelaunch, flight, and ferry-flight.

ATOMIC OXYGEN EFFECTS

Effects of the orbital atomic oxygen in the Shuttle environment were first noted by Leger on the thermal control material Kapton [VI-3]. Such effects were first noted for PSA samples when the STS-3 postflight inspection of the two osmium mirrors included in the array revealed the disappearance of the osmium films. A similar osmium mirror was mounted in the subsequent PSA for the STS-4 mission; silver and carbon films on quartz substrates were also included on the basis of projected interactions

5. Scanning electron microscopy with energy dispersive spectroscopy performed by Ms. Alice Dorries, NASA/MSFC.

with atomic oxygen.[6] Postflight inspection of these samples revealed that the osmium and the carbon films had both disappeared, and that the opaque silver film (225 ± 5 nm) had been changed to a transparent blue-green interference film approximately 125 nm thicker than the original silver film. All of these effects were attributed to the interaction of these materials with the orbital atomic oxygen. Details of the observations, and results of the analyses of these samples have been separately published [VI-4].

CONCLUSIONS

From analysis of results from the OEM and the PSA, there is no significant evidence of molecular film deposition on the optical OEM samples, excepting only early mission self-contamination of OEM samples mounted near the OEM venting apertures. Most of the measured degradation of samples is probably due to the effects of adhering particles. Much of the particulate accumulation can be attributed to the postlanding ferry-flight environment.

The measured optical change of the samples exposed to the Shuttle cargo bay environment is generally small, limited in magnitude to levels comparable to or less than the associated levels of measurement uncertainty.

Orbital atomic oxygen effects were detected and analyzed on silver, carbon, and osmium mirrors. There was no systematic evidence of morphological change, such as erosion or pitting, observed on samples of the PSA or OEM.

In general, the optical effects of exposure to the Shuttle cargo bay environment were minimal in the measured spectral regions. With removable covers and coordinated shuttering of optical payloads, the applicable contamination design limits are achievable and realistic for Shuttle payloads.

6. At the suggestion of and cooperation of Dr. Palmer Peters, NASA/MSFC.

REFERENCES

VI-1. Miller, E. R. (Editor): STS-2 Induced Environment Contamination Monitor (IECM) – Quick-Look Report. NASA TM-82457, January 1982, pp. 30-48.

VI-2. Miller, E. R. and Fountain, J. A. (Editors): STS-3 Induced Environment Contamination Monitor (IECM) – Quick-Look Report. NASA TM-82489, June 1982, pp. 17-26.

VI-3. Leger, Lubert J.: Oxygen Atomic Reaction with Shuttle Materials at Orbital Altitudes. NASA TM-58246, 1982.

VI-4. Peters, P. N., Linton, R. C., and Miller, E. R.: Results of Apparent Atomic Oxygen Reactions on Ag, C, and Os Exposed During the Shuttle STS-4 Orbits. SSL Preprint No. 82-125, December 1982, submitted to Journal of Geophysical Research.

APPENDIX VI–A

STS-2 PASSIVE SAMPLE ARRAY

MSFC SAMPLE DIRECTORY

MIRROR
SUBSTRATES: Fused silica, 1.000" dia., 0.125 ± 0.010" thick, 1/4 wavelength flat, front surface polished – same for all mirrors unless otherwise specified.

Type	Symbol	Number in Array	Description
Aluminum: Magnesium Fluoride overcoat	MgF_2/Al	10	1000 (± 300) Angstroms Aluminum, overcoated with 250 (± 20) Anglstroms Magnesium Fluoride melles-griot.
Gold	Au	8	200 (± 25) Angstroms gold (purity: 99.999%), semi-transparent
Platinum	Pt	4	400 (± 50) Angstroms platinum (purity: 99.999%), opaque acton
Vacuum Ultraviolet Filter	2000 Åf.	1	Vacuum ultraviolet filter, peak wavelength 1850 Å, 260 Å bandwidth.
Vacuum Ultraviolet Filter	1400 Åf.	1	
WINDOWS:			
Calcium fluoride	CaF_2	1	25 mm dia., 3 mm thick.
Fused Silica	fusi	6	Mirror substrate, front surface polished 1/4 λ, flat: 1.000" dia., 0.125 (±0.010)" thick.
Stainless steel	SS	1	1 in. dia., 1/8 in. thick, 304 SS CRES, polished included for chemical analysis purposes.
Electrets	E	8	Teflon-Polytetrafluorethylene $(C_2F_4)_n$, sheets, in one (1) in. dia. annulus holder; electrets are thin sheets of teflon with a permanent surface polarization of charge.

PASSIVE SAMPLE ARRAY
SAMPLE LOCATION MATRIX

ARRAY 02 FOR STS-2 (SEE TEXT FOR EXPLANATION OF SYMBOLS)

GUEST SAMPLES						
P_T A	MgF_2/AL A	MgF_2/AL A	MgF_2/AL A	P_T A	MgF_2/AL A	P_T A
MgF_2/AL B	Au B	Au B	Au B	FUSI B	Au B	MgF_2/AL B
Au C	FUSI C	P_T C	CaF_2 C	2000A F. C	Au C	FUSI C
FUSI D	Au D	FUSI D	FUSI D	FUSI D	FUSI D	FUSI D
MgF_2/AL E	Au E	MgF_2/AL E	1400 A f. E	MgF_2/AL E	MgF_2/AL E	MgF_2/AL E
Au F	ELECT-RETS F	ELECT-RETS F	ELECT-RETS F	ELECT-RETS F	ELECT-RETS F	SS F
AEROSPACE SAMPLES						
COMP.						

STS-3 PASSIVE SAMPLE ARRAY

MSFC SAMPLE DIRECTORY

MIRROR
SUBSTRATES: Fused silica, 1.000" dia., 0.125 ± 0.010" thick, 1/4 wavelength flat, front surface polished – same for all mirrors unless otherwise specified.

Type	Symbol	Number in Array	Description
Aluminum: Magnesium Fluoride overcoat	MgF_2/Al	10	1000 (± 300) Angstroms Aluminum, overcoated with 250 (± 20) Angstroms Magnesium Fluoride.
Gold	Au	9	3: 200 (± 25) Angstroms gold (purity: 99.999%), semi-transparent 6: 600 (± 50) Angstroms gold, opaque
Platinum	Pt	2	400 (± 50) Angstroms platinum (purity: 99.999%), opaque acton
Osmium	Os	2	125 (+25/–0) Angstroms 99.999% purity osmium, semi-transparent.
Vacuum Ultraviolet Filter	1820 Å	1	Vacuum ultraviolet filter, peak wavelength 1850 Å, 260 Å bandwidth.
Zinc Telluride	$ZnTe_2$	1	120 Å thick, semi-transparent, compound semiconductor material
WINDOWS:			
Calcium fluoride	CaF_2	1	25 mm dia., 3 mm thick.
Barium fluoride	BaF_2	1	1/4 λ flat, UV transmissive calcium fluoride window same as above, except UV transmissive barium fluoride.
Fused Silica	fusi	6	Mirror substrate, front surface polished 1/4 λ, flat: 1.000" dia., 0.125 (±0.010)" thick.

Pyrex	pyrex	1	1 in. dia., 1/8 in. thick,
Electrets	E	8	Teflon-Polytetrafluorethylene $(C_2F_4)_n$, sheets, in one (1) in. dia. annulus holder; electrets are thin sheets of teflon with a permanent surface polarization of charge.

PASSIVE SAMPLE ARRAY
SAMPLE LOCATION MATRIX

ARRAY 03 FOR STS–3

(SEE TEXT FOR EXPLANATION OF SYMBOLS)

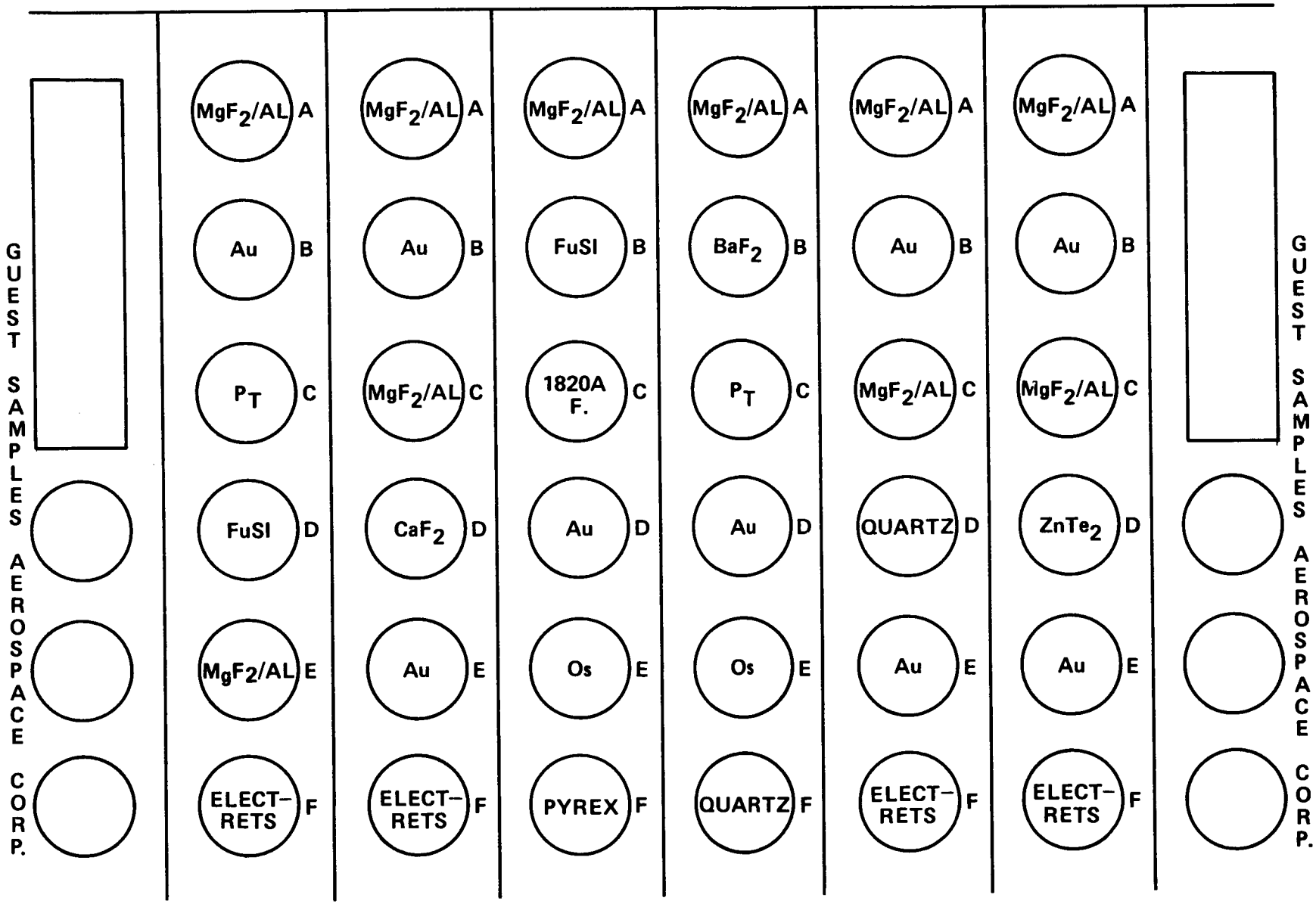

STS-4 PASSIVE SAMPLE ARRAY

MSFC SAMPLE DIRECTORY

MIRROR
SUBSTRATES: Fused silica, 1.000" dia., 0.125 ± 0.010" thick, 1/4 wavelength flat, front surface polished – same for all mirrors unless otherwise specified.

Type	Symbol	Number in Array	Description
Aluminum: Magnesium Fluoride overcoat	MgF_2/Al	4	1000 (± 300) Å Aluminum, overcoated with 250 (± 20) Å Magnesium fluoride
Gold	Au	4	200 (± 25) Å gold (purity: 99.999%), semi-transparent.
Platinum	Pt	4	400 (± 50) Å platinum (purity: 99.999%), opaque
Osmium	Os	1	125 (+25/-0) Å 99.999% purity osmium, semi-transparent.
Silver	Ag	1	2250 (± 50) Å 99.999% purity silver, opaque.
Carbon	C	2	100-300 Å carbon, one opaque, one translucent.
Vacuum Ultraviolet Filter	1850 Å	1	Vacuum ultraviolet filter, peak wavelength 1850 Å, 260 Å bandwidth.
WINDOWS:			
Calcium fluoride	CaF_2	1	25.4 mm dia., 3 mm thick, 1/4 λ flat, UV transmissive calcium fluoride window
Barium fluoride	BaF_2	1	Same as above, except UV transmissive barium fluoride.
Lithium fluoride	LiF	1	Same as above, except UV transmissive lithium fluoride.
Fused Silica	fusi	1	Mirror substrate, front surface polished 1/4 λ flat: 1.000" dia., 0.125 (+0.010/-0.000)" thick.
Stainless Steel	SS	1	1 in. dia., 1/8" thick, 304 SS CRES, polished; included for chemical analysis purposes.
Electrets	E	4	Teflon-Polytetrafluorethylene $(C_2F_4)_n$, sheets, in one (1) in. dia., annulus holder; electrets are thin sheets of teflon with a permanent surface polarization of charge.

PASSIVE SAMPLE ARRAY
SAMPLE LOCATION MATRIX

ARRAY 04 FOR STS–4 (SEE TEXT FOR EXPLANATION OF SYMBOLS

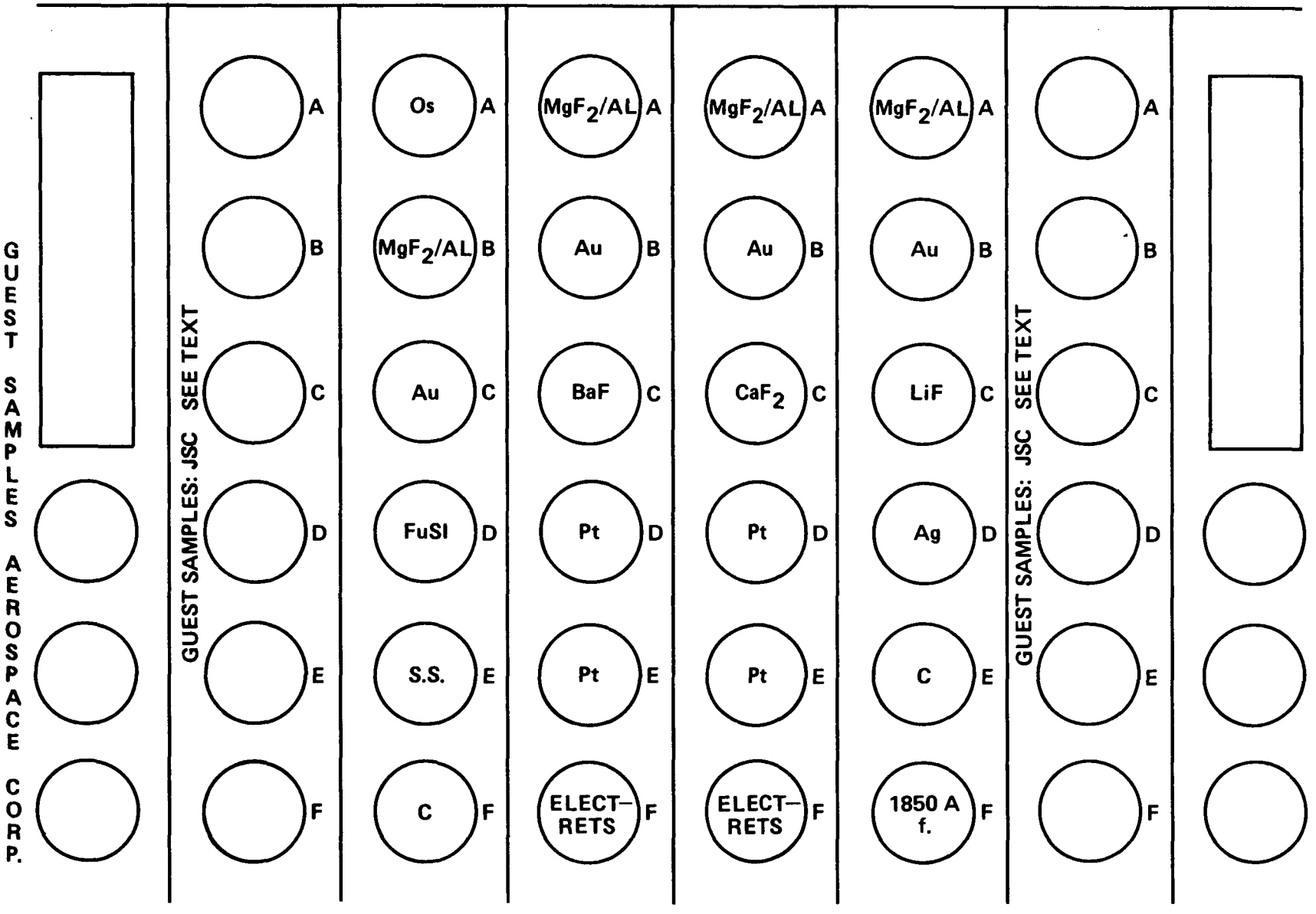

APPENDIX VI-B

ELECTRET RESULTS FROM THE PASSIVE SAMPLE ARRAY FOR STS-2, -3, AND -4

M. Susko

On each orbital and ferry-flight mission of the PSA, a number of samples (Table B-1) called "electrets" were included because of their enhanced attractive force for charged contaminant effluents. Electrets are teflon-polytetrafluorethylene $(C_2F_4)n$ dielectrics with a permanent surface polarization of charge (approximately 10^{-8} C/cm^2 density). X-ray Energy Dispersive Spectroscopy (XEDS) was used to analyze particles collected on the electrets (0.707–30 keV, ± 0.17 keV). The area scanned was approximately 0.45 cm^2 in the center of the electret. The results show the elemental abundance of an aggregate of particles on the electret surface.

The electrets were oriented normal to the Shuttle Z-axis (–Z) and down (+Z) for directionality analysis. In all cases, the negatively-polarized surface was exposed. For each detectable element, the postflight microprobe "counts" were subtracted from the preflight "counts." These values provide a means of estimating the relative increase in measured abundance of a given element detected on the electrets.

Table B-1 lists the averaged relative abundance of electret results for STS-2, -3, and -4. The difference of the total mission and ferry-flight values provides an estimate of the orbital contribution. There were ten electrets computed in the average for the orbital flights as compared to three for the ferry-flights.

Figure B-1 compares the particle size distribution of the average of the ten electrets in-cargo bay during the orbital flight for STS-2, -3, and -4 with the average of three electrets mounted in the cargo bay during the ferry-flight in the (–Z) orientation.

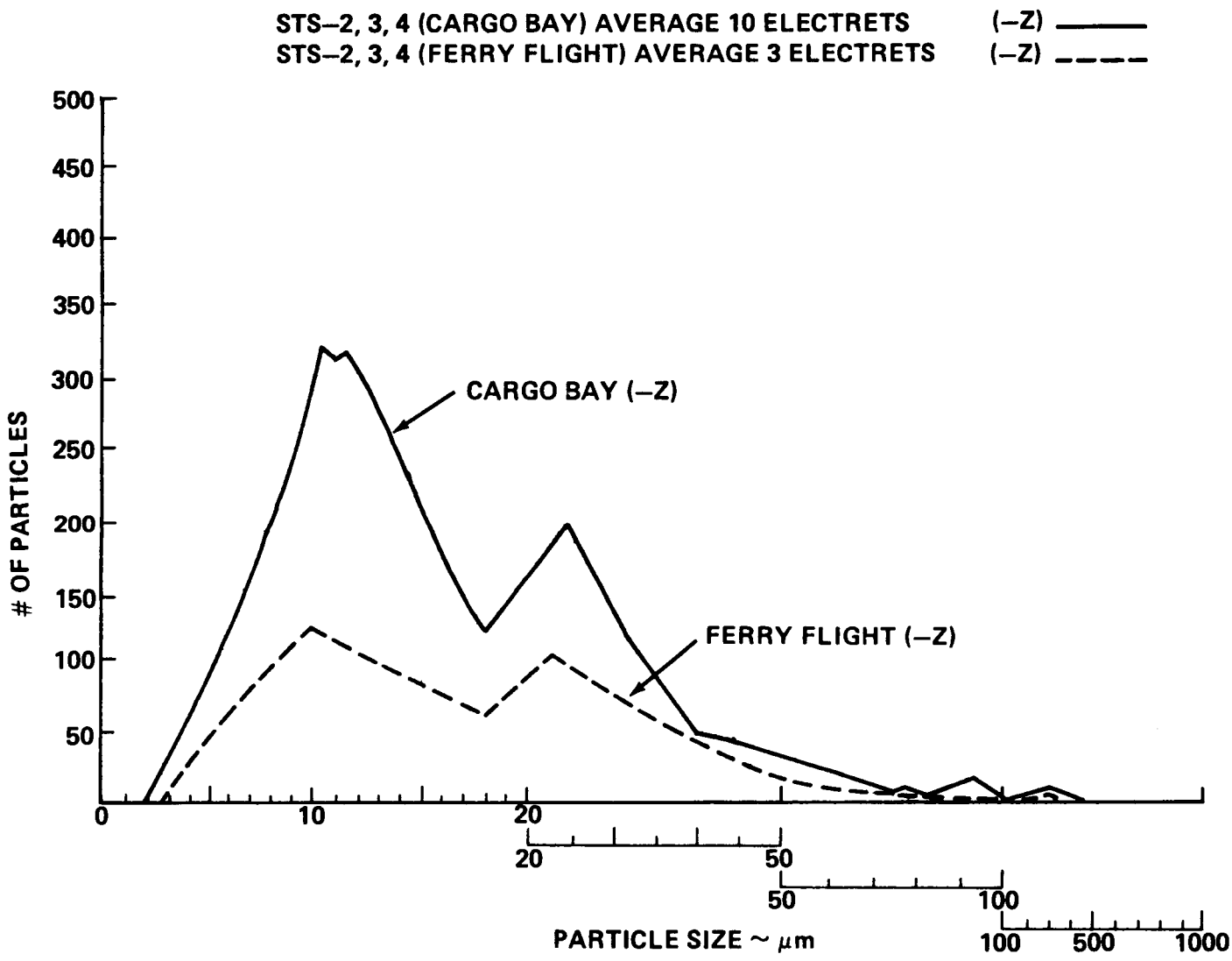

Figure B-1. Comparison of average of particle size distribution for 10 electrets in cargo bay (STS-2, -3, and -4) with average of 2 electrets from ferry-flight (STS-2, -3, and -4) for (-Z) orientation.

TABLE B-1. AVERAGE ELECTRETS RESULTS STS-2, -3, AND -4

RELATIVE ELEMENTAL ABUNDANCE INCREASE**				
ELEMENT	ELECTRET ORIENTATION (SHUTTLE Z–AXIS)	TOTAL MISSION AVERAGE (10 ELECTRETS) STS–2, 3, 4	FERRY–FLIGHT AVERAGE (3 ELECTRETS) STS–2, 3, 4	Δ = (MISSION –FERRY FLIGHT)
CHLORINE	(–Z)	80	0	80
	(+Z)	35	15	20
SILICON	(–Z)	350	165	185
	(+Z)	305	150	155
POTASSIUM	(–Z)	40	0	40
	(+Z)	30	15	15
CALCIUM	(–Z)	120	50	70
	(+Z)	30	40	*
ALUMINUM	(–Z)	90	350	*
	(+Z)	120	550	*
COPPER	(–Z)	15	5	10
	(+Z)	15	5	10
PHOSPHORUS	(–Z)	35	0	35
	(+Z)	35	0	35
SULPHUR	(–Z)	100	0	100
	(+Z)	40	375	*
CHROMIUM	(–Z)	45	20	25
	(+Z)	35	15	20
IRON	(–Z)	90	50	40
	(+Z)	65	90	*

**X–RAY MICROPROBE PROPORTIONAL COUNTS PER ELEMENT

*FERRY–FLIGHT PARTICLES EXCEED ORBITAL VALUES

VII. TEMPERATURE-CONTROLLED QUARTZ CRYSTAL MICROBALANCE AND CRYOGENIC QUARTZ CRYSTAL MICROBALANCE

J. A. Fountain

A. TEMPERATURE-CONTROLLED QUARTZ CRYSTAL MICROBALANCE (TQCM) MEASUREMENTS

The TQCM system measures condensible molecular deposition in the payload bay of the Space Shuttle Orbiter as a function of temperature, direction, and time [VII-1–VII-3]. The system consists of a controller and five sensors, one pointing in each of the Orbiter axes (except +Z) (Fig. II-1). Each sensor has approximately a 2 π sr field-of-view, and the +X, -X, +Y, and -Y sensors view both space and payload bay area about equally. The -Z sensor has almost a clear view of space. The temperature of each sensor is controlled by a thermoelectric device so molecular accumulation can be measured periodically at four pre-programmed temperature settings: +30°, 0°, -30°, and -60°C. The sensors also have a +80°C clean-up mode which is commanded between each measurement period. The signal outputs from the TQCM sensors are (1) a frequency which is proportional to mass accumulation per unit area at a sensitivity of 1.56×10^{-9} g cm^{-2} Hz^{-1}, and (2) the temperature of the sensor in degrees Celsius measured by a platinum-resistance thermometer.

The Shuttle flights are divided into three phases: ascent, orbital, and descent. The sensors are not controlled during ascent and descent but are allowed to seek ambient temperature. This is done as a power conservation measure, because the IECM is on battery power during these phases. During the orbital phase, the temperature control command program is implemented by the Data Acquisition and Control System (DACS). The command sequence was changed between each flight, and the differences are shown in Figure VII-1. Figure VII-1 shows that for STS-2 the +80°C clean-up periods were 30 min each, and the measurement periods were 120 min. For the second flight, the clean-up periods were shortened from 30 to 20 min, the +30° and 0°C measurement periods were shortened to 100 min, and the -30° and -60°C measurement periods were extended to 255 min. For the third flight, all measurement periods were made 255 min, with the first measurement being 0°C instead of +30°C. The command sequences were continuously repeated during the flights except for power interruptions and the scheduled remote arm deployment on STS-4. Whenever the power was interrupted for any reason, the command sequence recycled, so several partial cycles resulted.

Orbital Phase Measurements

Mass accumulation measurements made during the orbital phase represent the bulk of the data taken. Ascent and descent data will be discussed separately in the next section. Figures VII-2, VII-3, and VII-4 summarize the orbital data taken on the three flights. Each data point represents the net mass accumulation rate for the particular collection period. Refer to Figure VII-1 to determine whether a particular data point represents a 100-, 120-, or a 255-min collection period. The values are obtained in two ways. First, most are obtained by taking the difference between the frequency at the onset of mass accumulation (soon after the set temperature has been reached) and the frequency at the end of the collection period. This frequency difference is converted to mass and is divided by the number of minutes in the period, then multiplied by 60 to convert it to mass accumulation per hour. The second method to obtain a data point is used when the TQCM output shows a periodic nature such as in Figure VII-5 in which the above method would produce a meaningless value. In these cases, a peak-to-peak

value is obtained to show the mass accumulation rate during these periods. The value of 142 ng cm^{-2} hr^{-1} is the rate at which molecular mass is being retained from one orbit to the next. These net values are given as the best way to make comparisons between the different flights because of the different conditions during the flights, such as Orbiter attitude, whether the Orbiter is in daylight or shadow, etc. This method of data analysis averages over short-term contamination events. Two examples of short-term events will be given: Figure VII-5 shows the "worst case" example of diurnal variation in molecular deposition. The TQCM output shown from 133 hr, 42 min to 134 hr, 45 min MET is when the Orbiter was in a sunlit portion of the orbit during the bay-to Sun "hot soak" attitude. Mass accumulated at a rate of 1028 ng cm^{-2} hr^{-1} during this 63-min period. As shown, however, this contamination dissipated for the most part during the shadowed part of the orbit. Figure VII-6 shows an instantaneous increase in molecular mass measurement of 175 ng cm^{-2} in 1 min. This event has been identified with the test firing of a Primary Reaction Control System (PRCS) engine. The point to be made by Figures VII-5 and VII-6 is that there are numerous occurrences of short-term contamination events which are included in the net values which comprise this summary report. These events will be investigated individually and treated in future publications.

The net mass accumulation results from the STS-2 flight are given in Figure VII-2. The STS-2 orbital phase lasted 53 hr, and most of it was spent in the bay-to-Earth attitude. The most notable trend is the preponderance of accumulation measured in the +X axis. Since the IECM sits at the back of the payload bay, and the +X sensor looks forward over the bay, it is evident that most of the contamination is coming directly from the bay. The second-most amount comes from the +Y direction. While most of the values lie between 0 and 50 ng cm^{-2} hr^{-1}, higher values are seen early in the mission at +30° and –60°C, and some very low values and even negative values are seen at each temperature throughout the mission. Not shown on the graph are two large negative values at +30°C during the first cycle.

Figure VII-3 shows the results from the STS-3 flight. This flight saw many Orbiter attitude changes, of which only the major ones are indicated on the graph. The mission lasted 8 days, but an electronic malfunction resulted in no TQCM data being taken after 168.5 hr of Mission Elapsed Time (MET). This eliminated data from the final hours of the bay-to-Sun "hot soak" and the descent phase of the mission. Figure VII-3 shows clearly the trend of the preponderence of molecular flux coming from the +X axis, directly from the bay, as on STS-2. However, the second-most amount came from the –X direction which indicates offgassing from the aft bulkhead. The highest value measured was 174 ng cm^{-2} hr^{-1} from –X at –60°C at 136 hr MET which was during the "hot soak." A value of 106 ng cm^{-2} hr^{-1} was recorded from the +X axis sensor during this same time, while the +Y, –Y, and –Z sensors measured levels only slightly higher than in the nose-to-Sun attitude. This seems to indicate that during the "hot soak," molecular accumulation was a result of direct deposition, and that redirection by ambient atmospheric molecules played a less significant role. Again as on STS-2, mass accumulation rates for most of the mission were below 50 ng cm^{-2} hr^{-1}, and again some negative values were recorded.

The STS-4 mission lasted 7 days; and, as seen on Figure VII-4, was also characterized by many attitude changes. However, for the most part, the attitudes were benign thermally, and this is reflected in the data as shown. There is little evidence of directionality at +30° and 0°C; and, although it is clear that most of the molecular flux came from the aft direction on the –30° and –60°C plots, the magnitudes of the differences are quite small. This directionality seems to be due to a Freon 21 leak in the heat exchanger in the flash evaporator system in the aft section which was confirmed by the IECM Mass Spectrometer. During the gravity gradient attitude from 25 hr to 31 hr MET, two relatively high

values are seen: 115 and 86 ng cm^{-2} hr^{-1} from the +X and -X axes, respectively. The values from the -Z, -Y, and +Y axes at this time period remain at normal levels. Overall, on STS-4, the majority of fluxes measured were less than 25 ng cm^{-2} hr^{-1}, and many negative values was recorded.

Ascent and Descent Phases

The ascent and descent phases of the Shuttle flights represent quite different environments for TQCM measurements as opposed to the orbital phases. Ascent and descent are characterized by rapid changes in pressure from atmospheric pressure to orbital vacuum and back to atmospheric pressure, respectively. Also, the temperatures of the sensors during this period are not controlled. Therefore, it is a period of transient conditions which makes the data obtained not directly comparable to the orbital data. However, the TQCM sensors continued to operate during ascent and descent, and the data are presented.

The ascent phase for the TQCM's begins at lift-off (00 hr, 00 min MET) and continues until the on-orbit command is received from the DACS. For STS-2, -3, and -4, the ascent phase lasted for 36, 36, and 18 min, respectively.

Figure VII-7 shows a comparison of representative behavior of the +Y TQCM sensors during ascent. Table VII-1 summarizes all of the ascent data for the three flights. Mass accumulates on the sensors during ascent, and generally reaches a peak in less than 1 min. As orbital altitudes are reached and the vacuum level approaches the 10^{-5} torr region, the accumulated mass begins to dissipate and in most cases reaches a level which is below the original level.

The descent phase covers re-entry of the Orbiter through the Earth's atmosphere, landing, and postlanding. At the de-orbit command, the IECM switched from orbital operation to descent operation. For the TQCM's, this meant termination of the temperature control command sequence, causing the sensor crystals to seek ambient temperature. Figure VII-8 shows a representative plot of mass accumulation during the entire descent phase for the +Y axis sensors and their temperatures. On STS-2 the sensors were in the +80°C clean-up mode when the de-orbit command occurred. On STS-4, the sensors were at -30°C at de-orbit command. (As mentioned previously, no descent data were taken on STS-3.) Figure VII-8 shows that it takes about 15 min for the temperatures to settle out and become fairly stable. An increase in mass accumulation is seen at Orbiter landing with a slow rate of increase after landing until IECM power-down.

Table VII-2 gives a summary of descent data for STS-2 and STS-4 for all TQCM sensors referenced to a zero mass accumulation value which was chosen at the reference point when the temperatures had become relatively stable. As seen on Figure VII-8, this point for STS-2 was chosen at 16 min after de-orbit command (53 hr, 50 min MET). For STS-4, the point chosen was at 15 min after de-orbit command (168 hr, 45 min MET). The descent data as summarized in Table VII-2 shows that after near stable temperature conditions are reached, there is generally a mass accumulation on most sensors at low and sometimes negative levels. The largest value recorded over the 75-min collection period is the 413 ng cm^{-2} on the +X axis sensor on STS-4.

B. CRYOGENIC QUARTZ CRYSTAL MICROBALANCE (CQCM) MEASUREMENTS

The CQCM is a molecular contamination measuring device with quartz crystal microbalance sensors which are identical to the TQCM sensors except that they are not temperature controlled, but are radiatively cooled by a passive radiator system. The two -Z axis pointing sensors, -Z1 and -Z2, are thermally coupled to an array of second surface mirrors which have optical properties designed to reflect and radiate heat away. Thus, when the -Z axis of the Orbiter is pointed away from the Sun, such as in the tail-to-Sun or nose-to-Sun attitude for long periods of time, the sensors will reach cryogenic temperatures. The -Z2 sensor is designed to lag the -Z1 sensor in temperature. The CQCM is a low-power-consumption device, only 40 mW, and operates from lift-off to power-down at the end of the mission. The signal outputs of the CQCM are (1) the two QCM frequencies which are proportional to mass accumulated on the surface of the crystal, and (2) the sensor temperatures as measured by platinum-resistance thermometers. The CQCM sensors have fields-of-view and viewing areas which are almost identical with the -Z axis TQCM sensor.

Data are presented for the two CQCM sensors for each of the three flights with the exception of the -Z1 sensor on STS-4. This sensor showed extreme sensitivity to direct solar radiation causing the data to be unreliable. It is therefore omitted. The frequency plot from the CQCM showed some repeatable patterns from mission to mission. After orbital altitude was reached and the payload bay doors opened, the frequencies decreased until a minimum was reached. In Tables VII-3, VII-4, and VII-5, it can be seen that the minimum was reached as early as 3 hr, 32 min on STS-3, and no later than 6 hr, 45 min on STS-4. It is this minimum that is used as a reference point for the rest of the mission. After this point, the frequencies generally increase for the remainder of the orbital phase, depending on the Orbiter attitude. In Tables VII-3, VII-4, and VII-5, three summary mass accumulation rate values are calculated for each mission (1) from lift-off to power-down, (2) from frequency minimum-to-maximum in orbit, and (3) from frequency minimum to the end of the orbital phase. The mass accumulation rates for the entire mission show small negative values for STS-2 and STS-4, while the rate for STS-3 shows a small overall increase. The largest value from minimum-to-maximum in orbit is the 12 ng cm^{-2} hr^{-1} on STS-2. Probably the most significant value is the one from the reference minimum to the final frequency in orbit. The largest value is from STS-2: 5 ng cm^{-2} hr^{-1}. The value on STS-4 was -1 ng cm^{-2} hr^{-1}. The lowest temperature reached was -102°C in the long tail-to-Sun attitude on STS-3, and the highest temperature was 34°C while the payload bay doors were still closed at the beginning of STS-4. During the "hot soak" of STS-3, the passive radiators kept the sensor temperatures no higher than 28°C.

During the three missions, the Orbiter changed attitude many times. Tables VII-6, VII-7, and VII-8 show net mass accumulation rates for attitudes that lasted for more than 1 hr, plus the ascent and descent phases. "Net values" indicates that the rates were calculated from the frequencies at the beginning and end of each attitude position as shown. As in the TQCM data, this averages over short-duration contamination events which may have occurred during the period. Also, the temperatures as shown at the beginning and end of each attitude position are the average values of the diurnal variations at that time. Tables VII-6, VII-7, and VII-8 demonstrate the volatile nature of the contamination with the periodic positive and negative values of accumulated mass as contamination is deposited and subsequently removes itself as conditions change.

CONCLUSIONS

The Contamination Requirements Definition Group (CRDG) set a contamination requirements goal for molecular deposition of 1×10^{-5} gm cm^{-2} for a 30-day mission on a 300 K surface in the -Z axis [VII-1]. In order to determine if this goal was met, each value of the +30°C data from the -Z axis sensor is extrapolated to a 30-day mission; i.e., the per hour mass deposition rates are multiplied by 720 hr, the number of hours in a 30-day mission. The 14 values from the STS-3 and -4 missions are shown in Table VII-9. Numbers in parentheses indicate from which flight the data is taken. This is a very conservative test, because it makes the assumption that a source of outgassing will outgas at the same rate for 30 days which is probably not the case. However, even assuming a constant rate, the table shows that the Shuttle is below the desired limit except for one value which exceeds the limit by only 0.1×10^{-5} gm cm^{-2}.

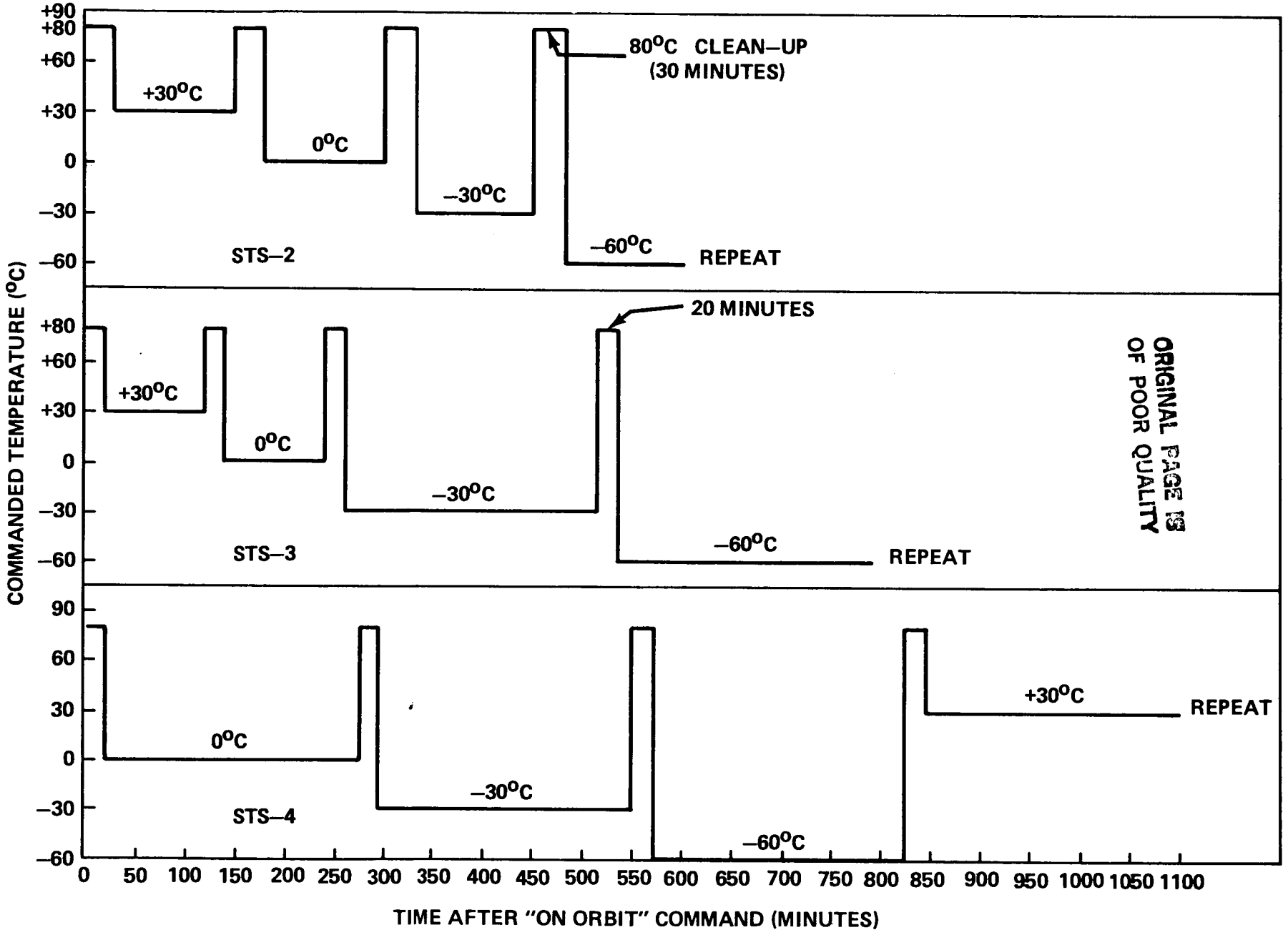

Figure VII-1. TQCM on-orbit command sequences for STS-2, -3, and -4.

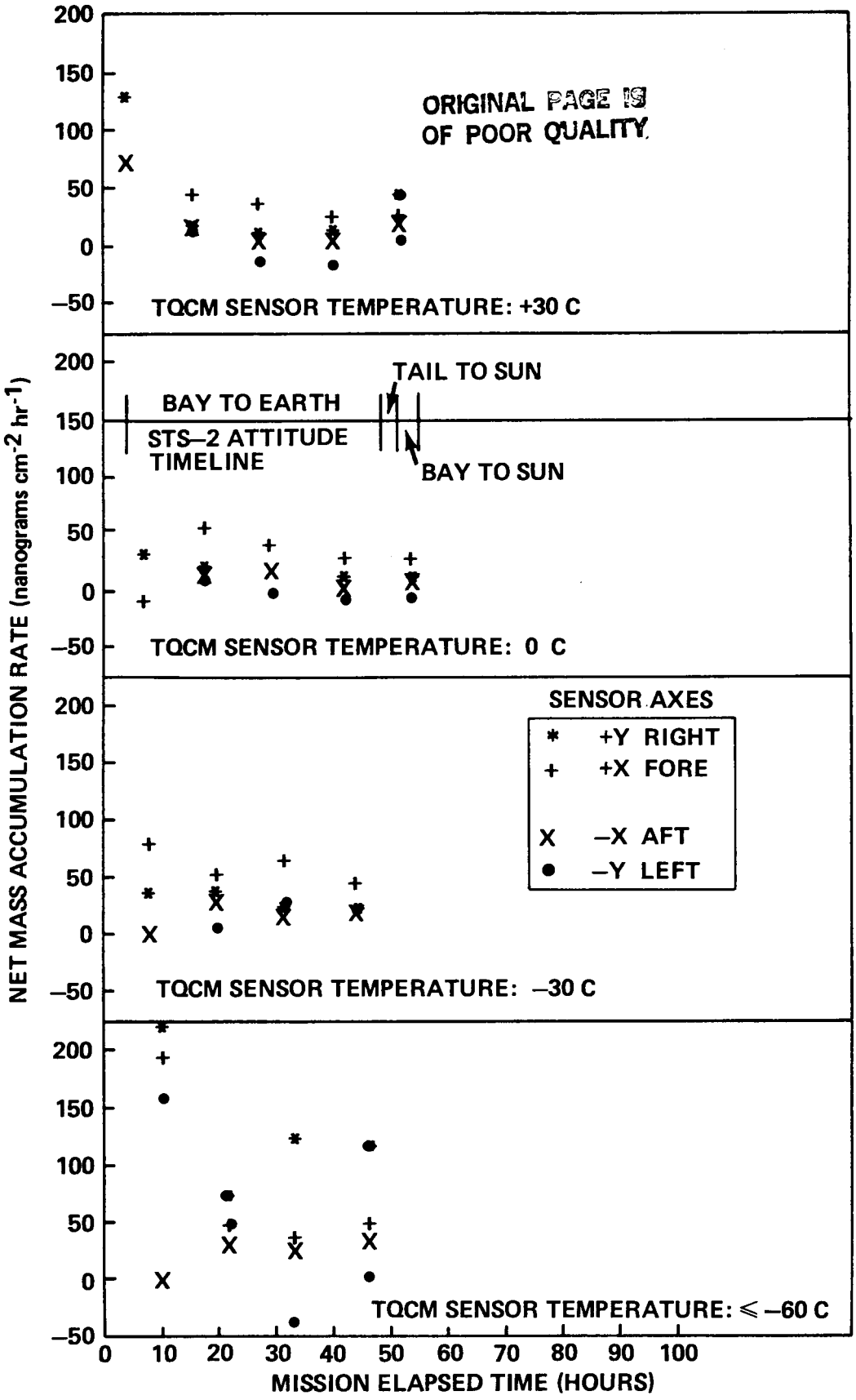

Figure VII-2. Values of net mass accumulation rate from STS-2 TQCMs.

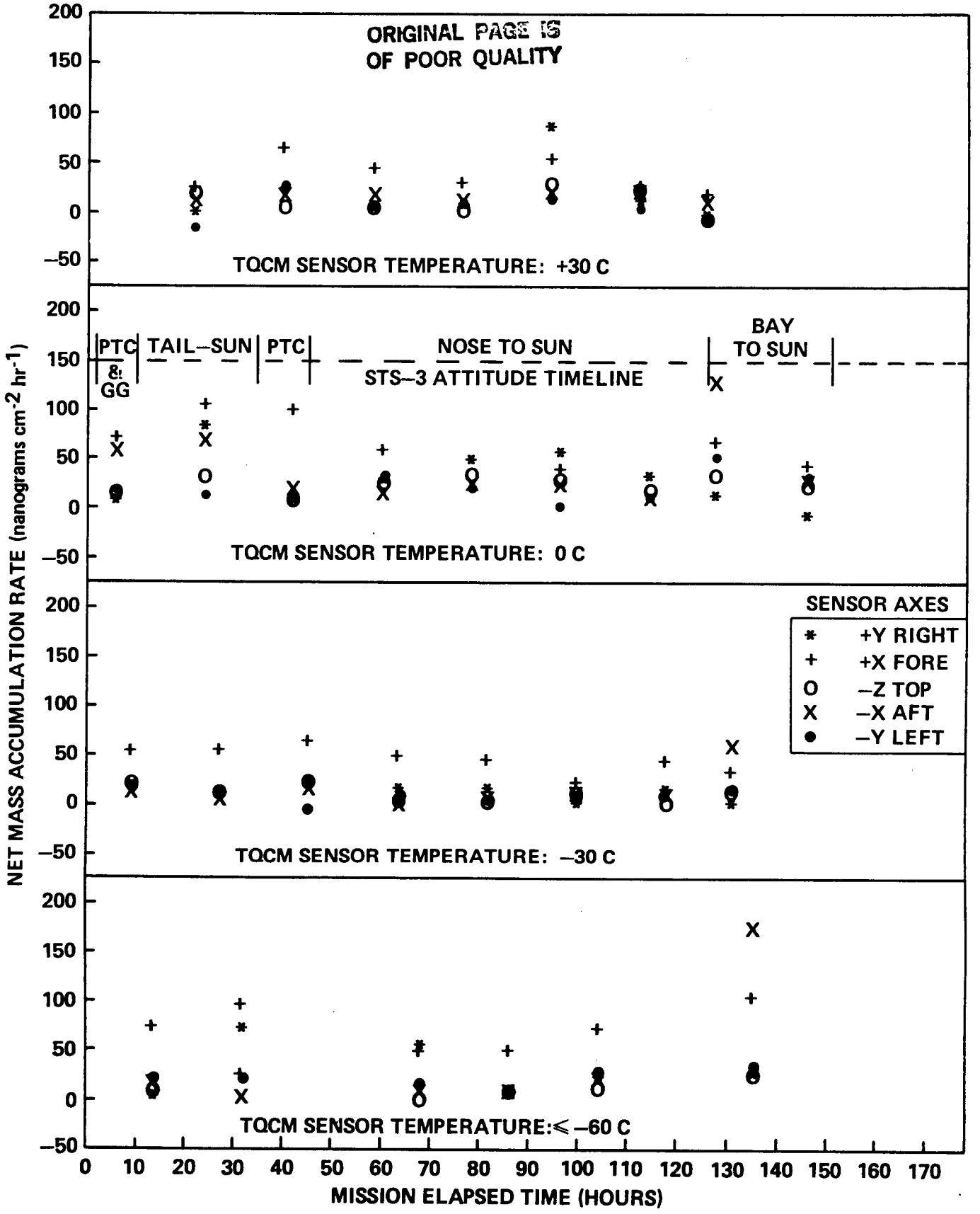

Figure VII-3. Values of net mass accumulation rate from STS-3 TQCMs.

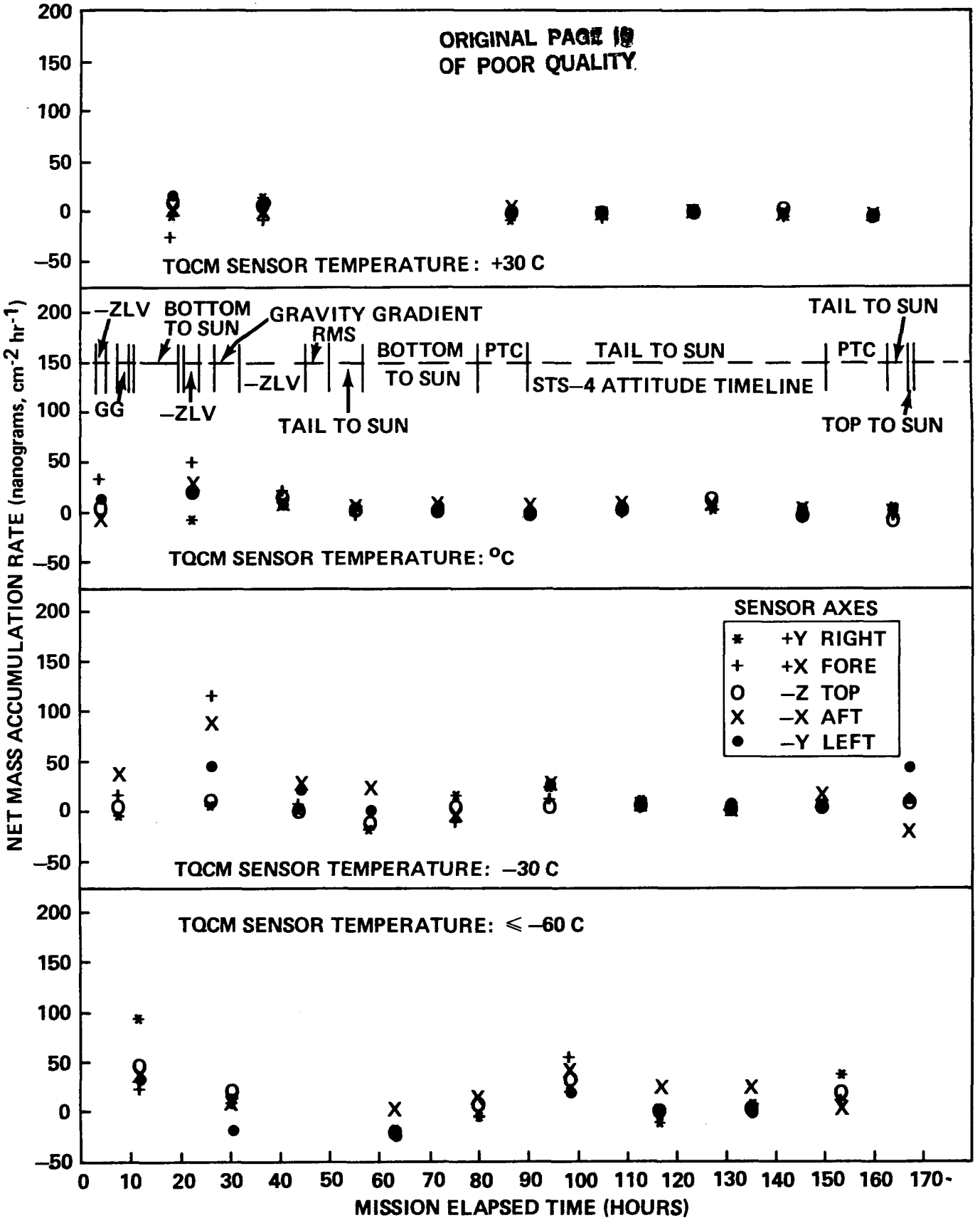

Figure VII-4. Values of net mass accumulation rate from STS-4 TQCMs.

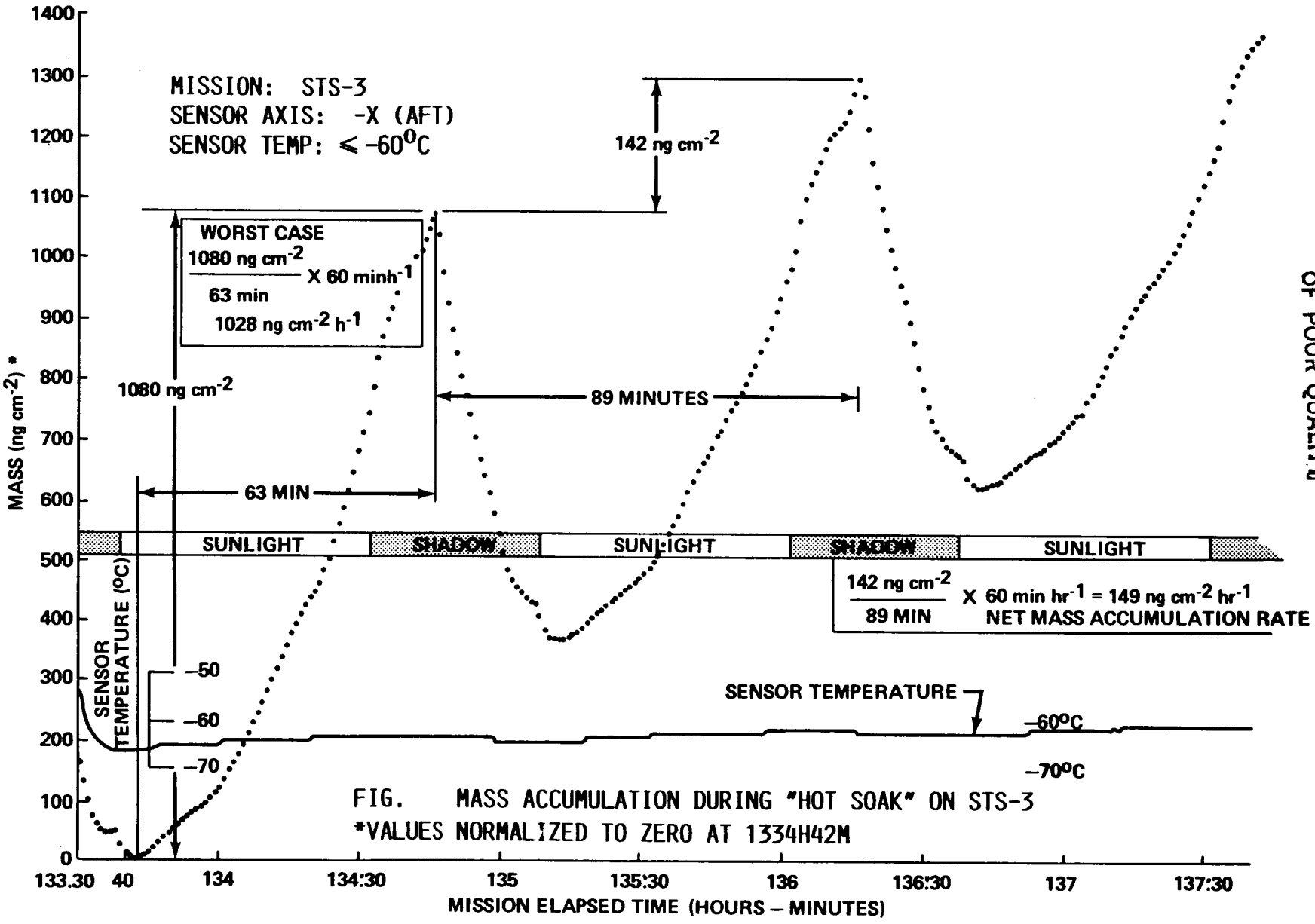

FIG. MASS ACCUMULATION DURING "HOT SOAK" ON STS-3
*VALUES NORMALIZED TO ZERO AT 1334H42M

Figure VII-5. Mass accumulation during "hot soak" on STS-3.

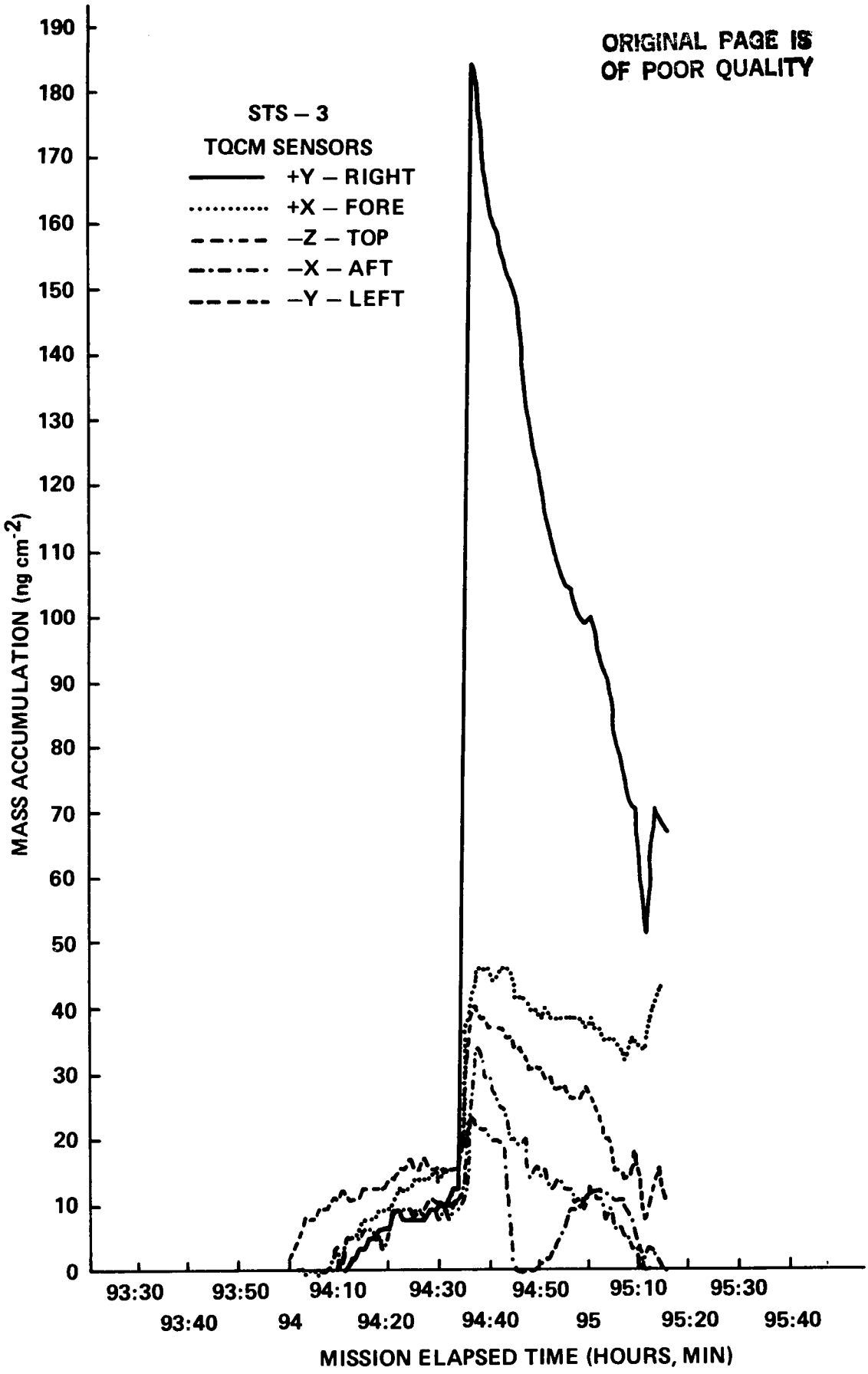

Figure VII-6. Mass accumulation during STS-3 L2U engine firing.

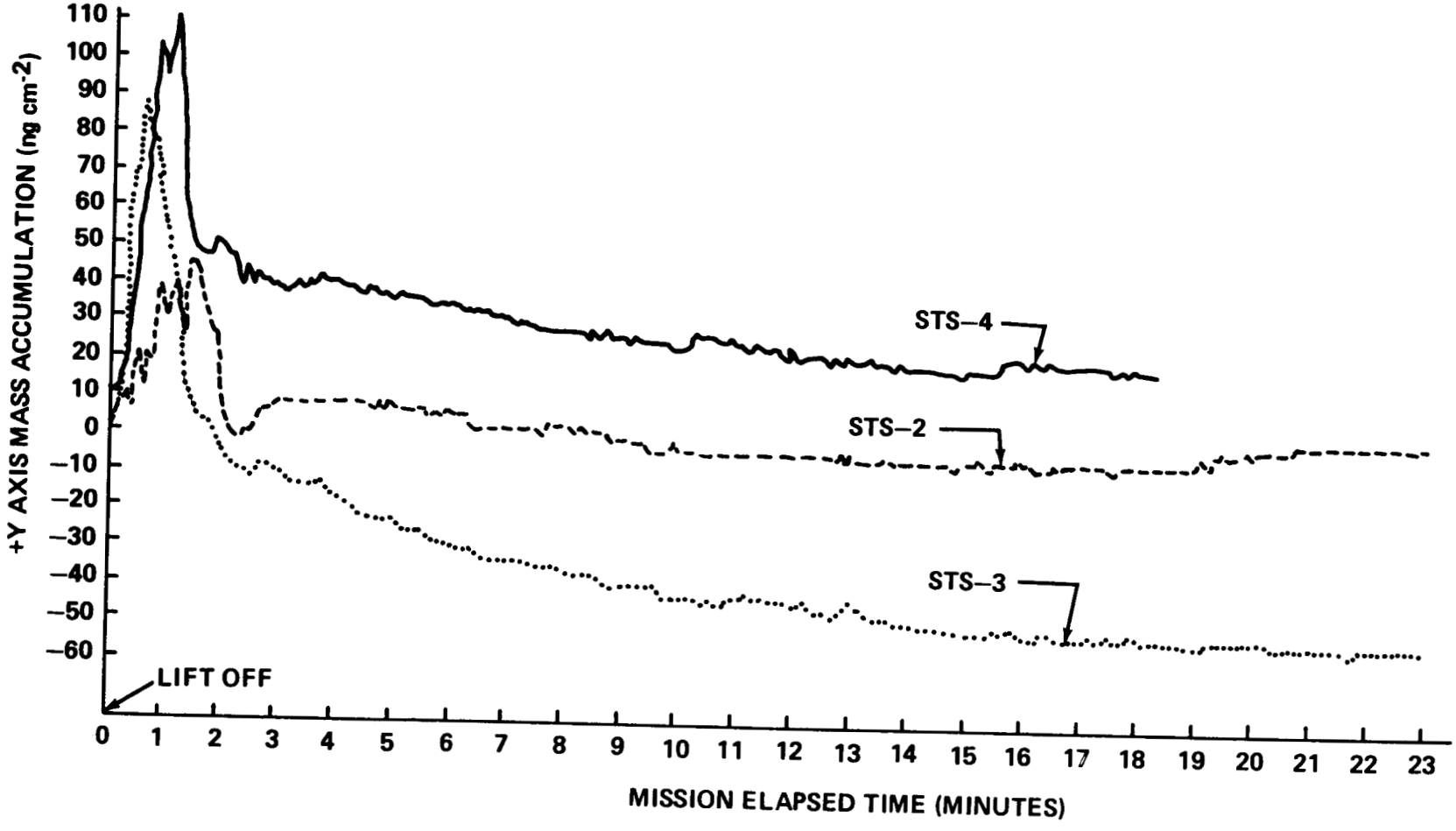

Figure VII-7. Comparison of +Y axis mass accumulation during ascent of STS-2, STS-3, and STS-4.

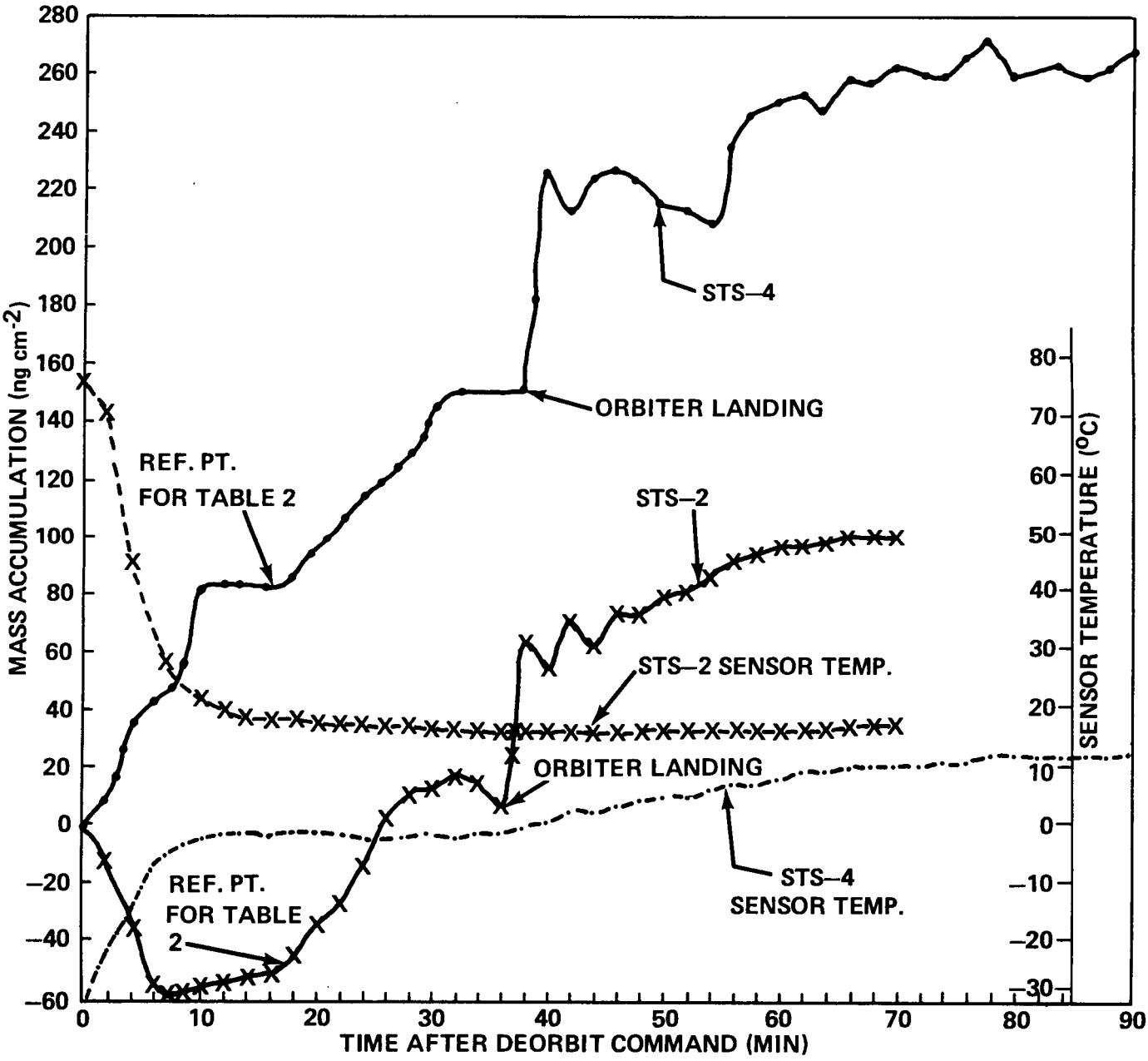

Figure VII-8. Mass accumulation during descent phase on +Y axis TQCM sensors on STS-2 and STS-4.

TABLE VII-1. MASS ACCUMULATION DURING ASCENT PHASE
(VALUES SHOWN IN ng cm^{-2})

STS-2 – Ascent

Sensor Axis	Mission Elapsed Time (min)						
	Max	Time	2	10	20	30	37
+Y	+45	1.5	-2	-6	-2	-43	-149
+X	109	0.8	-20	-16	-62	-69	-179
-Z	33	0.8	-27	+22	+61	+81	+94
-X	134	1.0	-8	-20	-8	-11	-11
-Y	129	2.0	–	+6	-739	-465	-674

STS-3 – Ascent

Sensor Axis	Mission Elapsed Time (min)						
	Max	Time	2	10	20	30	37
+Y	+87	0.7	-2	-45	-58	-69	-72
+X	+109	0.6	-16	-47	-67	-76	-81
-Z	+111	0.6	-9	-16	-20	-25	-25
-X	+145	0.8	-9	-61	+75	+70	+75
-Y	+145	0.8	+8	0	+2	-12	-27

STS-4 – Ascent

Sensor Axis	Mission Elapsed Time (Min)						
	Max	Time	2	5	10	15	18
+Y	112	1.2	+47	+36	+22	+17	+17
+X	195	0.9	-114	-265	-535	-449	-412
-Z	41	0.8	-2	-11	-25	-45	-53
-X	144	1.0	+23	+6	-3	-9	-12
-Y	192	0.9	+11	+20	+43	+28	+27

TABLE VII-2. MASS ACCUMULATION DURING THE DESCENT PHASE

STS-2 Descent Phase Total Duration: 1 hr, 10 min

Mission Elapsed Time (hr:min)	Sensor Axis	53:50	54:00	54:10	54:20	54:30	54:40	54:44
Mass Accumulation Per Area (ng cm^{-2})	+Y	0	55	58	123	140	150	150
Sensor Temperature (°C)		18.0	17.1	16.2	16.2	16.2	17.1	17.1
Mass Accumulation Per Area (ng cm^{-2})	+X	0	78	80	374	395	413	413
Sensor Temperature (°C)		16.2	15.2	14.3	14.3	14.3	14.3	14.3
Mass Accumulation Per Area (ng cm^{-2})	-X	0	56.2	44	162	136	125	125
Sensor Temperature (°C)		17.1	17.1	17.1	19.0	20.8	21.8	21.8
Mass Accumulation Per Area (ng cm^{-2})	-Y	0	9.4	-36	-75	-115	-92	-92
Sensor Temperature (°C)		15.2	14.3	13.3	17.1	19.0	20.8	20.8

STS-4 Descent Phase Total Duration: 1 hr, 28 min

Mission Elapsed Time (hr:min)	Sensor Axis	168:45	169:00	169:15	169:30	169:45	170:00
Mass Accumulation Per Area (ng cm^{-2})	+Y	0	62	137	165	182	179.4
Sensor Temperature (°C)		-1.6	-2.5	3.1	7.7	10.5	+13.5
Mass Accumulation Per Area (ng cm^{-2})	+X	0	-19	0	16	8	8
Sensor Temperature (°C)		5.9	+4.9	+4.9	+5.9	6.8	8.8
Mass Accumulation Per Area (ng cm^{-2})	-Z	0	-13	343	360	349	360
Sensor Temperature (°C)		6.8	6.8	5.9	6.8	8.7	9.6
Mass Accumulation Per Area (ng cm^{-2})	-X	0	4.7	190	195	208	220
Sensor Temperature (°C)		7.7	6.8	10.5	13.3	15.2	16.2
Mass Accumulation Per Area (ng cm^{-2})	-Y	0	2	-183	-206	-192	-178
Sensor Temperature (°C)		4.0	3.1	7.7	10.5	13.3	14.3

TABLE VII-3. STS-2 CQCM MISSION SUMMARY VALUES

	-Z1			-Z2		
	MET hr min	Frequency Hz	Temperature °C	MET hr min	Frequency Hz	Temperature °C
Frequency and temperature at lift-off	000 00	1422	23	000 00	1425	23
Minimum orbital frequency and its temperature	04 17	1089	-35	04 22	839	-31
Maximum orbital frequency and its temperature	50 44	1301	-13	36 43	1084	-38
Final orbital frequency and its temperature	53 34	1263	4	53 34	986	4
Frequency and temperature at power-down	54 45	1313	27	54 45	1053	26
Minimum orbital temperature	36 50		-52	37 05		-43
Maximum orbital temperature	02 14		30	02 15		26

CQCM Summary: Net Molecular Mass Accumulation Rates (calculated from the above values)

	-Z1				-Z2			
	Frequency Change Hz	Mass Change ng cm^{-2}	Time Interval min	Mass Accumulation Rate ng cm^{-2} hr^{-1}	Frequency Change Hz	Mass Change ng cm^{-2}	Time Interval min	Mass Accumulation Rate ng cm^{-2} hr^{-1}
From lift-off to power-down	-109	-170	3285	-3	-372	-580	3285	-11
From minimum frequency to maximum frequency in orbit	212	331	2787	7	245	382	1941	12
From minimum frequency to final frequency in orbit	174	271	2957	5	147	229	2952	5

TABLE VII-4. STS-3 CQCM MISSION SUMMARY VALUES

	-Z1			-Z2		
	MET hr min	Frequency Hz	Temperature °C	MET hr min	Frequency Hz	Temperature °C
Frequency and temperature at lift-off	000 00	1749	23	000 00	1346	24
Minimum orbital frequency and its temperature	03 49	1542	-14	03 32	1197	5
Maximum orbital frequency and its temperature	151 27	1951	25	166 49	1590	-41
Final orbital frequency and its temperature	191 28	1882	14	191 28	1487	23
Frequency and temperature at power-down	192 59	1868	25	192 59	1490	25
Minimum orbital temperature	29 40 30 25		-102 -102	28 21 30 38		-87 -87
Maximum orbital temperature	01 59		27	137 32 151 46		28 28

CQCM Summary: Net Molecular Mass Accumulation Rates (calculated from the above values)

	-Z1				-Z2			
	Frequency Change Hz	Mass Change ng cm^{-2}	Time Interval min	Mass Accumulation Rate ng cm^{-2} hr^{-1}	Frequency Change Hz	Mass Change ng cm^{-2}	Time Interval min	Mass Accumulation Rate ng cm^{-2} hr^{-1}
From lift-off to power-down	119	186	11,580	1	144	225	11,580	1
From minimum frequency to maximum frequency in orbit	406	638	8,858	4	393	613	10,009	4
From minimum frequency to final frequency in orbit	340	530	11,488	3	290	452	11,276	2

TABLE VII-5. STS-4 CQCM MISSION SUMMARY VALUES

	-Z1			-Z2		
	MET hr min	Frequency Hz	Temperature °C	MET hr min	Frequency Hz	Temperature °C
Frequency and temperature at lift-off	000 00	2551	25	000 00	1270	25
Minimum orbital frequency and its temperature				06 45	1080	-23
Maximum orbital frequency and its temperature				47 43	1367	2
Final orbital frequency and its temperature				168 30	1263	-4
Frequency and temperature at power-down	170 02	2394	22	170 02	1238	23
Minimum orbital temperature	149 05		-66	149 06		-63
Maximum orbital temperature	01 44		34	01 45		32

CQCM Summary: Net Molecular Mass Accumulation Rates (calculated from the above values)

	-Z1				-Z2			
	Frequency Change Hz	Mass Change ng cm^{-2}	Time Interval min	Mass Accumulation Rate ng cm^{-2} hr^{-1}	Frequency Change Hz	Mass Change ng cm^{-2}	Time Interval min	Mass Accumulation Rate ng cm^{-2} hr^{-1}
From lift-off to power-down	-157	-245	10,202	-1	-32	-50	10,202	-0.3
From minimum frequency to maximum frequency in orbit					287	448	2,458	11
From minimum frequency to final frequency in orbit					183	285	9,705	-1

TABLE VII-6. STS-2, CQCM NET MOLECULAR MASS ACCUMULATION RATES AS A FUNCTION OF ORBITER ATTITUDE

			Sensor -Z1			Sensor -Z2		
Attitude	MET	Δ Time	Sensor Temp.	Mass Change	Mass Accum. Rate	Sensor Temp.	Mass Change	Mass Accum. Rate
	HHH MM	Min	°C	ng cm^{-2}	ng cm^{-2} / hr	°C	ng cm^{-2}	ng cm^{-2} / hr
Ascent	000 00 000 37	37	23 21	67	109	23 20	-6	-10
IMU Alignment	002 40 004 02	82	-2 -36	-328	-240	14 -29	-153	-112
-ZLV	004 15 007 14	179	-38 -6	106	36	-32 -4	170	57
-ZLV	009 10 010 55	105	-11 -4	23	13	-9 -2	-67	-38
-ZLV	012 35 047 19	2084	-6 -6	111	3	10 -1	73	2
Tail-to-Sun	047 21 048 25	64	-6 -16	-3	-3	-2 -12	-44	-41
Top-to-Sun*	050 28 053 34	186	-19 4	-37	-12	-27 4	119	38
Descent	053 34 054 45	71	4 27	78	66	4 26	112	95

*Payload bay doors closed.

TABLE VII-7. STS-3, CQCM NET MOLECULAR MASS ACCUMULATION RATES AS A FUNCTION OF ORBITER ATTITUDE

			Sensor -Z1			Sensor -Z2		
Attitude	MET	Δ Time	Sensor Temp.	Mass Change	Mass Accum. Rate	Sensor Temp.	Mass Change	Mass Accum. Rate
	HHH MM	Min	°C	ng cm^{-2}	$\frac{ng\ cm^{-2}}{hr}$	°C	ng cm^{-2}	$\frac{ng\ cm^{-2}}{hr}$
Ascent	000 00 000 37	37	23 20	-4	-8	24 21	-28	-47
-ZLV	001 22 002 54	92	22 12	83	54	21 17	133	86
PTC	003 19 006 30	191	-2 -25	-136	-43	8 -15	-14	-4
Gravity Gradient	007 28 009 14	106	-29 -45	-17	-10	-18 -36	0	0
Tail-to-Sun	010 45 031 00	1215	-57 -97	16	1	-47 -76	112	6
PTC	034 20 045 50	690	-42 -14	70	6	-28 -2	75	7
Nose-to-Sun	046 00 125 50	4790	-14 -32	186	2	-2 -22	187	2
Top-to-Sun	126 13 153 00	1607	-30 2	193	7	-19 10	66	2

TABLE VII-7. (Concluded)

			Sensor -Z1			Sensor -Z2		
Attitude	MET	Δ Time	Sensor Temp.	Mass Change	Mass Accum. Rate	Sensor Temp.	Mass Change	Mass Accum. Rate
	HHH MM	Min	°C	ng cm^{-2}	$\frac{ng\ cm^{-2}}{hr}$	°C	ng cm^{-2}	$\frac{ng\ cm^{-2}}{hr}$
PTC	153 30 164 38	668	-6 -26	-21	-3	4 -13	8	1
Tail-to-Sun	164 38 167 29	171	-26 -38	48	17	-14 -25	101	36
Top-to-Sun	167 30 170 30	180	-38 6	2	1	-25 12	-66	-22
PTC	171 45 185 05	800	-4 -9	70	5	7 2	-16	-1
Tail-to-Sun	185 30 188 13	163	-15 -13	22	8	-2 -3	56	21
Top-to-Sun*	188 13 190 55	162	-13 14	48	18	-3 23	-62	-23
Descent	191 29 192 59	90	14 25	0	0	23 25	37	25

*Payload bay doors closed.

TABLE VII-8. STS-4, CQCM NET MOLECULAR MASS ACCUMULATION RATES AS A FUNCTION OF ORBITER ATTITUDE

			Sensor -Z1			Sensor -Z2		
Attitude	MET	Δ Time	Sensor Temp.	Mass Change	Mass Accum. Rate	Sensor Temp.	Mass Change	Mass Accum. Rate
	HHH MM	Min	°C	ng cm^{-2}	ng cm^{-2} / hr	°C	ng cm^{-2}	ng cm^{-2} / hr
Ascent	000 00 000 17	17				25 22	17	61
-ZLV	001 30 003 45	135				30 5	-80	-37
Gravity Gradient	005 45 007 45	120				-10 -42	-41	-20
Bottom-to-Sun	008 46 018 42	596				-46 -37	115	13
-ZLV	019 36 022 08	152				-37 -3	6	2
Gravity Gradient	025 17 030 46	329				-3 -45	-14	-3
-ZLV	032 02 043 19	677				-52 4	140	12
Top-to-Sun*	044 00 048 00	240				-6 -3	87	47

*IECM on remote arm, out of bay.

TABLE VII-8. (Concluded)

			Sensor -Z1			Sensor -Z2		
Attitude	MET	Δ Time	Sensor Temp.	Mass Change	Mass Accum. Rate	Sensor Temp.	Mass Change	Mass Accum. Rate
	HHH MM	Min	°C	ng cm^{-2}	$\frac{ng\ cm^{-2}}{hr}$	°C	ng cm^{-2}	$\frac{ng\ cm^{-2}}{hr}$
Tail-to-Sun	048 20 055 21	421				-3 -45	-78	-11
Bottom-to-Sun	055 22 078 06	1364				-45 -30	-253	-11
PTC	078 06 088 20	614				-30 -21	176	17
Tail-to-Sun	088 21 148 32	3611				-21 -49	-34	-1
PTC	149 02 161 04	722				-50 -26	-34	-3
Tail-to-Sun	161 20 165 26	246				-26 -42	-51	-13
Top-to-Sun*	165 56 167 56	120				-26 -7	34	17
Descent	168 30 172 02	92				-4 23	-41	-26

*Payload bay doors closed.

TABLE VII-9. DATA FROM -Z AXIS TQCM SENSORS AT 30°C EXTRAPOLATED TO 30-DAY MISSION

MET hr	Measured Value ng cm^{-2} hr^{-1}	Value Extrapolated to 30-Day Mission gm cm^{-2}/30 days
003.8(3)	<0	<0
016.6(4)	5.7	4.1×10^{-6}
021.9(3)	14.6	1.0×10^{-5}
034.9(4)	3.2	2.3×10^{-6}
040.0(3)	1.0	7.2×10^{-7}
058.0(3)	0	0
076.0(3)	<0	<0
084.7(4)	0.4	2.9×10^{-7}
102.9(4)	4.2	3.0×10^{-6}
112.5(3)	14.8	1.1×10^{-5}
121.4(4)	4.2	3.0×10^{-6}
125.7(3)	<0	<0
139.5(4)	7.6	5.5×10^{-6}
157.9(4)	<0	<0

TABLE VII-10. DATA FROM A11 TQCM SENSORS AT 30°C EXTRAPOLATED TO 30-DAY MISSION

MET hr	Measured Value ng cm^{-2} hr^{-1}	Value Extrapolated to 30-Day Mission gm cm^{-2}/30 days
2.1(2)	<0	<0
3.8(3)	<0	<0
13.8(2)	20	1.4×10^{-5}
16.6(4)	<0	<0
21.9(3)	5	3.6×10^{-6}
25.4(2)	7.7	5.5×10^{-6}
34.9(4)	1.8	1.3×10^{-6}
38.2(3)	4.6	3.3×10^{-6}
40.0(3)	23	1.7×10^{-5}
50.0(2)	22.6	1.6×10^{-5}
58.3(3)	9.7	7.0×10^{-6}
76.3(3)	7.9	5.7×10^{-6}
84.7(4)	<0	<0
94.4(4)	35.3	2.5×10^{-5}
102.9(4)	2.5	1.8×10^{-6}
112.5(3)	11.1	8.0×10^{-6}
121.4(4)	3.8	2.7×10^{-6}
125.7(3)	<0	<0
139.5(4)	2.7	1.9×10^{-6}
157.9(4)	<0	<0

REFERENCES

VII-1. Miller, Edgar R. and Decher, Rudolf (Editors): An Induced Environment Contamination Monitor for the Space Shuttle, NASA TM-78193, August 1978.

VII-2. Miller, Edgar R. (Editor): STS-2 Induced Environment Contamination Monitor (IECM) – Quick-Look Report. NASA TM-82457, January 1982.

VII-3. Miller, E. R. and Fountain, J. A. (Editors): STS-3 Induced Environment Contamination Monitor (IECM) – Quick-Look Report. NASA TM-82489, June 1982.

VIII. CAMERA/PHOTOMETER

J. K. Owens and K. S. Clifton

Optical measurements of background brightness and the size and velocity distributions of contaminant particles were undertaken by the Camera/Photometer instrument during the OFT series. These measurements were made in order to ascertain whether Orbiter-induced contamination was within limits recommended by the Contamination Requirements Definition Group (CRDG). The criteria concerning particulate contamination are as follows:

> Production of particles by the STS shall be limited so that an average of less than one particle per orbit enters a 1.5×10^{-5} sr field of view along any line within 60 deg of the -Z axis, and this field-of-view contains no discernible particles for 90 percent of the operation period. A discernible particle is a particle with diameter of 5 μm within a range of 10 km.

The definition of a discernible particle is the result of the calculated particle detection by an infrared telescope with a 300 K particle in the field-of-view [VIII-1]. The Camera-Photometer could not approach this detection capability, and the definition of the particulate environment in this size and distance range is not addressed here. This problem must await flight of the Shuttle Infrared Telescope (IRT) aboard Spacelab 2. The Camera/Photometer only measures particles of size greater than 25 μm in the immediate vicinity of the payload bay.

The recommendations for background brightness are expressed as spectral intensity for ultraviolet and visible radiation as follows:

> The total ultraviolet and visible radiation background from spacecraft-induced particulate and molecular scattering and emission must be less than the envelope defined by the following spectral intensities:

Wavelength (nm)	Spectral Intensity at 90 deg Sun Angle ($W\ m^{-2}\ sr^{-1}\ nm^{-1}$)
155	3.5×10^{-11}
191	1.9×10^{-11}
246	1.3×10^{-11}
298	5.9×10^{-11}
332	1.0×10^{-10}
425	2.5×10^{-10}
550	2.0×10^{-10}
1000	1.0×10^{-10}

This yields a total brightness of approximately $4.85 \times 10^{-14}\ B_o$ over the interval from 155 to 1000 nm. Over the photographic interval; i.e., about 332 to 550 nm in the table above, the brightness is about $1.53 \times 10^{-14}\ B_o$. It is important to note that the recommendations do not say that these numbers should be the background brightness, but they say they are the "radiation background from spacecraft-induced particulate and molecular scattering and emission." Since the total mean sky brightness from natural sources is $1.06 \times 10^{-13}\ B_o$, [VIII-2] the intent is to make the contribution due to the

induced environment much less than the natural sources. Violation of criteria are permitted for dumps and maneuvers provided such violations are controllable and do not persist for more than 10 percent of the operational time and do not occur more frequently than once per 30 min [VIII-3].

The Camera/Photometer experiment consists of two 16-mm photographic cameras separated by a distance of 0.4 m and electrically slaved together such that stereoscopic observations can be performed. Figure VIII-1 is a cutaway view of a Camera/Photometer. Each is housed within a pressurized canister and operated automatically throughout the mission, making simultaneous exposures on a continuous basis every 150 sec. The cameras are equipped with 18-mm f/0.9 lenses and subtended overlapping 32 deg (0.24 sr) fields-of-view in the -Z direction relative to the spacecraft. An integrating photometer is used to inhibit the exposure sequences during periods of excessive illumination and to terminate the exposures at preset light levels. During the exposures, a camera shutter operates in a chopping mode in order to isolate the movement of particles for velocity determinations [VIII-4,VIII-5]. Calculations based upon the pre-flight film calibration indicate that particles as small as 25 μm can be detected under ideal observing conditions; i.e., background brightness of about 4×10^{-14} B_0 with bright objects such as the Sun and Earth at angles greater than 60 deg from the optical axis.

Kodak Double X film, Type 7222, was used to allow exposures to about 10^{-2} erg/cm^2 with good detective quantum efficiency. In this way, more of the 150 sec frame period could be covered by the active observation while maintaining small particle detection capability, whereas high-speed film such as type 2485 would limit the exposure to about 10 sec for peak detection efficiency. Since the detective quantum efficiency curve falls off relatively rapidly after reaching a peak, it is desirable to shift the curve to longer exposures by use of a slower film such as Double X. Also, the resolution of Double X is superior to that of high-speed films.

The Camera/Photometers operated throughout each mission during the on-orbit phase except during Remote Manipulator System (RMS) activities involving the IECM or periods of power interruption to the IECM. The number of opportunities available for observing contamination is quite dependent on spacecraft orientation as well as mission duration. The Camera/Photometer operational times and principle orientations during those times were as follows:

Mission	Principal Orientation	Time (hours)
STS-2	Earth-directed	44.5
STS-3	Celestial attitudes	45.0
STS-4	Celestial attitudes	138.8

The short operational times for STS-2 and -3 resulted from the short mission duration of STS-2 and a random component failure in the master timing circuitry which halted both cameras during STS-3. It is possible for the Camera/Photometer to observe particulate contamination in two circumstances: (1) during sunlit passes in which the Orbiter -Z axis (Fig. II-1) is directed away from both the Earth and Sun, and (2) twice each orbit when the spacecraft is between the terrestrial terminator and the umbra of the Earth's shadow and the Orbiter -Z axis is Earth-directed along the local vertical.

The appearance of particulate contamination varied throughout each mission. Sometimes, the contamination recorded by the cameras took the form of "snowstorm" events, such as that shown in Figure VIII-2, with sometimes better than 30 individual particle tracks visible in a single frame. Many of these events have been temporally correlated with water dumps, engine firings, and payload bay door activities [VIII-6,VIII-7]. Most frames show a few individual tracks which can be discriminated from background (e.g., lights of cities).

All three missions provided data during the first 48 hr of mission time to the Camera/Photometer data base. Only STS-4 provided data beyond 48 hr. Table VIII-1 shows the percentage of those frames for which the above criteria for observing particles are met during which contaminant particles were actually observed. It may be seen that particles were observed on all such frames for the first 7 hr of the missions. Each of the missions indicated an initial "clean-up" period during the first 15 hr of the mission. After this period, there is a relatively low level of particulate contaminants primarily due to isolated events related to spacecraft activities. Figure VIII-3 illustrates this very well, as well as the general increase of clear observing time (X = 0 particles/frame) with MET.

Examining the particle data after the 24-hr point in more detail and omitting data recorded in the vicinity of a water dump or when the Shuttle was in a bottom-to-Sun orientation a quiescent particle rate may be obtained. Particles were recorded during such periods at the average rate of 500/orbit throughout the camera's 0.24 sr field-of-view. This corresponds to about 0.03 particles/orbit in a 1.5×10^{-5} sr field-of-view. Normalizing the data to exposure durations of 1 sec, the probability of seeing one or more particles within the field-of-view per exposure is 36 percent. The average stay time for a typical particle in the Camera/Photometer's field-of-view is 5 sec.

Water dumps, APU tests, and payload bay door opening/closings appear to be the only onboard activities which can be clearly correlated to particulate contamination events. Thruster firings for spacecraft maneuvers did not consistently correlate to particle observations, as can be seen in an excerpt from the STS-2 correlations shown in Table VIII-2. It is likely that any particles generated by the firing itself would be far too fast to be detected. Those apparent correlations with maneuvers may be the result of a particle being shaken loose by spacecraft firing vibration.

The photometer section of the system is capable, in the configuration used on these flights, of measuring brightness levels, B, between $B/B_0 = 2.972 \times 10^{-15}$ and $B/B_0 = 5.53 \times 10^{-12}$, where B_0 is the solar brightness. The primary sources of error in the measurement are high voltage to the photomultiplier tube (PMT) and integration time, which were measured during the mission. It is estimated that the error in PMT gain due to the uncertainty of the high-voltage value is approximately 10 percent, and the integration time is known to ±1 sec. Therefore, the error in the background brightness measurement is $\Delta(B/B_0) = \pm 1.04 \times 10^{-14}$ for the longest exposure recorded; i.e., about t = 80 sec, or $B/B_0 = 6.9 \times 10^{-14}$. The more typical sky observations at Sun angles greater than 90 deg (or nighttime) show B/B_0 to be in the 10^{-13} range. This is consistent with measurements from Apollo 15 and 16 as well as Skylab, and this is also on the order of the natural sources; e.g., unresolved stars, zodiacal light, etc.

An approximation, using the fact that stars as faint as about $m_v = 10$ have been seen on the film, indicates that a background brightness on the order of 10^{-13} B_0 is also consistent with the photographic data. Using a typical detection criterion of S/N = 5, where S/N is the signal-to-noise ratio, and a flux ratio of the star relative to the Sun of about 2×10^{-15}, the background brightness integrated over the field-of-view is approximately 2×10^{-13} B_0. This is roughly the same brightness as measured by the photometer over the same field-of-view.

In conclusion, the Camera/Photometer experiment indicates that within the detection capabilities of the instrument the recommendation of the CRDG relative to particulate contamination has been met on the OFT missions. Although the sensitivity of the film only permits detection to a 25 μm particle size, the observed value of 0.03 particles/orbit in a 1.5×10^{-5} sr field-of-view is sufficiently less than the

goal of one particle/orbit in this field-of-view to make it unlikely for the goal to be exceeded significantly by extension to the 5 μm size limit. Since the CRDG recommendations for background brightness are expressed as spectral intensities within specific wavelength bands, it is difficult to express the goals in terms of a white light value. However, since the usually observed values are on the order of the naturally occurring background brightness, any contribution to background brightness from "Spacecraft-induced particulate and molecular scattering and emission" does not appear to be measurable during quiescent periods. Exceptions occur as provided for by the CRDG recommendations, e.g., water dumps, and during the first 15 hours of the mission. After this initial "clean-up" period, major contamination events can generally be correlated with spacecraft activities and thus avoided in terms of data acquisition for Shuttle-based experiments.

REFERENCES

VIII-1. Simpson, J. P., and Witteborn, F. C.: Effect of the Shuttle Contaminant Environment on a Sensitive Infrared Telescope. Applied Optics, Vol. 16, August 1977, pp. 2051-2073.

VIII-2. Allen, C. W.: Astrophysical Quantities, Third Edition. University of London, The Athlone Press, 1973.

VIII-3. STS Contamination Control Requirements for Induced Environment, STS Payload Contamination Requirements Definition Group Report, NASA/Marshall Space Flight Center, July 1975.

VIII-4. Clifton, K. S., and Owens, J. K.: Camera/Photometer, in an Induced Environment Contamination Monitor for the Space Shuttle. NASA TM-78193, edited by Edgar R. Miller and Rudolf Decher, August 1978, pp. 118-131.

VIII-5. Clifton, K. S., and Owens, J. K.: Monitoring of Particulate Contamination and Background Brightness from IECM Based Instrumentation. AIAA/IES/ASTM 10th Space Simulation Conference: A Collection of Technical Papers, Bethesda, Maryland, October 16-18, 1978, pp. 55-62.

VIII-6. Owens, J. K., and Clifton, K. S.: Camera/Photometer, in STS-2 Induced Environment Contamination Monitor (IECM) – Quick-Look Report, NASA TM-82457, Edited by E. R. Miller, January 1982, pp. 63-66.

VIII-7. Clifton, K. S., and Owens, J. K.: Camera/Photometers, in STS-3 Induced Environment Contamination Monitor (IECM) – Quick-Look Report, NASA TM-82489, Edited by E. R. Miller and J. A. Fountain, June 1982, pp. 33-37.

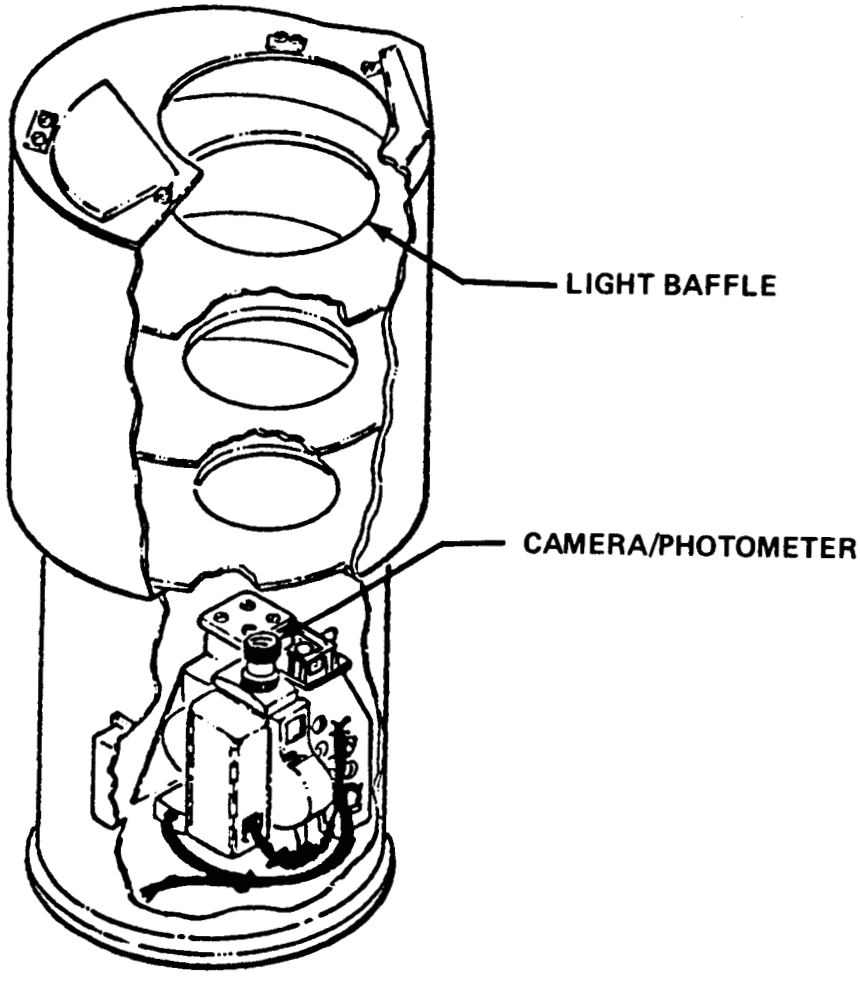

Figure VIII-1. Cut-away view of the Camera/Photometer instrument in which the camera is located within a canister pressurized to 14.7 lb/in.^{2} Observations are made through a quartz window above which is located a baffle. The baffle has a diameter of 32.4 cm and a length of 26.8 cm and was constrained to the envelope defined by the IECM.

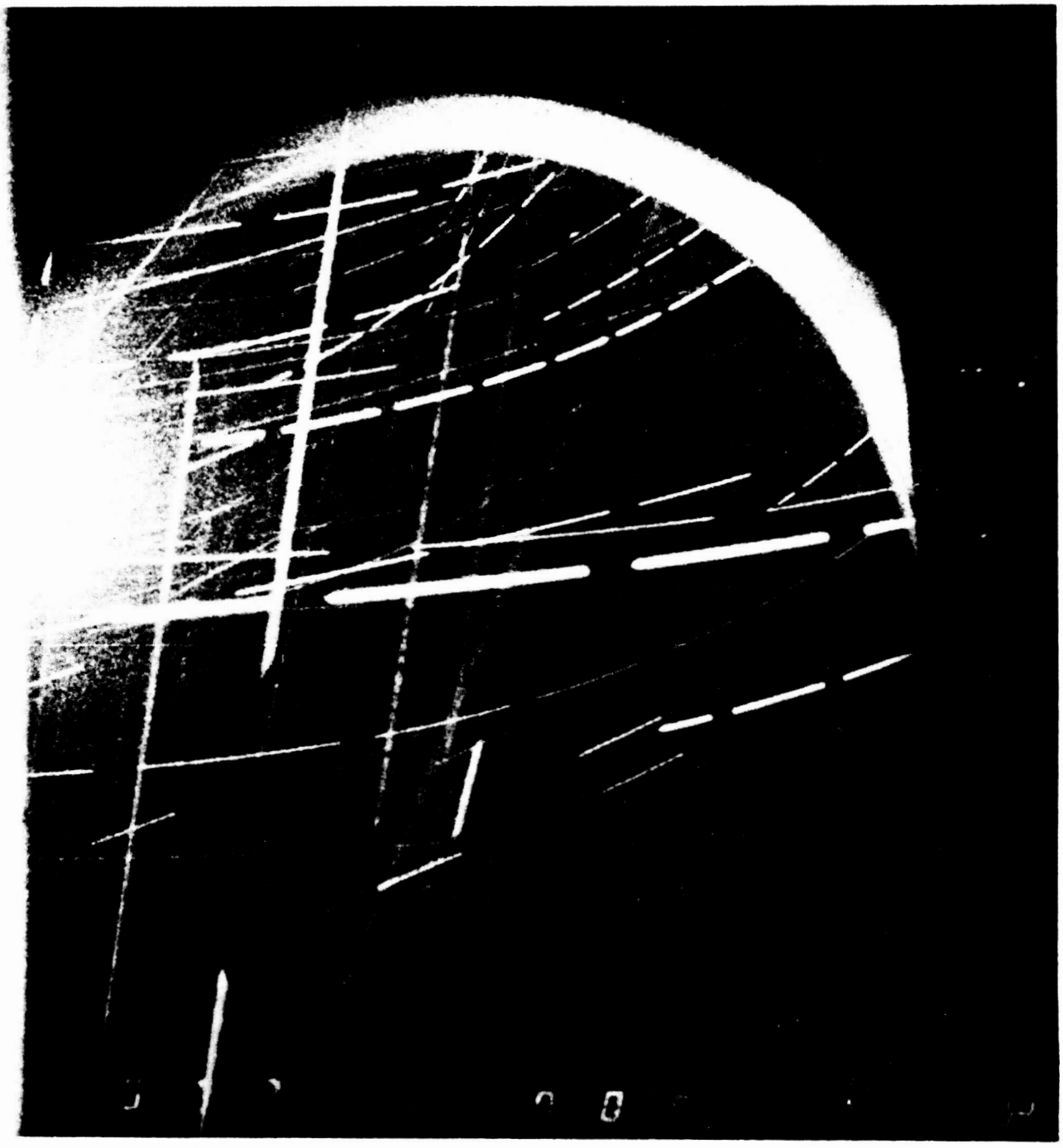

Figure VIII-2. A photograph of heavy contamination typical of that seen during the very early portions of the OFT missions. In this photograph, two populations of particles are evidenced by their directions of travel. The action of the camera shutter acting in a chopper mode can be seen splitting the particle tracks into segments of 800 m sec duration.

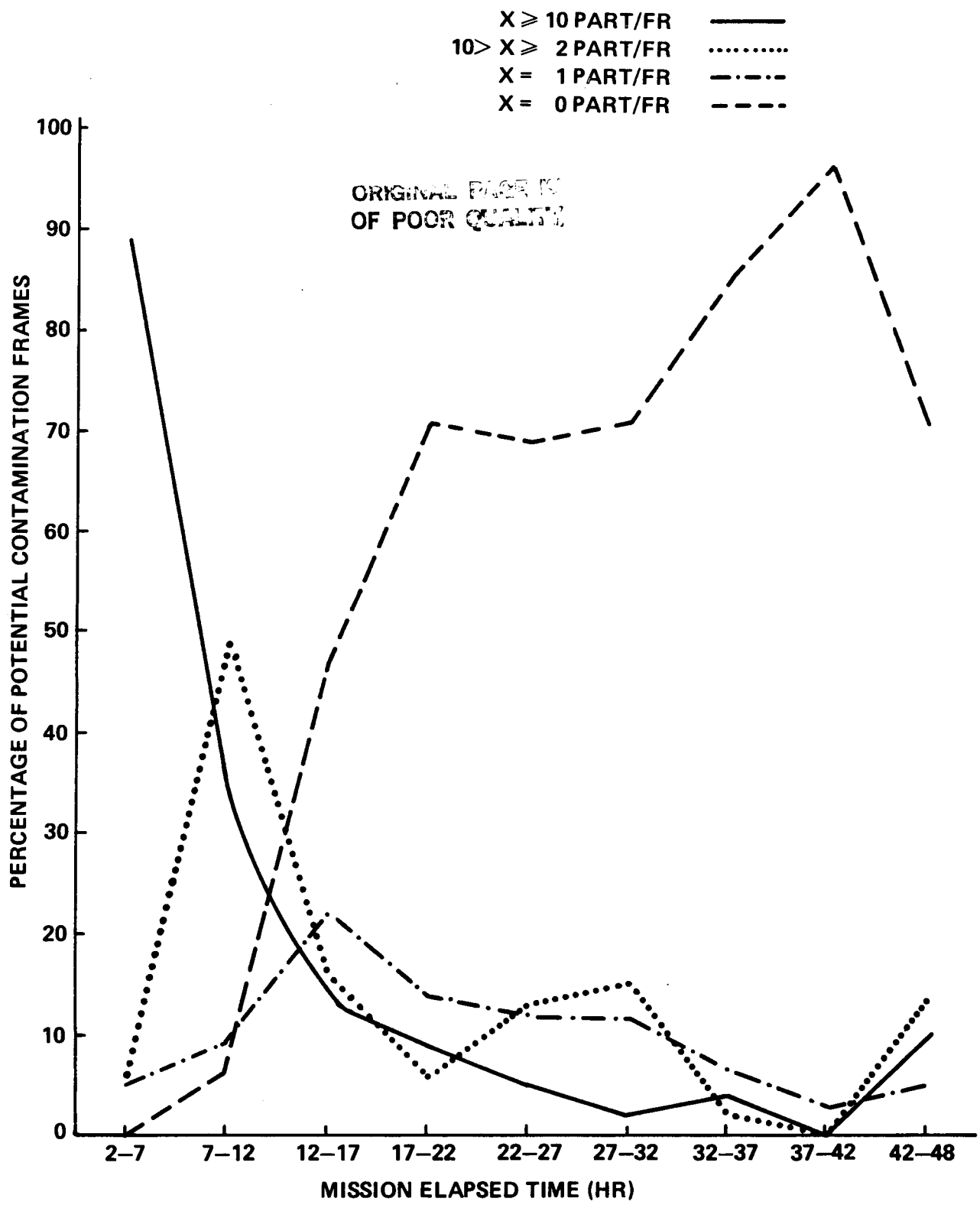

Figure VIII-3. A summary of the contamination observed during the first 48 hr combined from the STS-2, -3, and -4 missions. Curves are presented showing the time histories of particle concentrations (particles/frames) recorded by the cameras. Heavier concentrations of particles are recorded very early in the mission, with fewer particles being recorded as the mission progresses.

TABLE VIII-1. THE NUMBER OF FRAMES WITH X NUMBER OF EVENTS AS A PERCENTAGE OF POTENTIAL CONTAMINATION FRAMES. THE DATA IS A SUMMARY OF THE STS-2, -3, AND -4 MISSIONS DURING THE FIRST 48 hr OF THE RESPECTIVE MISSIONS

	Mission Elasped Time								
Number of Events per Frame	2-7h	7-12h	12-17h	17-22h	22-27h	27-32h	32-37h	37-42h	42-48h
$x \geq 20$	81%	25%	10%	3%	2%	0%	2%	0%	10%
$20 \geq x \geq 10$	8	12	4	6	3	2	2	0	0
$10 > x \geq 5$	6	16	5	1	2	5	0	0	5
$5 > x \geq 2$	0	32	11	5	11	10	2	0	10
1	5	9	22	14	12	12	7	3	5
0	0	6	48	71	70	71	87	97	70
Total Contamination	100	94	52	29	30	29	13	3	30

Data frames as a percentage of potential contamination frames as seen in the first 48 hours during STS-2, 3, and 4.

TABLE VIII-2. CORRELATION OF OBSERVED CONTAMINATION WITH ONBOARD SPACECRAFT ACTIVITIES, SUCH AS MANEUVERS, WATER DUMPS, ENGINE BURNS, ETC. THE DATA WAS RECORDED DURING THE STS-2 MISSION.

EVENT	MET	ΔT	TOTAL AVAIL. FRAMES	NUMBER OF CONTAM. FRAMES	AMOUNT OF CONTAM. (PART/FR)
MANEUVER	12:35	7	1	0	0
		25			
		150	1	0	0
		180	1	2	2
		240	1	0	0
		270	1	0	0
		330	1	0	0
		510	1	0	0
MANEUVER	21:55	5	1	1	2
MANEUVER	22:18	40	1	0	0
RMS TESTS	23:00–	––	4	1	1
	27:00				
		150	1	0	0
		210	1	1	3
		240	2	0	0
		270	1	0	0
MANEUVER	32:05	25	1	0	0
		50	1	0	0

IX. MASS SPECTROMETER

G. R. Carignan[1] and E. R. Miller

INTRODUCTION

A Mass Spectrometer system was developed for application on the IECM to measure the on-orbit gaseous environment around the Shuttle.[2] The inlet to the Mass Spectrometer is collimated by a three-stage skimmer to a field-of-view of 0.1 sr. The back side of the skimmers is pumped by an array of zirconium oxide getters so that the collimation is effective only for those gases which are pumped by zirconium oxide. The principal contaminants, except for the noble gases, helium and argon, are well pumped by the getters so that generally the flux of contaminants into the instrument arrives inside a cone of 10 deg half angle.

The instrument covers the mass range from 2 to 150 amu. In normal operation, a 600-sec cycle format is employed during which each mass number from 2 to 150 is sampled for 2 sec and during the subsequent 300 sec, mass 18 (H_2O) is sampled continuously with a 2-sec integration period. This format reflects the importance attributed to water contamination. Other formats used during special events allow the integration period to be shortened from 2.0 to 0.2 sec reducing the cycle time to 60 sec. It is also possible to truncate the spectrum at 50 amu and to eliminate the alternate H_2O sample in either integration period so that the best temporal resolution of masses 2 to 50 of 10 sec (50 x 0.2) can be achieved.

Two Mass Spectrometer systems, essentially identical, were built so that the turnaround time between flights could be accommodated. After each flight it is necessary to evacuate the vacuum enclosure, reactivate the getters, check the calibration, and vacuum bake and reseal, a process that cannot be confidently accomplished between successive flights.

The systems were flown on STS-2, -3, and -4 and operated remarkably well without any known equipment malfunctions. During the first flight, STS-2, the H_2O background in the instrument was higher than desirable and limited the ability to quantity the contaminant fluxes of H_2O. This problem was largely eliminated on subsequent flights. The results of the analysis of the data to date are presented in the following paragraphs.

Most of the measurements were made with the Mass Spectrometer on the IECM in the payload bay with its field-of-view looking outward along the -Z axis (see Fig. II-1). Thus, contaminants originating from Shuttle surfaces must, for the most part, scatter off atmospheric gases back into the instrument. Knowledge of the scattering cross sections or assumptions about them must be used to relate the measured return fluxes to source strengths or column densities. To mitigate this limitation, a gas calibration was incorporated as part of the instrumentation. A known collimated flux of isotopically labeled neon and water were released over a few tens of minutes. The gas calibration is discussed in a subsequent section. Operational problems have delayed a full analysis of the results. Therefore, the scattering cross sections used in the data reduction are calculated, and their uncertainty generally dominates the uncertainty in the reported column densities.

---

1. The University of Michigan, Space Physics Research Laboratory.
2. An Induced Environment Contamination Monitor for the Space Shuttle, edited by Edgar R. Miller and Rudolf Decher, NASA TM-78193, August 1978.

RESULTS

Predominant Masses

The gases observed by the Mass Spectrometer are, for the most part, those with molecular weight below about 50 amu. The various contributors (contaminant, atmospheric, and background) are given below:

Mass 1 – Hydrogen atoms, entirely the product of dissociative ionization of hydrogen-bearing species, notably H_2O, the ionization of which yields a significant 17 and 1 fraction.

Mass 2 – Molecular hydrogen which is almost entirely background of the zirconium oxide getters. No significance can be attached to this measurement.

Mass 3 – Statistically insignificant (SI).

Mass 4 – Helium. This measurement provides a good indicator of atmospheric helium abundance. Angle of attack excursions are clearly seen as is the diurnal variation in helium seen as a modulation with the period of the orbit. Helium is also a significant contaminant.

Mass 5 – SI.

Mass 6 – SI.

Mass 7 – SI.

Mass 8 – SI.

Mass 9 – SI.

Mass 10 – SI.

Mass 11 – Small but statistically significant, probably a minor contaminant containing boron, possibly borane.

Mass 12 – All carbon-containing molecules contribute to this peak.

Mass 13 – Mostly a product of dissociative ionization of CH_4. This peak together with 14, 15, and 16 is used to separate methane from other gas contributing to these various peaks.

Mass 14 – A complex sum of doubly and dissociatively-ionized N_2, doubly-ionized CO, and dissociatively-ionized CH_4. Its amplitude is heavily modulated by angle of attack because of the N_2 contribution and also modulated by methane-producing events.

Mass 15 – Almost exclusively from methane; a very small fraction from the 15 isotope in nitrogen compounds. It is a good mass for measuring the methane because it is uncontaminated by zero atoms and is almost equally sensitive to methane.

Mass 16 – Methane and zero atoms. Ambient atomic oxygen does not survive the many surface collisions before ionization. It forms other molecules, CO and CO_2 and O_2. The contribution to the 16 peak is thus indirect through dissociative ionization of oxygen-bearing molecules. In the STS-2 mission, most (at least half) of the 16 peak appears due to CH_4 which is a major background peak from the zirconium oxide getters. CH_4 is however a Shuttle contaminant, apparently having thruster firings as a source.

It is known that monomethyl hydrazine is catalytically converted to methane by zirconium oxide. It is suspected that unburned thruster fuel is the major source of the methane peaks observed during thruster firings.

Mass 17 – Dissociatively-ionized H_2O; i.e., OH^+; amplitude is about 40 percent that of mass 18.

Mass 18 – Water. The density of H_2O in the ion source is the sum of the instrument background and contaminant H_2O backscattered by the atmospheres into the instrument orifice. The level of the background was high on STS-2; but, on STS-3 and -4, the background level did not seriously degrade the contamination measurement.

Mass 19 – A statistically significant but unknown contaminant. It is possibly a fluorine compound, but the associated spectral peaks have not been identified.

Mass 20 – Mostly doubly-ionized argon with a small $H_2{}^{18}O$ contribution.

Mass 21 – Statistically insignificant except during gas calibration when the sum of ^{21}Ne and cross talk from the very large 22 peak contribute to the relatively large amplitude. The mass 20 peak is also slightly contaminated for similar reasons.

Mass 22 – Doubly-ionized CO_2 except during gas calibration when ^{22}Ne from the calibration source took the count to the highest observed for any mass during the flight test program. The density of ^{22}Ne in the ion source is consistent with the model values for scattering at 90 deg, which was the only angle of attack achieved during the period of gas calibration on STS-2.

Mass 23 – SI.

Masses 24, 25, 26, and 27 – An instrument contaminant of unidentified origin.

Mass 28 – Molecular nitrogen-ambient and contaminant, and carbon monozide which is a relatively large instrument background probably from the zirconium oxide getters but also from the instrument surfaces. Because the getters pump N_2 and degas CO, the analysis of the 28 peak at angles of attack other than near zero is very complex. At small angles the results are dominated by ambient atmospheric N_2, and the numbers are consistent with atmospheric models.

Mass 29 – Mostly $^{14}N\ ^{15}N$.

Mass 30 – Presumed to be NO with large peaks observed during thruster firings.

Mass 31 – Not analyzed.

Mass 32 – Molecular oxygen mostly of atmospheric origin through the recombination of atomic oxygen.

Mass 33 – SI.

Mass 34 – Not analyzed; partly O^{16} O^{18}.

Mass 35 – SI.

Mass 36 – An unknown minor contaminant, possibly HCL, plus a small component of ^{36}A.

Masses 37, 38, 39, 41, and 42 – Small but statistically significant peaks characteristic of propene.

Mass 40 – Mostly atmospheric argon.

Mass 44 – CO_2. Mostly instrument background with some small contribution from Shuttle environment – too small with respect to background to quantify.

Water

The measurement of H_2O was emphasized throughout the flight test program. Generally half the measurement time is devoted to water measurement. Specific events of short duration; e.g., 875-lb thrust Primary Reaction Control System (PRCS) thruster test firings, therefore frequently take place when H_2O is being continuously sampled. The geometry of the process that scatters thruster exhaust into the instrument is complex and has not been rigorously solved. It can be said, however, that the largest fluxes of water observed, except during payload bay door closings, result from PRCS test firings. Contributions to the water, or other species, return flux from the 25-lb thrust Vernier RCS engines were fired tens of thousands of times during the missions, are not detectable.

The envelope of counts at mass 18, proportional to the source density of H_2O, is shown in Figure IX-1 for STS-4. The large increase in H_2O count rate in correlation with PRCS firings can be clearly seen. It is stressed that the payload bay door closings and PRCS firings, often consisting of simultaneous firings of more than 1 PRCS in order to maintain a given attitude, were tests and would not normally occur during operational missions.

Aside from the thruster firings and payload bay door closings, the maximum level of H_2O contamination on STS-4 occurs at the beginning of the flight and decreases with a time constant of about 10 hr to near the instrument background. (Time constant is used to mean the time required to decrease to 1/e of a given level.) The count rate of $2 \times 10^4/2$ sec observed early in the flight corresponds to a source density of 2.5×10^8 cc^{-1} which at thermal velocities is a flux of 2.1×10^{14} cm^{-2} sr^{-1} sec^{-1}. Using a calculated scattering cross section yields a column density of 3.2×10^{13} cm^{-2}. This is the highest value observed on any of the flights and is attributed to the tile hail damage and rain environment experienced by Columbia during the STS-4 preparation. STS-2 was also subjected to a heavy rain on the launch pad and had a thin application of water protection coating consisting of 50-50 trichlorethane and flouroalthatic resin. Thick coating thickness was increased for STS-3 and STS-4. The following table summarizes the H_2O column densities observed on STS-2, -3, and -4.

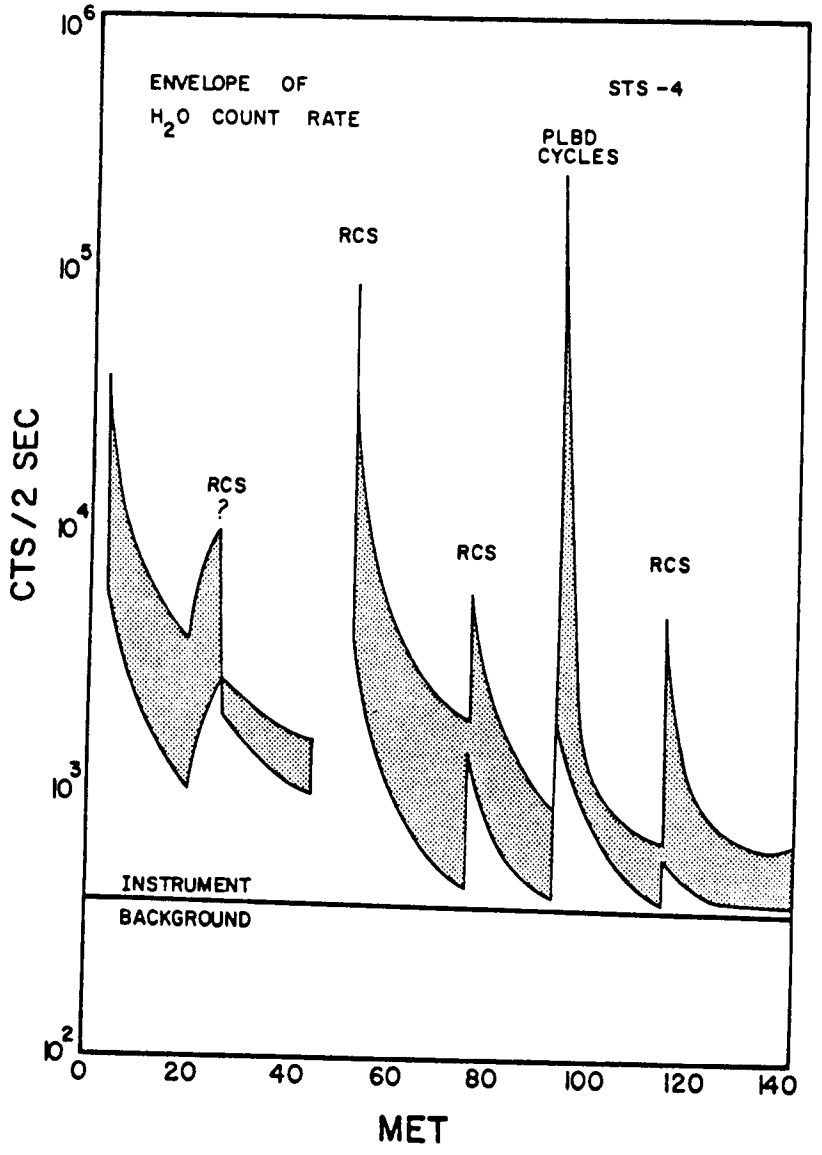

Figure IX-1. Envelope of H_2O count rate over the duration of the flight of STS-4. The values within the envelope are strongly modulated by the instrument angle of attack.

TABLE IX-1. H_2O CONTAMINANT COLUMN DENSITY

	Max*	Final
STS-2**	2.0×10^{13}	2.7×10^{12}
STS-3	1.5×10^{11}	4.0×10^{10}
STS-4	3.2×10^{13}	1.0×10^{12}

*Except for RCS firings and payload bay door closings
**The STS-2 values are considered upper limits.

Liquid water dumps, typically 150 lbs/hr for about 1 hr each, did not increase the mass 18 count rate with the possible exception of an increased count rate correlated in time with a water dump early in the STS-2 mission [2]. Also, the Flash Evaporator System (FES), which ejects molecular water in both sides of the lower aft section of the vehicle, did not significantly increase the water return flux, probably due to shielding by the eleven surfaces.

On STS-4, the IECM with the Mass Spectrometer was grasped by the RMS and moved and oriented to look back toward the Shuttle. The survey of contamination during this maneuver is discussed in a subsequent section, but a few comments with respect to H_2O contamination are appropriate here. A plot of H_2O counts/0.2 sec is shown in Figure IX-2. During most of this interval, the IECM was in two different locations with various pointing vectors.

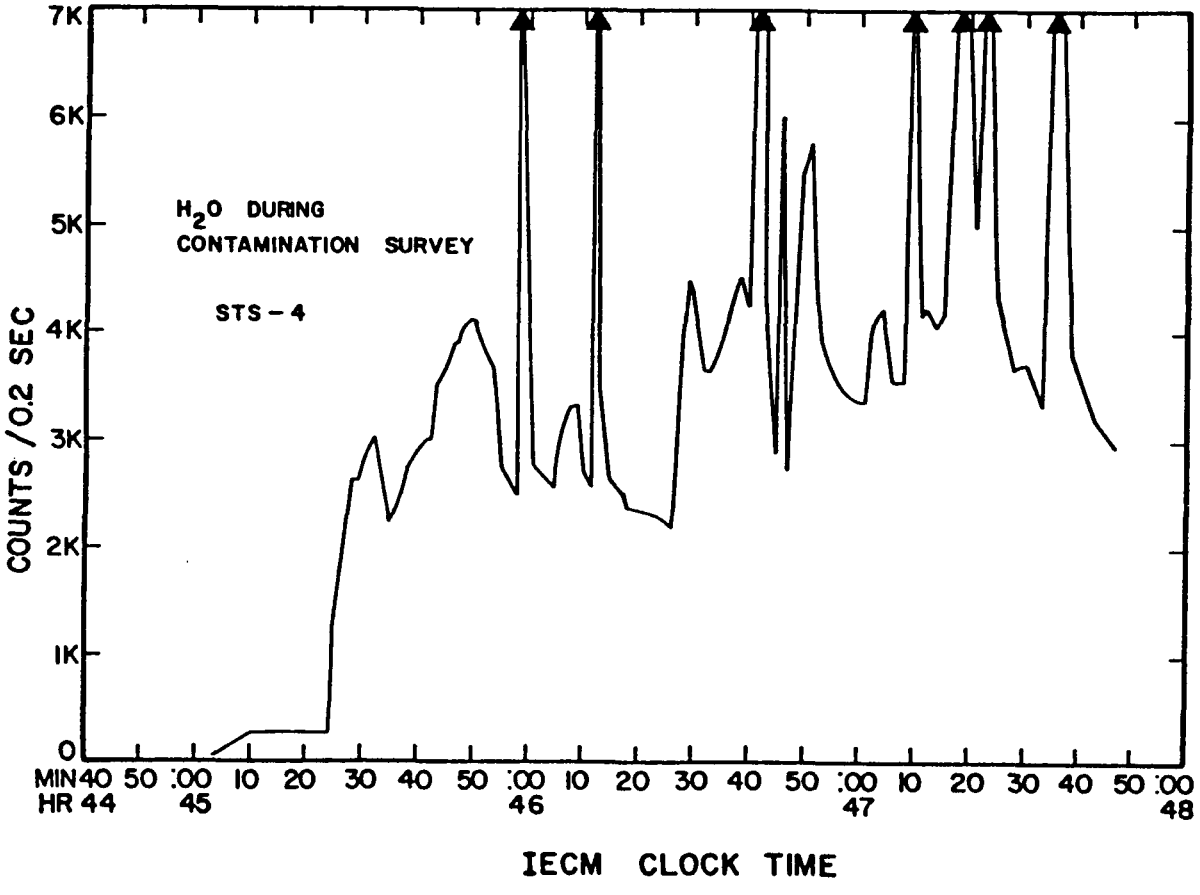

Figure IX-2. H_2O during contamination survey, STS-4.

The variation with distance from payload bay surfaces is slight suggesting that the source is distributed, largely filling the field-of-view of the instrument, at both locations. In fact, the small decrease at the outer location is probably the result of part of the field-of-view falling outside the bay in the Y axis. The ratio of the outbound flux to the inbound flux is about 50. The altitude of Columbia during this interval was about 305 km. This ratio is in qualitative agreement with the assumption of isotropic scattering in the center of mass system. A quantitative analysis of this complex scattering process will entail additional effort.

Helium and Argon

Helium is an important contaminant during all three flights analyzed. It is probable that small leaks in the many helium pressurized systems account for much of the helium observed. The most striking manifestation of the helium leaks is observed during door closing events. In Figure IX-3, a door closing at about 167 hr MET during the flight of STS-3 is plotted. The helium pressure in the payload bay is seen to rise, in a period of a few minutes to about 1.5×10^{-6} torr. On STS-4, the rate of increase was even greater and the final pressure somewhat higher.

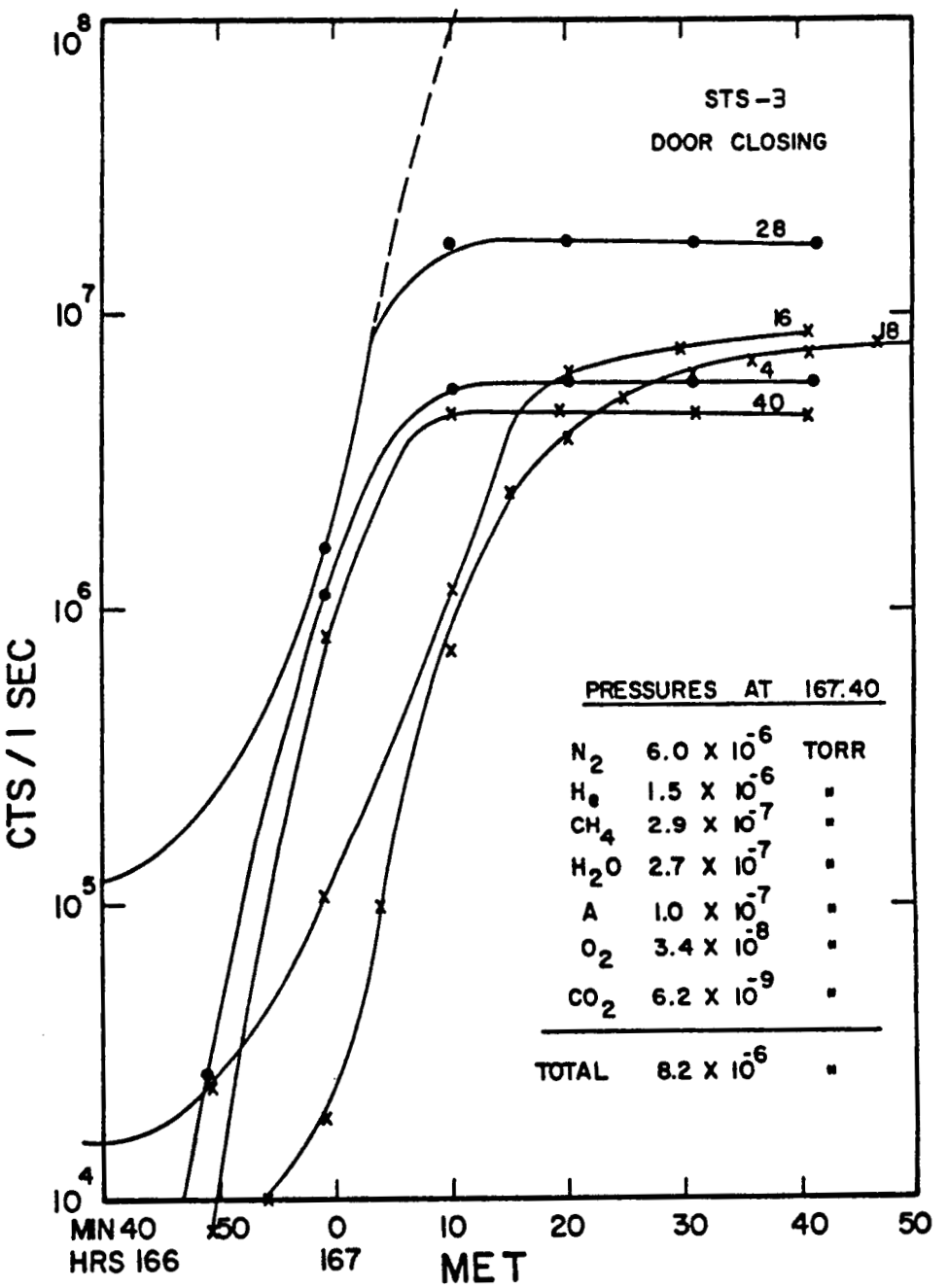

Figure IX-3. Pressure rise and composition in the payload bay during the door closing exercise at 167 hr MET on STS-3.

The partial pressure of argon on STS-3 is about 0.067 that of helium; and, during the door closing, the rise is virtually parallel suggesting that argon might be a 6 percent contaminant in the pressurization system helium.

During normal operation, atmospheric helium and argon can be measured. One orbit of data on helium and argon during the flight of STS-3 is shown in Figure IX-4. The large modulation is due to angle of attack variation over the orbit. The "bite-out" in the argon peak is caused by the deployed arm of the RMS intercepting the flow. The effect on helium can hardly be seen because of the filling in of the wake of the arm by the faster helium atoms.

Atmospheric helium and argon abundances have been obtained for each of the three flights using data of the kind shown in Figure IX-4. The results agree very well with model atmosphere values adding confidence to the other results.

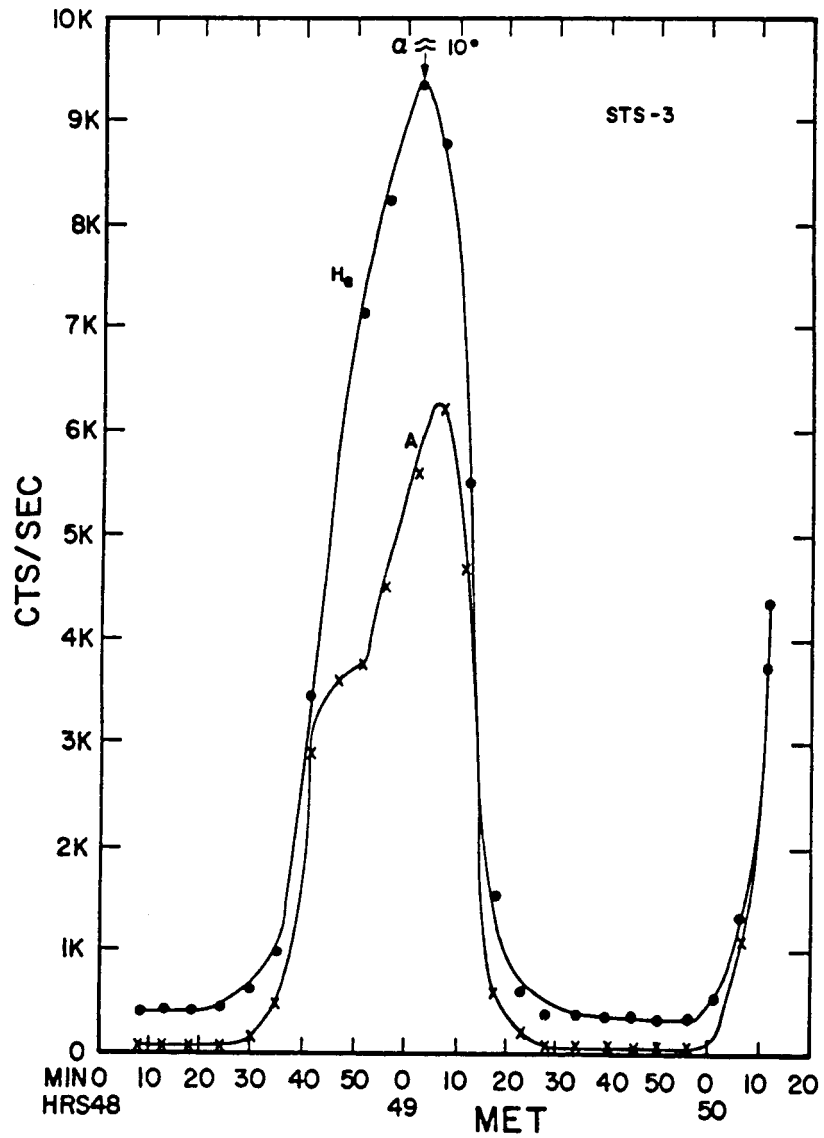

Figure IX-4. Variation in measured helium and argon as instrument angle of attack varies from 170 deg to 10 deg. The atmospheric densities obtained from many such observations on STS-2, -3 and -4 agree well with model values.

C-2

Methane

An unexpected result of the Mass Spectrometer measurements is a large, unambiguous peak in methane during PRCS thruster tests. Methane is a relatively large background contaminant of the instrument, but the large increases associated with thruster firings rise well out of this background. A vernier thruster firing event, viewed directly during the RMS contamination survey on STS-4, is shown in Figure IX-5. The methane peak increases more than tenfold in correlation with the indicated vernier firings. The observed increases in molecules other than methane are given and agree fairly well with predicted values. The methane is not predicted and is ascribed to the catalytic production of methane over the zirconium oxide getters from unburned monomethyl hydrazine. This assertion requires additional study but does seem to adequately explain the results.

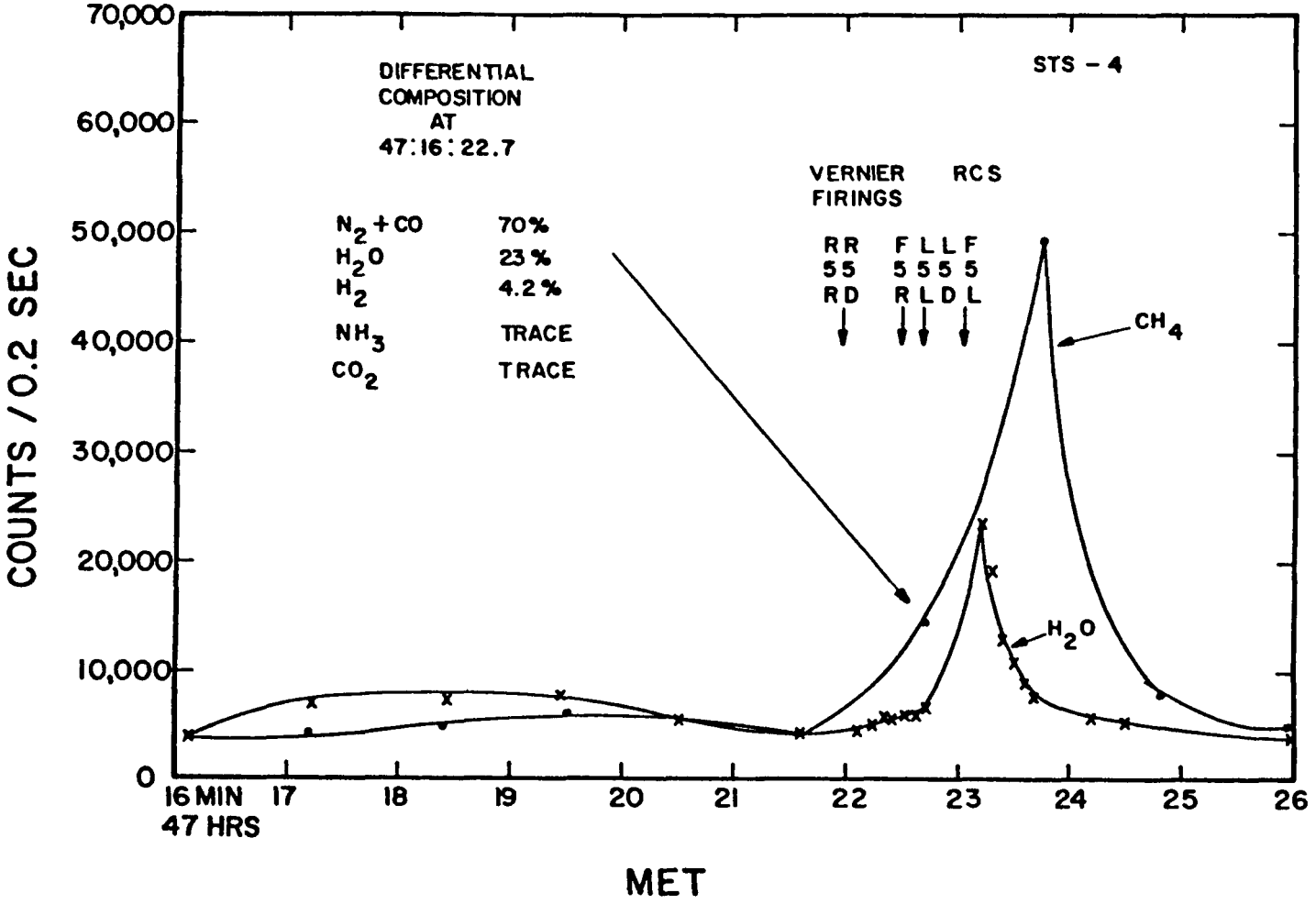

Figure IX-5. Signature of a vernier RCS firing during mapping. Methane is believed to be artificially produced on the zirconium oxide getters of the collimator. Nitrogen, water, and hydrogen are the principal products observed.

Because the zirconium oxide of the collimator pumps is assumed to be the catalyst, there is no collimation, and the full 2π sr uncollimated field-of-view of the instrument participates in the acceptance of the monomethyl hydrazine. Taking this factor into account, together with the source densities and sensitivities, it is computed that a 1.5 percent excess fuel in the thruster firings would explain the result.

Methane is also a significant contaminant during door closings. In the door closing case, however, it is difficult to rule out a pressure-dependent methane background in the instrument. An alternative explanation is that the monomethyl hydrazine from previous thruster firings is slowly outgassing from payload bay surfaces. The entire methane issue deserves further study.

Heavy Molecules

On all three flights contaminants of high molecular weight (>50) are at very low levels. Heavy molecules are measurable during door closing events and, on STS-4, during the contamination survey. Molecules that have been identified include trichlorethylene, Freon 12, and other hydrocarbons typical of chemically cleaned surfaces. On STS-4, during the contamination survey, a relatively large flux of Freon 21 (dichlorofluoromethane) is observed when the instrument is pointed at the aft payload bay bulkhead.

Generally, it can be stated that the contamination environment in heavy hydrocarbons is low. The levels are too small to be accurately quantified. Freon leaks in cooling systems can, however, cause higher values particularly in the vicinity of the leak as was apparently the case on STS-4.

Door Closings

On both STS-3 and STS-4, the composition and pressure in the payload bay was measured during door closing events. The results are similar except that on STS-4 a much larger partial pressure of helium was observed. The composition and pressure during the door closing at 167 hr and STS-3 is shown in Figure IX-3. The total pressure of 8×10^{-6} is dominated by N_2, and the levels of other gases are indicated. During the next spectrum after the one at 167 hr, 40 min MET, the pressure was approximately 5×10^{-5} torr, too high for spectrometric analysis. This door closing was in preparation for end-of-mission de-orbit. The doors were opened after about 4 hr when the mission was extended due to weather conditions at the landing sites.

Nitrogen which is an obvious contaminant during door closings is undoubtedly present at all times. The presence of atmospheric nitrogen, however, masks the contaminant flux so its level has not been quantified. Further analysis should yield a more quantitative result.

Gas Calibration

At 34 hr MET on STS-2, a controlled release of isotopically-labelled neon and water was initiated. The purpose of the release was to calibrate the measurement including the scattering cross section. ^{22}Ne and $H_2{}^{18}O$ are expelled through a capillary array providing a known flux directed outward. A fraction of the gas is scattered backward into the instrument very much like a contaminant flux. Since the flux out in the calibration source is known, the return flux measurement can, in principle, be interpreted in terms of the scattering cross section. However, to eliminate the component of the measurement arising from self scattering, the plan called for a maneuver that would sweep the -Z axis through all angles of attack between 180 and 0 deg. In the wake, near 180 deg, the measured value should arise entirely from self scattering. For operational reasons, the maneuver was not carried out so the calibration is not yet complete. The angle of attack was 90 deg throughout. The values of some key mass numbers

during the release are plotted in Figure IX-6. The 22 peak from the isotopically-labelled neon is seen to rise from virtually zero to a very high value (3×10^6), close to the predicted level. It stays near constant over a period of about 30 min just short of the predicted lifetime of the source. The 20 and 21 peaks are the result of impurities from the other neon isotopes. The $H_2{}^{18}O$ is not seen; subsequent laboratory tests indicate that the simple technique employed will not reliably produce a water vapor flux but will rather produce only solid water.

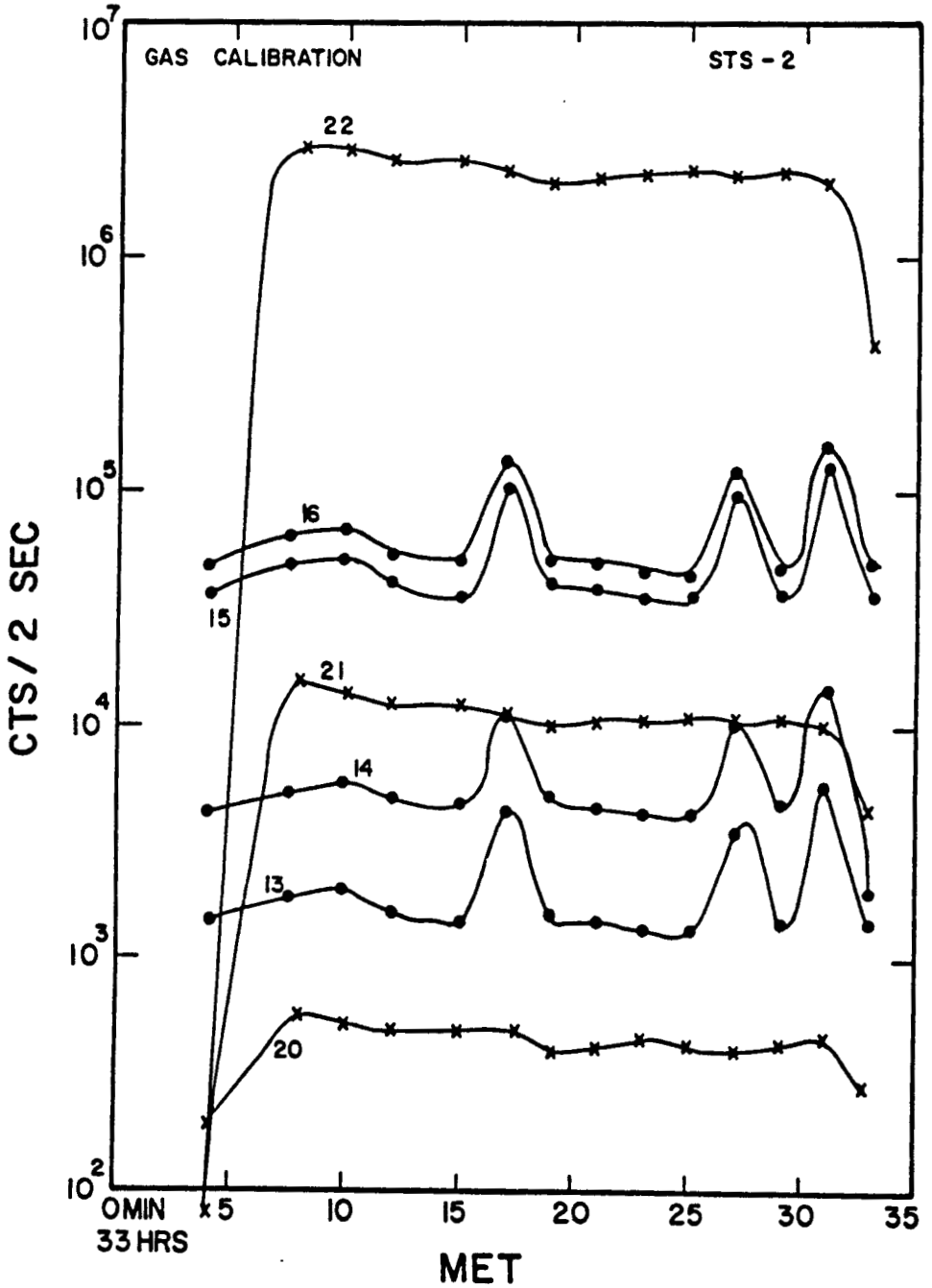

Figure IX-6. The calibration gas release at 33 hr MET on STS-2. The mass 22 isotope of neon dominates the spectrum. The isotopically labeled water at mass 20 which was released simultaneously is not seen. The mass 20 and 21 count rates are consistent with the purity of the neon-22 gas load.

Thruster firings are evident during the calibration by their strong methane signature. The duration of these thruster events is short; the figure is misleading because of the temporal resolution of the methane measurement.

On STS-3, the gas calibration was not initiated; and, on STS-4, the release was not synchronized with the associated maneuver. The STS-4 results, when understood, should enable an evaluation of the self-scattering component which can then be used to correct the STS-2 result to obtain a scattering cross section for the 90 deg angle of attack case. Altogether, the gas calibration has been something less than successful. It would be highly desirable to improve the technique, separate the gas source from the vicinity of the spectrometer, and synchronize the release with an angle of attack maneuver.

Contamination Survey

On STS-4, the IECM was picked up by the RMS and maneuvered to enable an inward look at the payload bay and some other surfaces. The survey was performed between 45.5 and 47.8 hr MET in top-to-Sun attitude, attained at 44 hr MET. Night cycles occurred between 45.8 and 46.4 hr MET and 47.3 and 47.9 hr MET during the survey. A total of 15 different configurations was achieved. Nine of these are depicted in Figures IX-7 and IX-8. The field-of-view of the instrument, 10 deg half angle, is shown in positions 11 and 18. In all the cases shown, the IECM is located on the center line of the Y axis. The average value at each position of three of the observed contaminants is shown in Figure IX-9, IX-10, and IX-11. For H_2O, discussed earlier, the vertical spikes correspond to thruster firings. The highest levels of H_2O other than these spikes, are at positions 9, 10, and 18 corresponding to the center of aft payload bay.

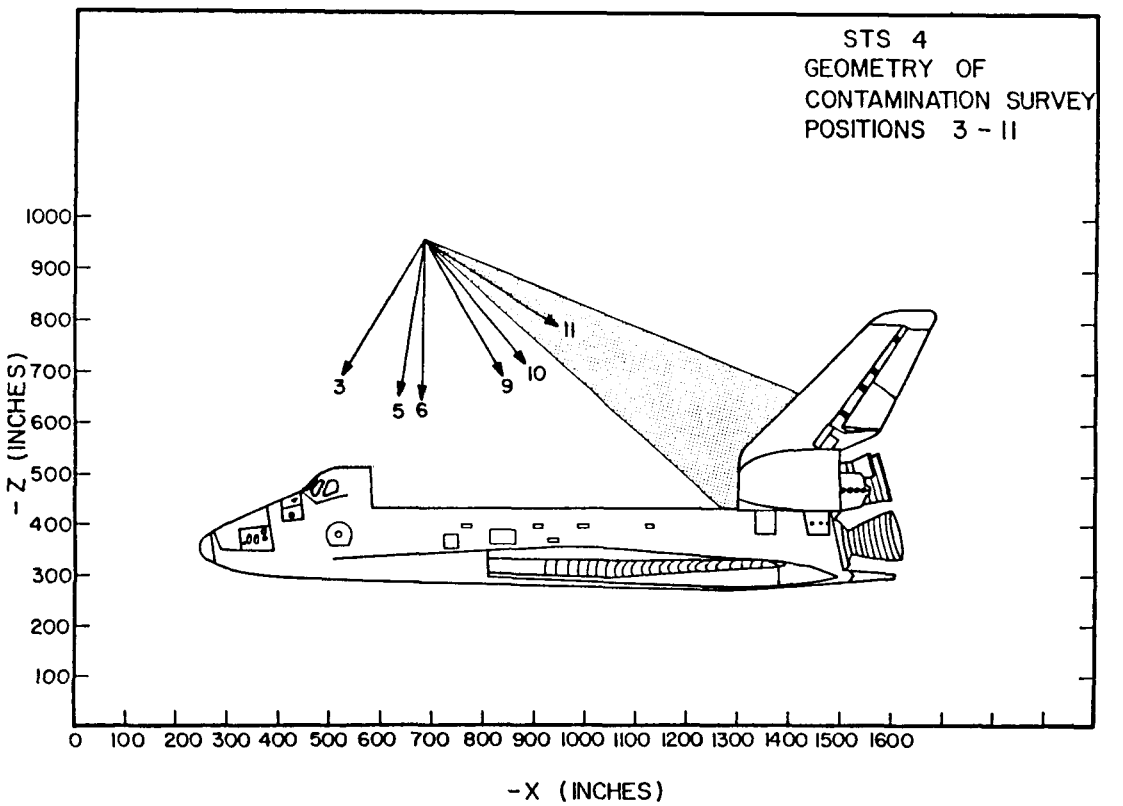

Figure IX-7. STS-4 geometry of contamination survey positions 3 through 11.

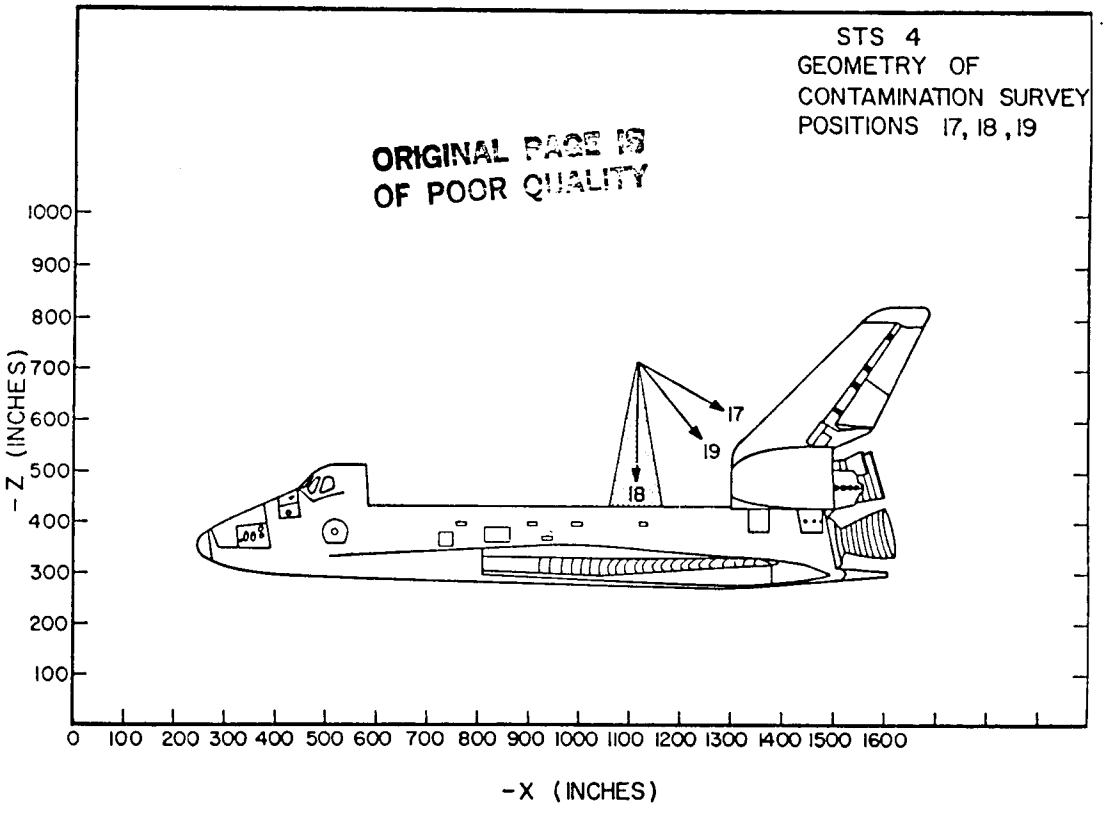

Figure IX-8. STS-4 geometry of contamination survey positions 17, 18, and 19.

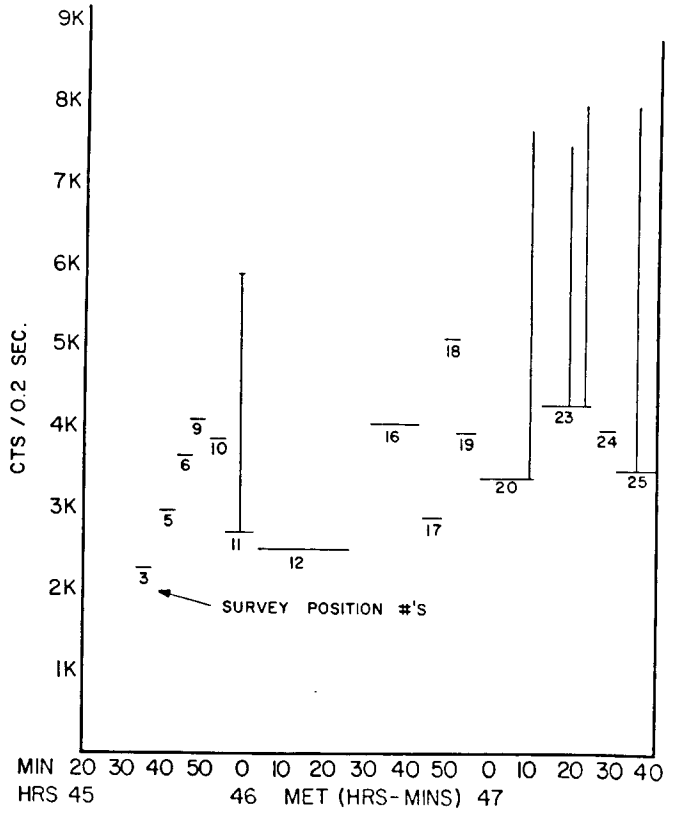

Figure IX-9. STS-4 H_2O counts during contamination survey.

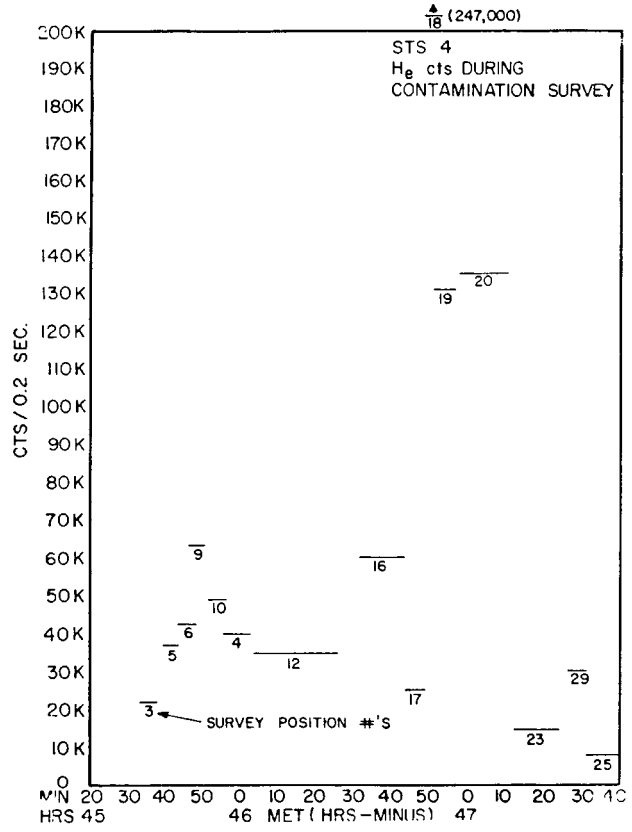

Figure IX-10. STS-4 He counts during contamination survey.

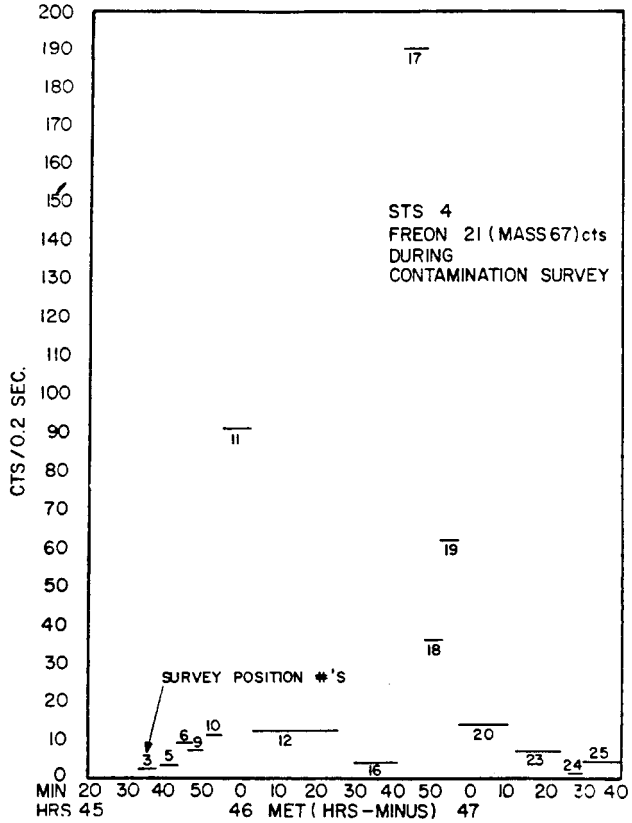

Figure IX-11. STS-4 freon 21 (mass 67) counts during contamination survey.

The helium contaminant survey has a pattern similar to that for H_2O except that a very large source at position 18 is seen.

Freon 21, used in thermal control systems, has a distinct spectrum. It was observed clearly during the survey. The fraction of mass 67 is plotted in Figure IX-11. Positions 11 and 17 seem to localize the source of the leak in the vicinity of the aft bulkhead and tail root.

All of the masses of interest have been tabulated and plotted for the period of the survey. Vehicle outgassing and leakage of cabin gas appears to be very low as determined by the contamination survey and, as mentioned for H_2O, appears consistent with in-bay return flux measurements. Further analysis is necessary to quantify outgassing by species taking into account atmospheric contributions, vehicle attitudes, and temperatures.

CONCLUSIONS

The gaseous environment in the vicinity of the Shuttle Orbiter has been well characterized by the Mass Spectrometer measurements on STS-2, -3, and -4. The results are less quantitative than desired largely because of the complex scattering processes involved.

Despite the complexities and the limitations of the measurement, the H_2O contamination level has been quantified and a number of other contaminants identified. Helium venting and leaks in onboard systems are particularly large sources of contamination. Large fluxes of methane are observed in the instrument during PRCS thruster test firing events. The major source of the methane is tentatively identified as unburnt monomethyl hydrazine catalytically converted, in the instrument, to methane.

Atmospheric gases, particularly helium and argon, which are not collimated by the getters have been measured. The results agree very well with model values adding confidence to the other results. The inflight calibration was less successful than anticipated. This deficiency and the rather high instrument background in several gases because of the presence of the getters gives rise to a desire to repeat the measurements on a future flight or flights. Several obvious changes based on what was learned on STS-2, -3, and -4 could improve the quality of the measurements and facilitate their interpretation.

X. CONCLUSIONS

Based on results from the IECM flights on STS-2, -3, and -4, the Space Shuttle has met requirement goals established as defined by the Particles and Gases Working Group (PGWG) and the CRDG for on-orbit particulates and gaseous induced environment.

The Camera/Photometer experiment provided excellent and consistent data on particulates down to approximately 2.5 μm diameter. The stereo pair images with 0.24 sr (32 deg) fields-of-view showed -Z axis particles with 25 μm or greater diameters at an average rate of 500/orbit. For a field-of-view of 1.5×10^{-5} sr (0.25 deg), 3 particles of 25 μm diameter or greater would be seen in 100 orbits (0.03 particles/orbit). The CRDG goal requires less than one 5 μm diameter or larger particles per orbit in a 1.5×10^{-5} sr field-of-view.

Early mission particulates were shown to dissipate in approximately 15 hr, and the large number of particulates produced by water dumps dissipated in 20 to 30 min after cut-off. Induced background brightness due to molecular and particulate scattering of sunlight was not measurable above the natural star and zodiacal light backgrounds (CRDG goal).

No background lighting from the few PRCS or many VRCS engine firings or from the so-called "surface glow" phenomenon have been specifically identified in the Camera/Photometer data at this time.

On-orbit optical degradation was within measurement accuracies of the OEM which monitors specular transmittance and diffuse reflectance at 253.7 nm wavelengths. Laboratory optical measurements of the OEM and PSA samples from 120 to 2500 nm verified the flight measurements. Postflight Auger measurements did not reveal non-volatile condensable materials on the surfaces. Also, data from the Mass Spectrometer and the TQCM and CQCM instruments confirm the general absence of heavy molecules (above 50 amu) and mass accumulation (approximately 10^{-6} g/cm^2/30 days), respectively. The goals for optical degradation are 1 percent and 10^{-5} g/cm^2/30 days mass accumulation on surfaces with a 2π sr view in the -Z axis.

Mass spectrometric measurements of molecular return flux indicate that water is the most prevalent outgassant. Early mission (approximately 3.5 hr MET) water return flux values were as high as 2.1×10^{14} molecules/cm^2/sr/sec on STS-4, presumably as a result of hail damaged tiles, resulting in a calculated column density of 3.2×10^{13}/cm^2.

On STS-3, with sufficient water protective coatings, measurements indicate early mission H_2O return fluxes of about 1×10^{12}/cm^2/sr/sec, corresponding to 1.5×10^{11}/cm^2 column density. Initial values decreased with a time constant of about 10 hr. The goals for H_2O return flux and column densities are $<10^{12}$/cm^2/sr/sec and 10^{12}/cm^2, respectively, after 24 hr MET. Water return flux during water dumps, flash evaporation cooling, and vernier engine operation did not significantly increase.

The environmental measurements during preflight ground operation reflect the pre-STS operational development phase of the OPF, which is to be upgraded in the near future. Only dustfall was identified as a problem during these periods, which contributed to airborne particulates during ascent. Dustfall was also noted as a result of the ferry-flights and subsequent exposure upon return to the OPF.

Non-volatile residues were well below the 10^{-6} g/cm^2 goal during ground operations.

Ascent and descent measurements detected no ingestion of exhaust products into the payload bay.

The fact that the Space Shuttle has met the induced environment requirement goals is a tribute to foresight, planning, and engineering. Testing and selecting materials, placement of engines, placement of the Auxiliary Power Unit and Flash Evaporator exhausts, and provision for payload bay door vent controls all contribute to meeting these goals.

Much of the credit for the establishment of requirement goals, planning, and implementing the efforts necessary to meet these goals belongs to the PGWG under the direction of Lubert J. Leger, JSC, and the CRDG chaired by Robert J. Naumann, MSFC.

APPROVAL

STS-2, -3, -4 INDUCED ENVIRONMENT CONTAMINATION MONITOR (IECM) SUMMARY REPORT

Edited by E. R. Miller

The information in this report has been reviewed for technical content. Review of any information concerning Department of Defense or nuclear energy activities or programs has been made by the MSFC Security Classification Officer. This report, in its entirety, has been determined to be unclassified.

A. J. DESSLER
Director, Space Science Laboratory

☆ U.S. GOVERNMENT PRINTING OFFICE 1983—646-058/190